nagra.

Arbeitsbericht NAB 17-34

Literature Review of Past and Future Climate Simulations

August 2017

Professor Dan Lunt,
Natalie Lord & Alan Kennedy

School of Geographical Sciences
University of Bristol

National Cooperative
for the Disposal of
Radioactive Waste

Hardstrasse 73
P.O. Box 280
5430 Wettingen
Switzerland
Tel. +41 56 437 11 11

www.nagra.ch

nagra.

Arbeitsbericht NAB 17-34

Literature Review of Past and Future Climate Simulations

August 2017

Professor Dan Lunt,
Natalie Lord & Alan Kennedy

School of Geographical Sciences
University of Bristol

KEYWORDS
Literature review, long term evolution, climate, LGM, simulation, paleoclimate, future climate

National Cooperative
for the Disposal of
Radioactive Waste

Hardstrasse 73
P.O. Box 280
5430 Wettingen
Switzerland
Tel. +41 56 437 11 11

www.nagra.ch

Nagra Arbeitsberichte ("Working Reports") present the results of work in progress that have not necessarily been subject to a comprehensive review. They are intended to provide rapid dissemination of current information.
This report was prepared on behalf of Nagra. The viewpoints presented and conclusions reached are those of the author(s) and do not necessarily represent those of Nagra.

Table of Contents

Electronic Appendix: A table including a summary of all publications discussed in this report is attached to the electronic version of this report (pdf). It is also available on request for paper versions.

List of Tables

List of Figures

1 Context

1.1 Background

Nagra (the National Cooperative for the Disposal of Radioactive Waste) is mandated to ensure the safe long-term disposal of radioactive waste generated in Switzerland by nuclear power plants and by medicine, industry and research, in deep geological repositories.

The significant timescales involved in the decay to safe levels of radionuclides incorporated in radioactive wastes means that geological disposal facilities containing low- and intermediate-level wastes must continue to function effectively for up to 100,000 years. For high-level wastes and spent nuclear fuel, repositories must remain functional for up to 1 million years. It is therefore essential to consider long-term climate evolution in post-closure performance assessments in order to evaluate a geological disposal system's response to, and robustness against, a variety of potential environmental changes.

One such environmental change which is crucial to consider is erosion. For Alpine environments, key processes of interest include river incision and glacial erosion. In particular, the process of overdeepening has been identified as a process that could result in the integrity of a repository being compromised under possible future glaciations. The variation in depth of the Opalinus clay host rock at the three sites currently under investigation for a repository for high level waste means that it is critically important to assess the likely magnitude of future erosion at these sites, to help to characterize the minimum depth at which a repository for radioactive waste should be placed.

For processes occurring on such long timescales, past observed changes provide a crucial test of our understanding of the underlying processes, and provide examples of the system operating under extreme conditions. In particular, past glacial-interglacial cycles have caused erosional processes at the sites of interest, and these can provide a key to possible future changes. In this context, Nagra has identified four key questions related to long-term climate change:

(Q1) When will the next glaciation occur?

(Q2) Which glaciations in the past were important for the formation of overdeepened valleys and which climates led to these glaciations?

(Q3) When do we expect the next glaciation with similar conditions to those in (Q2) to occur?

(Q4) Which climates are possible in the future and how do periglacial, non-glacial and interglacial climates affect the repositories (geosphere and biosphere)?

This literature review, whose aims and scope is outlined below, will provide a contribution towards addressing some aspects of these questions, in particular (Q1) and (Q4).

1.2 Aims and scope of the literature review

This literature review summarises key previous numerical modelling studies that address the long-term evolution of past and future climate change.

Section 2 provides an introduction to the modelling of long-term (~ 1 million year) climate change. This includes: a discussion of the principal forcings of long-term climate change, primarily atmospheric carbon dioxide and changes in insolation resulting from astronomical variations (Section 2.1); the climate feedbacks (both physical and biogeochemical) which mediate these forcings (Section 2.2); and an overview of the various modelling tools that are used to simulate long-term climate change, including General Circulations Models (GCMs), Earth system Models of Intermediate Complexity (EMICs), and conceptual models (Section 2.3).

Sections 3 and 4 summarise existing numerical model simulations of long-term past and future climate change respectively. Accompanying these is a spreadsheet giving details of the simulations, including model complexity, resolution, and boundary conditions.

Section 3 summarises 'snapshot' simulations of specific past time periods, usually carried out with full complexity models (Section 3.1), and transient simulations covering tens of thousands of years (Section 3.2, 3.3) to millions of years (Section 3.4), usually carried out with lower-complexity models. Many of the snapshot simulations have been carried out in the context of the Palaeoclimate Modelling Intercomparison Project (PMIP), and will thus concentrate on the Last Glacial Maximum (LGM), mid-Holocene (MH), and last interglacial (LIG). Focus will be on the LGM simulations as these are most relevant to Nagra in this context. Transient simulations are often focused on the last glacial-interglacial cycle, but simple conceptual models have been run over the entire 2 million year window. A particular focus will be on assessing the simulations in terms of any evaluation to proxy data that was carried out in the studies.

Section 4 addresses future climate simulations. A synthesis of the key forcings of future climate change is given (Section 4.1), and then a brief summary of IPCC-timescale simulations (next few hundred years, Section 4.2). This is followed by a discussion of future simulations on longer timescales; up to 50 kyr (Section 4.3), 100 kyr (Section 4.4), and 1 Myr (Section 4.5). The majority of studies in this context have focused on the question of the next glacial inception, and have been carried out with reduced-complexity models. Only a handful of studies (e.g. in the context of the BIOCLIM project) have carried out snapshot future simulations with full complexity models.

The studies in Sections 3 and 4 are critically assessed and intercompared in Section 5. In particular, there is a focus on the European region. Given the concept that "the past is the key to the future", this summary provides contextual information towards Nagra's question (Q4). In addition, a focus on the range and relative likelihood of predictions for the timing of the next glacial inception directly addresses question (Q1).

2 Introduction to modelling long-term climate change

This section provides an overview of the forcings that drive long-term climate change (Section 2.1), the mechanisms and feedbacks by which the Earth system responds to these forcings (Section 2.2), and a summary of the numerical modelling tools that are used to understand and simulate long-term climate change (Section 2.3).

2.1 Forcings of long-term climate change

On timescales of up to 1 million years, the primary external forcing of the Earth system is variation in incoming solar radiation at the top of the atmosphere. This variation results from changes in the Earth's astronomical parameters, which determine the seasonal and latitudinal distribution of incoming radiation. The key astronomical parameters are eccentricity (the extent to which the orbit of the Earth around the sun is elliptical), obliquity (the angle of the axis of rotation relative to the plane of the orbit of the Earth around the sun), and the precession (the timing of aphelion or perihelion relative to the vernal equinox). Due primarily to the gravitational effects of other bodies in the solar system, these three astronomical parameters vary on timescales of ~ 400 kyr and ~ 100 kyr (eccentricity), ~ 40 kyr (obliquity), and ~ 20 kyr (precession). Precession and obliquity modify the latitudinal and seasonal distribution of incoming radiation but do not affect the total global annual mean insolation. Eccentricity affects both the distribution of radiation and the total amount of radiation (albeit to a small degree), and also modulates the precession parameter.

Other external forcings include palaeogeographical (topography and bathymetry due to plate tectonics) and solar luminosity changes, but these act on much longer timescales than 1 million years and as such can be neglected (unless the period considered includes a significant change in ocean gateways, such as the closure of the Panama Seaway). In addition, the 11-year sunspot cycle, and longer timescale luminosity changes, such as those associated with the Maunder Minimum, can also be neglected as they occur on timescales shorter than those of relevance here. A similar comment applies to volcanic forcing, although the possibility of a supervolcano occurring over the timescale of interest is non-zero.

As a direct result of the astronomical forcing, Earth's climate has swung from glacial to interglacial state over at least the last 1 million years, despite the changes providing only a relatively weak forcing. The reason for the large response is due to positive feedbacks in the Earth system which amplify the forcing. The primary feedback is associated with the carbon cycle. Ice core records indicate that glacial periods are associated with relatively low atmospheric concentrations of carbon dioxide (CO_2) and methane (CH_4). However, the mechanism by which CO_2 changes through glacial-interglacial cycles is currently uncertain. Likely contributing effects are physical processes such as temperature dependence of the solubility of CO_2 in the ocean, ocean circulation affecting the lifetime of CO_2 in the ocean, and biogeochemical processes associated with the biological pump, such as iron fertilisation in the Southern Ocean increasing during glacial episodes (See IPCC AR5, Chapter 6, Figure 6.5). Feedbacks associated with the carbon cycle are so poorly understood that it is common practice to consider CO_2 changes in the past as a forcing on the climate system, rather than a feedback, and to impose CO_2 concentrations in long-term palaeoclimate simulations. Furthermore, anthropogenic emissions of CO_2 provide a genuine external climate forcing. Therefore, for the remainder of this report, we will consider CO_2 as a forcing on the climate system.

2.2 Climate feedbacks

There are multiple feedbacks, both positive and negative, that mediate the climate system response to the orbital and CO_2 forcings.

As stated previously, over the last million years the Laurentide and Fennoscandian ice sheets (and the smaller Alpine, Himalayan and Patagonian glaciers) have fluctuated in synchrony with CO_2, and paced by astronomical forcings. The orbital pacing of ice sheets is still not well understood, but the essence of Milankovic theory is thought to be broadly correct. That is, that the insolation in Northern Hemisphere summer is critical for determining the state of the Earth system, as this governs the likelihood of snow surviving summer ablation in regions where there is sufficient continental area to build up a large ice sheet. Thus, periods of low summer insolation in the Northern Hemisphere are generally associated with increasing ice volume. However, the system is highly non-linear and state dependent; for example, the Last Glacial Maximum, one of the periods of greatest ice volume in the last 2 million years, has similar astronomical forcing to the present day. These ice sheets play an important role in the atmosphere and ocean systems. They affect the radiation balance due to their high albedo (relative to vegetation or bare soil), affect atmospheric circulation directly through generation of Rossby waves and due to their effect on temperature, affect precipitation due to their orography, and can also affect ocean properties and circulation through interaction with the atmosphere and through the input of fresh melt-water.

Ocean circulation changes also play a role in the Earth system and their effect is important both for regional- and millennial-scale variability. Of particular importance are millennial-scale variations in temperature, which are recorded in ice and sediment cores, in particular in the North Atlantic during the last glacial-interglacial cycle. Antarctic and Greenland ice cores show a ‘bipolar seesaw’, whereby one pole warms as the other cools or remains at a steady temperature, before the pattern reverses (e.g. Broecker 1998; Stenni et al. 2010). The mechanisms behind these events are not fully understood and not captured by all model simulations (e.g. Smith and Gregory 2012). However, they are likely linked to changes in ocean circulation and the strength of overturning in the North Atlantic (Wolff et al. 2009) associated with the inputs of freshwater that accompany the decay of ice sheets.

Other processes, such as changes in atmospheric dust and vegetation feedbacks, likely played some role in shaping the exact nature of the glacial cycles. Dust is known to have varied over these timescales (Mahowald et al. 1999; Lambert et al. 2008), and could interact with the climate system through affecting the albedo of fresh snow (Warren 1984), absorption and/or scattering of radiation in the atmosphere (Tegen 2003), and ocean fertilisation (Jickells et al. 2005) for example. These processes may be very important, but their effect is much more uncertain than the orbital and CO_2 changes.

2.3 Modelling tools for long-term climate change

Over the last three decades, a wide range of numerical models of the Earth, of varying complexities, have been applied to predict and understand climate changes on long timescales. The models that have been used form a hierarchy or spectrum of complexity. It is often helpful to categorise models as one of four types, although recognising that many models sit at the boundaries of the categories. These are Earth system models (ESMs), General Circulation Models (GCMs), Earth system models of intermediate complexity (EMICs), and conceptual models. Here, we describe each of these, and discuss their strengths and weaknesses.

2.3.1 Conceptual models

Conceptual models represent a highly simplified version of the Earth, and usually include very few, if any, climatic mechanisms. They are often global in nature, with no latitudinal or zonal variations. They typically include a small number of poorly-constrained parameters which enable the models to be tuned to observations of some calibration period. Examples include (a) Rahmstorf (2007)'s sea level model, in which sea level change is predicted from temperature, based on a lagged response, and tuned to observations of the last century; (b) Paillard (1998)'s glacial-interglacial cycle model, in which ice volume is predicted from summer insolation at 65°N, based on a lagged response and asymmetric thresholds, and tuned to observations of the last 1 million years; and (c) Lunt et al (2011)'s hyperthermal model in which temperature is predicted from insolation, based on a lagged response to a time-varying threshold, and tuned to observations from 50 million years ago. The weaknesses of conceptual models are their simplicity, tunability, and lack of physical processes. However, they can usually be integrated almost immediately, and can provide insights into the properties of the processes responsible for climate change. Their simplicity means that their results can be relatively easily understood and interpreted. In particular, conceptual models are currently the only tool available to simulate climate change on timescales of 1 million years. Paillard's model of glacial-interglacial cycle, with extensions by Archer and Ganopolski (2005) remains the most accurate numerical representation of climate on these timescales. Furthermore, Paillard's work revealed the potential role of deep ocean processes for causing the mid-Pleistocene transition from a 40 kyr world to a 100 kyr world, and showed that changing thresholds could explain the gradual increase in intensity of glacials over the last 5 million years.

Conceptual models, very similar to those mentioned above, have been used in the context of the long-term geological storage of radioactive wastes in the BIOCLIM project (see Section 4.5), where they were used to make initial predictions of the state of the Earth system over the next 200 kyr, including predicting the onset of the next glaciation.

2.3.2 Earth System Models (ESMs)

At the opposite end of the spectrum are Earth system models. ESMs have been developed to represent the entire Earth system in as much detail as is computationally possible. As well as the dynamics and physics of the atmosphere and ocean, they represent the land surface and vegetation, ice sheets, marine biogeochemistry, and atmospheric chemistry and composition. Typically, they will include a dynamical core in the atmosphere and ocean which solves the Navier stokes equations and the appropriate thermodynamics, discretizing the equations on a fine spatial grid (currently typically at a resolution of about 0.5°×0.5°), and stepping forward at a timestep of typically about 10 minutes. However, many processes occur at a spatial scale smaller than this discretization, for example convection, clouds, and turbulence in the atmosphere, and eddies in the ocean. These processes are required to be 'parameterised', that is the consequences of these processes are approximated at the scale of the model. This results in tunable parameters in the model which can be constrained by process-based observations to a certain extent, but which nevertheless leave many relatively free parameters which allow the model to be tuned to global or regional observations, such as of sea surface temperature (SST) or top of the atmosphere radiative fluxes. ESMs are extremely complex, often incorporating over a million lines of computer code, and are extremely computationally expensive to run. Typically, ESMs will run at about 1–10 years per day on the most powerful supercomputers in the world. As such, they can only be used to carry out simulations of the order 100–300 years. ESMs are routinely used by national climate organisations, such as NCAR in the US (https://ncar.ucar.edu/), in the framework of the Coupled Model Intercomparison Project (CMIP, https://www.wcrp-climate.org/wgcm-cmip/wgcm-cmip6), which coordinates the

standard simulations synthesized by the Intergovernmental Panel on Climate Change (IPCC). They are the most accurate representations of the Earth system currently available, yet different models can give quite different predictions under identical forcings. In particular, aspects of the system that have to be parameterised, such as clouds, are simulated differently by different models, and as such we have relatively low confidence in predictions of these variables. Given that many of these variables, including clouds, play an integral role in the energy balance of the climate system, other variables, such as temperature, are also relatively uncertain. However, where many or all models predict similar outcomes, we can have high confidence in those outcomes, and the ensemble of simulations from different models allows the degree of confidence in predictions to be assessed. Such analysis allows statements such as those from the IPCC that "The global mean surface temperature change for the period 2016–2035 relative to 1986–2005 will likely be in the range of 0.3 °C to 0.7 °C (medium confidence)".

ESMs are very computationally expensive, and have only recently been developed; as such they have never yet been applied in the context of nuclear wastes.

2.3.3 General Circulation Models (GCMs)

GCMs are the longest-standing tools in climate science. They are similar to ESMs, but typically just represent the atmosphere, ocean, and land surface. ESMs have been developed from GCMs just in the past 5 years or so. Because they represent a subset of the Earth system, typically GCMs may run at a higher spatial resolution than the equivalent Earth system model. Some GCMs are not global, but represent a limited region of the earth, at very high spatial resolution. Such GCMs are called Regional Climate Models (RCMs), and are forced at their lateral boundaries by observations or outputs from a global GCM. The benefit of Regional Models is that the high resolution allows better representation of the boundary conditions, such as the underlying topography, and hence better representation of effects such as orographically-induced precipitation and rain shadows, and of dynamical processes such as storm tracks and hurricanes.

GCMs and Regional Models were used in the context of nuclear waste in the BIOCLIM project, where they were used to represent snapshots of extreme climates in the next 200 kyr (see Section 4.4). GCMs have also been used in the MODARIA project in an ensemble of simulations designed to represent a continuous climate evolution based on an emulator (see Section 4.5).

2.3.4 Earth system Models of Intermediate Complexity (EMICs)

EMICs sit between conceptual models and GCMs / ESMs in the climate modelling spectrum. They typically represent all aspects of the Earth system, but do so at a reduced complexity and resolution compared with ESMs and GCMs. The reduced complexity means that their predictions are associated with lower confidence, but they are sufficiently computationally efficient that they can typically be run over ten’s of thousands of years or more. EMICs are very variable in the degree to which they simplify the key processes. Many EMICs simplify the atmospheric circulation considerably. Some use an energy-balance atmosphere with no explicitly resolved dynamics (e.g. GENIE, http://www.seao2.info/mycgenie.html), or use the quasi-geostrophic approximation (e.g. LOVECLIM; Goosse et al. 2010). Others solve the fundamental Navier Stokes equations, but do so at a greatly reduced resolution (e.g. FAMOUS; Smith et al. 2008).

3 Previous simulations of the last 2 million years

The study of past climate evolution over multiple timescales can provide considerable insights into future climate evolution, by improving understanding of the principal features of long-term climate and the forcings and feedbacks that drive and mediate them. In addition, paleo-proxy data for a number of climatic variables provides a method for evaluating models and their simulations of past climates, which is not possible for simulations of future climate for which there is no data.

This section will provide a review of modelling studies that simulate the evolution of past climate, taking into account their uncertainties. Focus will be first on snapshot simulations of specific periods in the Earth's recent history (Last Glacial Maximum, mid-Holocene and last interglacial; Section 3.1) and then on transient model simulations of three approximate timescales (20 kyr, 200 kyr and 2 Myr before present (BP); Sections 3.2, 3.3, and 3.4 respectively). These timescales, which roughly equate to studies of the last deglaciation and Holocene, the last glacial cycle, and the glacial-interglacial cycles of the Pleistocene respectively, are chosen because the dominant forcings of climate and the commonly used modelling tools are different for each timescale.

3.1 Snapshot simulations during the last glacial-interglacial cycle

The Paleoclimate Model Intercomparison Project (PMIP, https://pmip4.lsce.ipsl.fr) represents a concerted effort by modelling groups around the world to simulate the climate of various key periods in the Earth's recent history. These experiments use standardised sets of boundary conditions to define experiments that allow models to be intercompared, and to be compared with proxy reconstructions of the periods, and therefore allow the strengths and weaknesses of models to be ascertained. PMIP is currently on its 4th phase (https://pmip4.lsce.ipsl.fr), and has consistently contributed to the IPCC process, including the most recent (5th) IPCC assessment report, AR5. The first phase of PMIP (Joussaume and Taylor 1995) included 12 atmosphere-only or slab ocean GCMs to simulate the LGM, forced by the ICE-4G ice sheet reconstructions (Peltier 1994) and CLIMAP (1981) SST reconstructions, with no changes in vegetation or dust fluxes. The second phase (PMIP2; Braconnot et al. 2007) included fully coupled GCMs (of generally the same complexity as the IPCC models of the time), updated ICE-5G ice sheet reconstructions (Peltier 2004), updated greenhouse gas (GHG) scenarios, and some simulations with dynamic vegetation models. PMIP3 consisted primarily of models that contributed to CMIP5, and included more forcing parameters with the aim of improving understanding of climate sensitivity and natural climate variability (Braconnot et al. 2012). Three main time periods contributed to the IPCC AR5: the Last Glacial Maximum (LGM; approx. 21 kyr BP), the mid-Holocene (MH; approx. 6 kyr BP) and the last millennium (850–1850 CE). Additionally, other periods were modelled outside of these including the last interglacial (LIG; approx. 130–115 kyr BP) and mid-Pliocene (3.3–3.0 Myr BP).

While there are stand-alone studies of the LGM climate using EMICs, such as the early work of Ganopolski et al. (1998) using the EMIC CLIMBER-2, here the focus will mostly be on the simulations that have been carried out as part of the PMIP projects, which primarily uses GCMs and ESMs. Being part of PMIP ensures there is consistency in the simulation setup allowing models to be easily compared and a consistent level of complexity (i.e. atmospheric-only GCM (AGCM) or fully-coupled atmosphere-ocean GCM (AOGCM)). Focus on studies carried out in the framework of PMIP in this report also allows inter-model dependence to be assessed, as highlighted in Section 2.3.2. Given the interests of Nagra, we focus on global mean trends and the results for the European region.

3.1.1 Last Glacial Maximum

At the Last Glacial Maximum (LGM; 21 kyr BP), carbon dioxide concentrations were close to their minimum value over the last 800,000 years (~ 190 ppmv, Luthi et al. 2008), global mean temperatures were reduced, large ice sheets had expanded over North America and Eurasia and glaciers and ice sheets expanded in other regions. Climatic changes resulted in a modified vegetation distribution with reduced forests and increased tundra and steppe over Northern Hemisphere continents. However, beyond these broad changes there were subtle regional patterns of change and interconnected processes and feedbacks shaping the Earth system that require the use of models to understand.

Kageyama et al. (1999) offer one of the earliest syntheses of the PMIP1 results, comparing the changes in Northern Hemisphere storm tracks in different AGCMs caused by the presence of the North American and Fennoscandian ice sheets. They find a consistent change across the models, with an eastward shift in both Atlantic and Pacific storm tracks associated with changes in atmospheric stationary waves and sea ice, which affects precipitation in northwest Europe. How much the storm tracks vary is somewhat model dependent, especially at their eastward extremities. Model resolution is found to be important for the simulation of storm tracks, and these simulations would now be considered relatively low resolution.

Kageyama et al. (2001) analyse the PMIP1 simulations specifically over Europe and western Siberia. Proxy reconstructions point to a 10–15 °C cooling in annual mean temperature over western Europe, 10–20 °C cooling over central Europe and up to 10 °C cooling over western Siberia compared to the present day. The model ensemble generally captures these changes, with variability between the models comparable to the uncertainties in the reconstructions. However, models are found to be too warm over western Europe, particularly in winter, by up to 10 °C. There is a much larger spread in precipitation from the models, compared to temperature. Although the general pattern of the LGM being drier than the present over all of Europe is captured, western Europe is found to be too wet compared to reconstructions. They note that possible causes for the discrepancies in temperature and precipitation could be the ice sheet reconstructions, SST reconstructions (as these are all AGCMs or slab-ocean models with no changes in ocean circulation), vegetation, dust or permafrost changes. They suggest that none of these missing processes will likely solve the issue of model biases over western Europe on their own; instead, some combination of missing processes is believed to be important.

Jost et al. (2005) test if any of three different approaches for increasing model spatial resolution reduce the model biases of the European LGM climate found by Kageyama et al. (2001). The three approaches they use are an AGCM (LMDZHR) with a zoomed grid over Europe, an AGCM with globally high resolution (CCSR1), and a high-resolution regional climate model (RCM; HadRM) nested in a lower resolution AGCM (HadAM3). These were compared to low-resolution simulations with the same models. The AGCMs are found to offer no improvement in the temperature biases over the lower resolution equivalents, but to improve precipitation trends (due to better resolved orography etc.). The RCM was found to improve the temperature bias, but has a very poor representation of the hydrological cycle. These results suggest it is not simply model resolution that limits performance in reconstructions, although this can lead to some improvements e.g. in precipitation. Missing processes such as evolving SSTs, vegetation and permafrost are highlighted as likely being important.

Braconnot et al. (2007) and Kageyama et al. (2006) review the progress of PMIP1 and PMIP2 simulations globally and over the North Atlantic/Europe area respectively. Braconnot et al. highlight that the model spread increases in the coupled PMIP2 simulations compared to PMIP1 because the SSTs and sea ice are no longer constrained. They find there is a greater cooling at the tropics as well as changes in the Northern Hemisphere due to the updated ice sheet configurations (Peltier 2004). Kageyama et al. focus on the SSTs and SATs of the North Atlantic and European region compared to MARGO (Multiproxy Approach for the Reconstruction of the Glacial Ocean surface, http://margo.pangaea.de/) SST and pollen-based SAT reconstructions. In the North Atlantic, the models are found to correctly simulate an increase in the meridional SST gradient (but not necessarily with the correct amplitude or location). The improvement of the ice sheet reconstructions from ICE-4G in PMIP1 to ICE-5G in PMIP2 improves the PMIP2 SAT distribution compared to PMIP1, but winter temperatures are still too warm particularly over western Europe in winter, shown in Figure 3.1. Reconstructions suggest temperatures over the Alps cooled more in the winter (by up to approx. 20 °C) than in the summer (up to approx. 10 °C cooling), but the models struggle in this region to capture the winter temperature anomalies in particular. Western Europe's temperature is strongly affected by oceanic changes and simulated sea ice varies significantly between models, meaning there is a larger spread for fully coupled models. They highlight an increase in inter-annual variability in cold month temperature and suggest that this could be biasing proxy reconstructions.

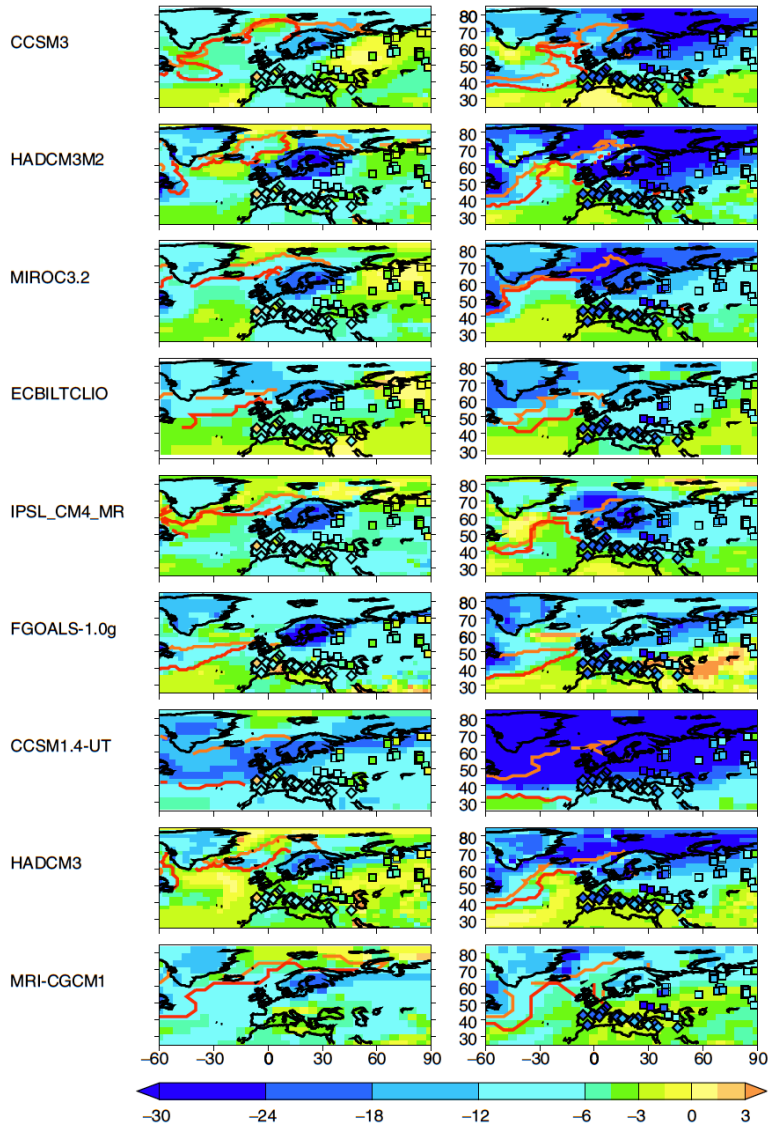

Fig. 3.1: Warm month (left hand column) and cold month (right hand column) temperature anomaly of the LGM relative to 1960-1990 for 9 PMIP2 models.

Squares and diamonds show observational data points. The orange contour shows the pre-industrial sea ice extent and the red line the LGM sea ice extent. Figure from Kageyama et al. 2006.

Ramstein et al. (2007) further investigate the results of Jost et al. (2005) and Kageyama et al. (2006) in an attempt to reconcile the temperature anomaly over western Europe. They find that dynamic vegetation in the models can account for up to 2 °C of cooling, but this is heterogeneous and other processes must also be important. They assess the impact of increased climatic variability (in terms of precipitation and cold month temperature) and CO_2 changes on the vegetation distribution and show that the latter particularly could be having an effect at the LGM. Using inverse modelling accounting for the effect of lower CO_2, they suggest that the error on proxy temperature reconstructions should be larger, bringing more consistency between the model results and observations.

The PMIP3 ensemble of simulations is presented in Harrison et al. (2014), wherein a comprehensive global model-data comparison is carried out. This model-data comparison is also summarised in the latest IPCC AR5 report (Section 9.4.1.5). This shows that even in the very latest climate models, there is still a warm bias in western Europe in winter, although the error bars on the paleo proxy reconstructions are large.

Zhang et al. (2013) highlight concerns that in the PMIP3 standard of models, initialisation of the ocean can lead to fundamentally different ocean states with a knock-on effect on the oceanic response to melt-water forcing. They use the model COSMOS (a coupled version of the ECHAM5 atmosphere, MPI-OM ocean and JSBACH vegetation models) initialised with glacial and pre-industrial ocean states. Although both models reach the PMIP criteria for steady state in the surface ocean (and hence would be eligible for inclusion in PMIP), they have very different stratification structures and respond differently to large freshwater inputs. They find it is not possible to force the model from one state to the other (e.g. with a large input of freshwater) and the bistability depends only on the initial state. When initialised with glacial conditions, North Atlantic Deep Water (NADW) is shallower and shows an overshoot of the Atlantic Meridional Overturning Circulation (AMOC) after a freshwater input takes place. This response was also found in the HadCM3M2 and CCSM3 PMIP simulations, which were also set up with glacial initial conditions.

Hargreaves et al. (2013) offer a quantitative statistical analysis of the simulated temperature from nine PMIP2 and two PMIP3 models for the LGM, compared with approximately 400 gridded data points over the land and ocean. The data (MARGO 2009; Bartlein et al. 2011) have errors in the range of 0.24–6.4 °C, but generally between 1–2.5 °C. They find the PMIP results for the LGM are generally in good agreement with the data, with qualitative trends captured with quantitatively reasonable magnitudes. Major patterns such as the land-ocean contrast and polar amplification are also captured. However, sub-continental scale features from the data are not simulated as strongly, with some features potentially lost due to low model resolution not capturing local orographic effects.

Ludwig et al. (2016) identify similar atmospheric circulation changes over Europe in four PMIP3 LGM simulations (from the models CCSM4, MIROC-ESM, MPI-ESM-P and MRI-CGCM3) as Kageyama et al. (1999) did with PMIP1 models. They show that during the LGM, western Europe was influenced by a stronger North Atlantic storm track producing prevailing circulation weather types from the west (similar to today) that enhanced rainfall. Central and eastern Europe were more affected by southerly and easterly flow patterns causing them to experience less rainfall, as shown in Figure 3.2. The Alps see a fractional drying on average in these four simulations, but the magnitude is small and on the margins of statistical significance (insignificant grid cells are indicated in Figure 3.2 by small black circles). The improvement in representation of strom tracks compared to PMIP1 is evident, highlighting the importance of model complexity and resolution. Analysis of the LGM precipitaiton and atmospheric circulation was also carried out by Hofer et al (2012a), who, using a high resolution version of CCSM4, showed that the presence of the Laurentide ice sheet resulted in a transition from north-south sea level pressure gradients to more west-east gradients, and that the resuting change in circulation type accounted for 60% of the precipitation change in southwest Europe at the LGM. Hofer et al (2012b) showed that the Laurentide ice sheet led to a southward displacement of the jet stream and the storm track in the North Atlantic region, generating a band of increased precipitation in the midlatitudes across the Atlantic to southern Europe in winter.

3.1.2 Mid-Holocene

The mid-Holocene (MH; 6 kyr BP) is another period modelled in the PMIP experiments, and, like the LGM, has been a part of PMIP since its conception. The MH differs from modern in terms of climate forcing through its astronomical forcing. Changes primarily in precession mean that it experienced relatively high insolation in Northern Hemisphere summer compared to modern. Other boundary conditions, such as CO_2 and ice sheets were very similar to those of pre-industrial. The MH is characterised as a relatively stable climate, but one in which the Earth system responded to the astronomical forcing with significant changes in temperature, precipitation, and vegetation compared to modern (Prentice et al. 2000; Braconnot et al. 2012). Studies specifically focussing on the MH using EMICs and GCMs/ESMs will be discussed here, although other studies with simpler models occasionally simulate this period to benchmark against GCMs (e.g. Crucifix et al. 2002).

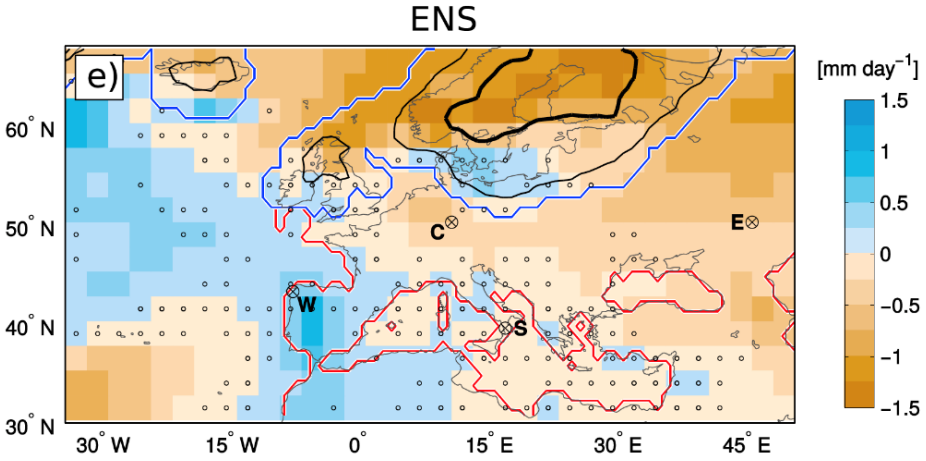

Fig. 3.2: Changes in the daily mean precipitation over Europe from four PMIP3 models.

Black circles show grid cells where the mean is not statistically significant. Blue and black contours mark ice sheet extent and thickness (thin black line at 500 m, bold black line at 1500 m) and the red contour shows the LGM coastline. Figure from Ludwig et al. 2016.

Ganopolski et al. (1998) model the MH using CLIMBER, a low resolution 2.5D coupled atmosphere-ocean-vegetation EMIC. By including components individually or in different combinations (atmosphere only, atmosphere and ocean, atmosphere and vegetation or all three components together) they show that all the model components act synergistically to reproduce the best approximation of the MH climate. With all three components, there is an increase in summer and winter temperatures by 4 °C and 3 °C respectively for Northern Hemisphere continents. This is caused by vegetation changes that affect planetary albedo and have a further effect on sea ice extent. Warming in the Southern Hemisphere is then caused by a reduced AMOC (due to temperature and salinity changes in the North Atlantic). The model suggests that the areas most sensitive to change in the MH are the high northern latitudes, the subtropics (particularly the Sahara) and the Atlantic.

Masson et al. (1999) analyse the PMIP1 results for the MH over Europe. Reconstructed vegetation changes suggest there were warmer, drier conditions in north western Europe and cooler, wetter conditions in southern Europe (particularly in summer) relative to the pre-industrial (i.e. a reduced climatic gradient across the continent). In lower latitudes, the models all agree on major cooling but over Europe there is larger uncertainty. The cooling over southern Europe is not captured well by the PMIP1 ensemble, but the warming in the northeast and some of the hydrological changes are captured by some models. Indeed, there is no consistency as to how the European temperature gradient changes in the models. The simulation of precipitation anomalies is slightly better, but the modelled and reconstructed seasonalities differ and there is still little spatial consistency between the models. It is concluded that processes are missing that influence the European climate. The lack of interactive vegetation and SSTs in the Atlantic and Mediterranean could be impacting on the temperature, while increased resolution could improve the simulated precipitation.

Bonfils et al. (2004) investigate the mechanisms behind the PMIP1 models that performed better over Europe using a cluster analysis. This analysis also investigated whether a model could simulate the correct response and mechanisms, but simply in an incorrect region. They identify two potentially important processes for representing the changes in the MH reconstructions. The first is increased westerly airflow relative to the present from southwest Europe toward the north east over winter. This accounts for the seasonal temperature (warming northern Europe in winter) and water budget changes identified in reconstructions. The second process is increased latent cooling in the summer due to increased winter soil moisture. This can reduce the warm summer anomaly over southern regions in the models relative to reconstructions, but requires the spatial distribution of precipitation to be accurate, which is a challenge for models of this age and resolution. They argue that the models are correctly simulating the gross climatic structures, but a lack of processes and resolution can mean that the models produce the climatic zones in slightly incorrect areas, making their performance relative to reconstructions appear biased.

Braconnot et al. (2007) also discuss the MH ensemble of simulations from the PMIP1 and 2 experiments. The general patterns in temperature are increased seasonality and summer warming over Northern Hemisphere continents. The Alps lie on the fringe of this warming, as it is less pronounced over the oceans and coastal regions. This seasonality change is due to changes in insolation and has a positive feedback with reduced sea ice extent. Changes in vegetation over the Sahara and other desert regions are due to enhanced monsoons and vegetation feedbacks, however, precipitation change is still underestimated. Over Europe no significant consistent change in precipitation is found in the models.

Brewer et al. (2007) carry out a similar analysis to Bonfils et al., using cluster analysis and fuzzy logic to compare three environmental parameters (moisture availability, cold month temperature and growing degree days) from 25 PMIP models to observations. The observational dataset is updated from Bonfils et al., but still shows the same reduced temperature gradient. Generally, the clustering in the models is similar and although the exact patterns and magnitude of change vary and are usually less than the reconstructions, models do project the correct sign of change. They do not find an obvious distinction between the PMIP1 and PMIP2 simulations, but find that higher resolution or less parameterised versions of the same model usually perform better.

Mauri et al. (2014) compare 14 PMIP3 GCMs to a large observational dataset for Europe. Previous studies (e.g. Bonfils et al. 2004) had suggested the winter climate anomalies in the reconstructions resembled increased westerly circulation (caused in the modern day by positive Arctic Oscillation/North Atlantic Oscillation (AO/NAO) modes), while summer anomalies

resembled modern day anticyclonic blocking events over northern Europe. The data set of Mauri et al. supports these two mechanisms. However, they show the PMIP3 models do not capture these circulation changes and temperature anomalies are instead driven most directly by insolation changes, resulting in poor representation of the spatial pattern of anomalies for the MH.

3.1.3 Last interglacial

The last interglacial (LIG or Eemian; 130–115 kyr BP) was the last period of reduced glaciation prior to the Holocene, compared to which it had a notably different climate (increased warming at high latitudes and increased global sea levels). The differences between the LIG and pre-industrial are primarily driven by insolation changes associated with astronomical forcing. It has attracted attention from modelling communities (e.g. PMIP3) as it is a good test for models in terms of representing a warm world with reduced ice sheets, but with different dominant driving factors compared to the future (in contrast to the future, CO_2 concentrations during the LIG were very similar to those of pre-industrial). The LIG has been modelled in a variety of ways, for example modelling the transient climate evolution and reglaciation through the LIG, snapshots of the climate as part of PMIP, or ice sheet modelling to assess the sources of sea level change (in particular, Greenland vs. Antarctica).

There are several simulations of the LIG using EMICs, which can be helpful for understanding how the climate transiently evolved over the period. One example is Crucifix and Loutre (2002) who use MoBidiC to simulate the period 126–115 kyr BP. They find climatic shifts through the period such as a precession-driven cooling over land between 122–120 kyr BP that results in some perennial snow accumulation, a southward shift of the northern treeline and increased sea ice. Snow, sea ice and vegetation feedbacks are found to be more important for driving the climate (nearly quadrupling the initial insolation forcing) than oceanic interactions. There is a small decrease in the North Atlantic overturning over the whole period, but this has little effect on Northern Hemisphere heat balance.

Stone et al. (2013) model the climate of the LIG using interpolated snapshots from the GCM HadCM3, primarily with the aim of forcing an ice sheet model (GLIMMER) over Greenland. Using a Latin Hypercube approach to cover the sensitivity to parameter uncertainty in the ice sheet model, they assess probabilistically how much of the Greenland ice sheet (GrIS) melted during the LIG. The interpolation of climate was done linearly between three orbital snapshots (at 120, 125, 130 kyr BP), each with three ice sheet states. Globally the climate is found to be marginally (0.13 °C) warmer than the pre-industrial, and is warmest at 130 kyr BP before cooling at 120 kyr BP. Over Greenland it is found to be around 3.5 °C warmer than pre-industrial, slightly less than proxies suggest (4–5 °C). However, with relatively few model simulations it is hard to account for uncertainties in the non-interactive vegetation, constant CO_2, etc. Feeding into the ice sheet model, they find there is a 90% probability melt was in the range 0.6–3.5 m of sea level equivalent, less than some other reconstructions (0.4–5.5 m). The most likely scenarios (based upon their representation of the modern ice sheet) show a 1.5 m sea level change and suggest the GrIS melts from its northern margin. This sea level change is not as much as records suggest, implying there must be additional sources of melt (e.g. from Antarctica or other glaciated regions).

Lunt et al. (2013) carry out a large intercomparison of snapshot simulations covering the period 130–125 kyr BP, including PMIP3 models and other experiments of lower complexity (11 GCMs and 3 EMICs). Because some of the simulations were carried out independently from PMIP, they do not all have the same boundary conditions, but this still offers a useful comparison of PMIP and non-PMIP model performance. Each model provides up to four

simulations with different boundary conditions or time slices (e.g. 130, 128 and 125 kyr BP). Because the insolation forcing of the LIG is seasonal, there is relatively little change in the annual mean values in the models and they are model dependent. This contrasts with reconstructions, which suggest there can be some large annual temperature anomalies, as shown in Figure 3.3. Seasonally the signal is stronger in the models, with summer warming in Northern Hemisphere mid-high latitudes and general cooling in winter (December-January-February; DJF). The modelled changes in the seasonal cycle are closer to the observations, but still have relatively little skill. Finally, an important conclusion is that the GCMs produce more complex and different responses compared with the EMICs (beyond just resolution differences), with less warming at high latitudes and more cooling in the African monsoon region than the EMICs. This suggests that there is considerable added-value in using GCM compared with an EMIC for modelling the LIG.

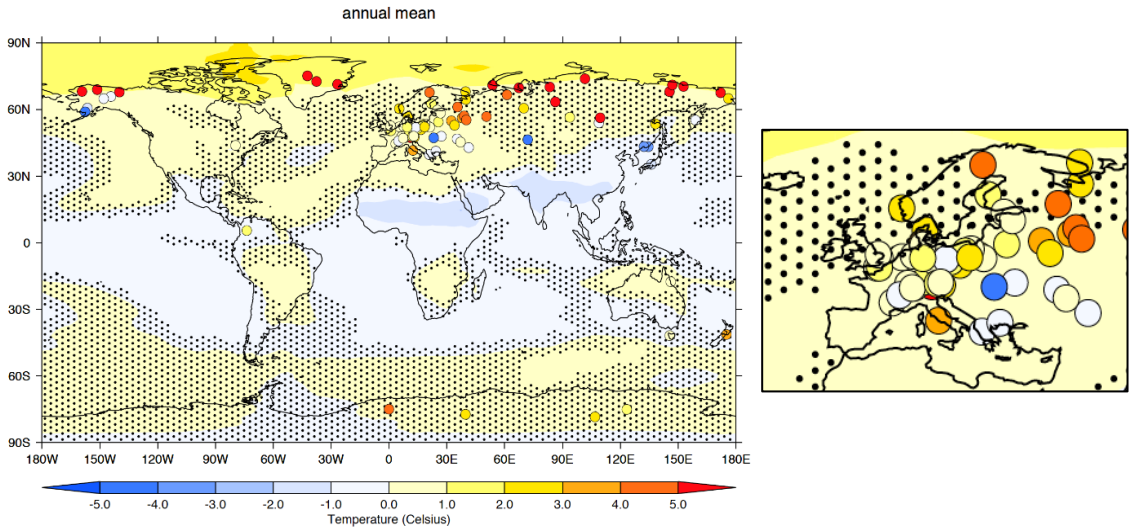

Fig. 3.3: Annual mean temperature anomaly at the LIG from a 14 model ensemble compared to the pre-industrial.

Data points are indicated by the coloured circles and stippling shows where less than 70% of the models agree on the direction of change. The smaller map is simply an enlargement of Europe. Figure from Lunt et al. 2013.

Bakker et al. (2013) carry out a similar intercomparison to Lunt et al., but focus on transient simulations of the LIG provided by 4 low-resolution GCMs and 3 EMICs covering the period 130– or 126–115 kyr BP. Although models struggle to capture spatial trends and magnitudes (Lunt et al. 2013), they do a reasonable job at capturing the temporal evolution through the LIG when and where it is driven by insolation. For example, a robust July temperature peak (ranging 0.3–5.3 °C) is found between 130–125 kyr BP, and a robust January temperature peak is found over the Arctic Ocean at 128–126 kyr BP and over Northern Hemisphere mid-latitudes between 121–117 kyr BP. Some aspects are not captured so well, when other processes besides insolation are important. For example, Southern Hemisphere temperature trends are captured better when GHGs are varied through the simulation and January temperatures at high northern latitudes are strongly influenced by highly model dependent sea ice changes. In contrast to Lunt et al. (2013), EMICs are found to adequately capture the long timescale (> 1 kyr) and large spatial trends (comparably to GCMs), suggesting they are better suited for this kind of analysis.

Various studies aim to understand the differences between proxy reconstructions and individual models. Due to the model-specific nature of these studies, they will be discussed only briefly. Nikolova et al. (2013) discuss snapshot simulation results from LOVECLIM and CCSM3 coupled to the vegetation model BIOME4. Their analysis of the climate is similar to the previous studies mentioned, but they do comment on the simulated vegetation over Europe from the two models. CCSM3-BIOME4 suggests there is more grassland over Europe compared to LOVECLIM, likely due to the relatively cool and dry climate simulated over the region. LOVECLIM generates warmer and more wet conditions in the region and as a result simulates more mixed forest, which is in line with vegetation reconstructions. Langebroek and Nisancioglu (2014) analyse six time slices from NorESM and show that seasonal changes are induced by the insolation forcing but GHGs are more important for global and annual mean changes. They suggest the mistiming of summer warmth in the Southern Ocean and Antarctica relative to the summer insolation peak is due to the ocean storing and integrating heat from other seasons, not just summer. Finally, Pedersen et al. (2016) use snapshots from the GCM EC-Earth with various prescribed boundary conditions to assess the direct and indirect (e.g. through ocean interactions) effects of insolation change. Through this they find that the changes in the tropics (a year-round cooling compared to the pre-industrial) are caused predominantly by insolation changes, while indirect effects of the insolation forcing on sea surface conditions are more important for the North Atlantic and European regions. This model is relatively high resolution compared to other PMIP models and is also exhibits an annual mean warming at the higher end of the PMIP model range.

Two other studies of interest include Loutre et al. (2014) and Pfeiffer and Lohmann (2016), who assess the importance of boundary conditions changes related to the GrIS at the LIG. Loutre et al. (2014) assess transient simulations of LOVECLIM and suggest that the presence of ice sheets and freshwater input to the North Atlantic from their melt could be important for the simulated climate. Generally, the magnitude of climatic change is too low and the summer temperature peak over the North Atlantic (at approx. 128 kyr BP) is too early compared to the reconstructions. Freshwater input can be a possible method for delaying the warming peak by causing a slowdown of the AMOC. This mechanism could be investigated in future studies. Pfeiffer and Lohmann (2016) assess the impact of the thickness and extent of the GrIS on the global and regional temperatures using a series of snapshot simulations with the GCM COSMOS. Major reductions in the size of the GrIS can result in additional warming in winter of up to 5 °C regionally and 0.48 °C globally. The effect is less pronounced in the summer, causing 0.24 °C of global warming. Although this generally improves the match of the model to the data, the magnitude of temperature change relative to the pre-industrial is still underestimated globally and is overestimated in Greenland compared to ice cores. They argue that there is likely a seasonal bias in the proxies and additionally a transient simulation with evolving ice sheet dimensions (which is not yet computationally possible) could help address these data mismatches.

Finally, Stone et al. (2016) provide a possible reconciliation of models and data during the LIG. They show that the relatively cool temperatures in the North Atlantic in the early LIG, which are not seen in simulations forced solely by insolation and GHG changes, can be explained by freshwater input in the North Atlantic associated with melting of remnants of the Laurentide ice sheet following the previous deglaciation. The freshwater leads to increased buoyancy of surface waters, a reduction in deepwater formation in the North Atlantic, a decrease in strength of the meridional overturning circulation and associated northwards heat transport, and therefore a cooling in the North Atlantic. Furthermore, Capron et al. (2014) in a related study show that great care must be taken in the interpretation of proxy records of the LIG for model-data comparison, in particular regarding their age control.

3.2 Transient simulations of the last 20 kyr

Studies of the past 20 kyr cover the last deglaciation and the Holocene. As the climate warmed from the LGM through to the end of the Pleistocene (approx. 11.7 kyr BP) the Northern Hemisphere ice sheets collapsed, but the warming and collapse was not spatially homogenous or monotonic in time. There were significant sub-millennial scale fluctuations and longer events superimposed on the cooling trend recorded over Greenland and Antarctica, as shown in Figure 3.4a. Sub-millennial events included Dansgaard-Oeshger (D-O) events (short warming spikes followed by prolonged cooling in the Northern Hemisphere) and Heinrich events (large ice loss events often preceding D-O events). Longer periods of change include the Bølling-Allerød (B-A; a phase of substantial warming around the North Atlantic region) and Younger Dryas (YD; a phase of cooling and minor reglaciation in the Northern Hemisphere). These events often have contrasting responses in the northern and southern hemispheres, linked to the idea of the bipolar seesaw (Crowley 1992; Stocker 1998).

After the deglaciation was complete (approx. 11.7 kyr BP), the Earth entered the relatively stable period (in terms of climate, CO_2 etc.) known as the Holocene, shown in Figure 3.4b. Temperatures generally rose to a maximum around the MH, after which there was a small gradual cooling. Climatic variations over the past one or two millennia up to the mid-19th century (e.g. the Medieval Warm Period, MWP; and the Little Ice Age, LIA) were relatively small (approx. < 0.5 °C) compared to the longer timescales considered in this report as shown in Figure 3.4c, but are still important to understand. Over this period, fluctuations in total solar irradiance (TSI) and the impact of volcanic events for example can be analysed, before the effects of anthropogenic CO_2 emissions become important for climatic change since the 19th Century.

20 kyr is at the limit of the time period that is possible to model transiently with a fully coupled GCM, meaning simulations discussed here are often of shorter sections of the period (e.g. only of the last millennium or deglaciation) or use accelerated GCMs, EMICs or conceptual models. Transient simulations that will be discussed here are those that fall wholly within the past 20 kyr BP. Longer simulations that cover this period but extend further back in time (e.g. 120 kyr BP – present) are discussed in the next section. Over this period, simulations can be compared to ice core records from around the world (GrIS, Antarctic ice sheet (AIS) as well as other glaciated regions), as well as tree ring records and historical documents for more recent periods. Shorter simulations of the last millennium (often from PMIP) will be discussed first, followed by simulations of the deglaciation and whole Holocene period.

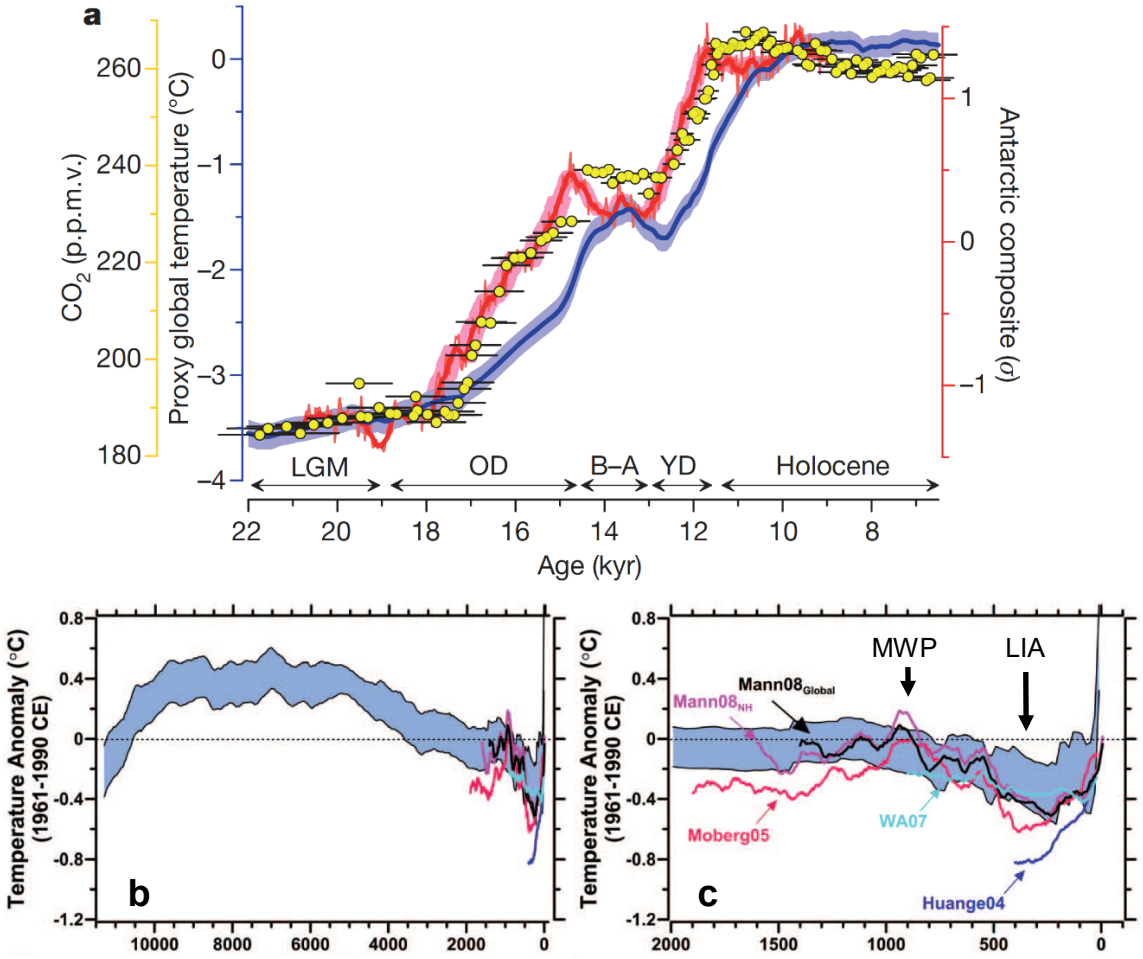

Fig. 3.4: Global proxy temperature stack and temperature anomalies of the Holocene and last two millenia.

a) A global proxy temperature stack (blue), Antarctic temperature record (red) and atmospheric CO_2 record (yellow dots) of the last deglaciation relative to the early Holocene mean (figure from Shakun et al. 2012). Major stages of the deglaciation are shown along the bottom: the Older Dryas (OD), the Bølling-Allerød (B-A) and Younger Dryas (YD). b & c) temperature anomalies of the Holocene and last two millennia respectively relative to 1961-1990 observations for a global stack (blue shading) and various other reconstructions (coloured lines) (figures from Marcott et al. 2013). The Medieval Warm Period (MWP) and Little Ice Age (LIA) have been annotated.

3.2.1 Last millennium

Crowley (2000) uses a simple vertically-averaged energy balance model of the ocean mixed-layer and atmosphere, coupled to a deep ocean store with a diffusion/upwelling equation to assess the impact of forced variability from TSI, volcanic and CO_2 changes over the last millennium. Results show that 41–64% of the variance between 1000–1850 CE can be explained by changes in TSI and volcanic forcing, with only modest contributions from CO_2 (0.05 °C). Other processes, such as changes in ocean circulation, appear to have played less of a role than TSI and volcanism in dictating events such as the MWP and LIA, with volcanism appearing to have been particularly important for the LIA.

Servonnat et al. (2010) use the fully coupled GCM IPSLCM4 to explore the effects of TSI, CO_2 and orbital changes over part of the last millennium (compared to static pre-industrial forcing). Like Crowley (2000), they find TSI is an important driver of the climate over this period (accounting for up to 59% of the low frequency variability), but unlike Crowley also find CO_2 to be important (particularly for the LIA), with volcanic forcing more important for annual and decadal variability. They find that no single forcing explains the signal as well as combined forcings and that these scale roughly linearly. They also show that, although the MWP and LIA stand out as hemispheric signals, events on a scale smaller than e.g. Europe will not be possible to pick up, highlighting the difficulties in modelling even relatively recent and well-constrained time periods.

Jungclaus et al. (2010) use the ESM MPI-ESM (which includes land surface, carbon cycle and ocean biogeochemistry modules) to run an ensemble of simulations through the last 1.2 kyr forced by TSI, volcanism, orbital insolation, GHGs, aerosol and land cover changes. Trends for the Northern Hemisphere climate are identified by the ensemble within the reconstruction uncertainty. They find that volcanism is important to events such as the LIA and that the simulated carbon cycle is not as dynamic as observations. Fluctuations in CO_2 are not driven solely by temperature and other processes must be important but are missing from the model. They acknowledge that these results will likely be model specific.

Fernandez-Donado et al. (2013) offer an overview of the PMIP3 simulations of the last millennium. Based upon 26 simulations from 8 different models there is broad agreement in the major hemispheric temperature trends and an approximately linear response to forcing at multi-decadal and lower frequencies. However, the spatial distribution of changes at the MWP and LIA are found to disagree with reconstructions and the models show different degrees of internal variability. For example, CCSM4 shows a larger variance in the Atlantic multidecadal oscillation (AMO) during the last millennium compared with the 1850 baseline, suggesting there is some long-term oceanic response to natural forcing (Landrum et al. 2013). However, CCSM4 shows no major changes in other internal variability such as the North Atlantic Oscillation (NAO), Southern Annular Mode (SAM), Pacific Decadal Oscillation (PDO) or El Nino – Southern Oscillation (ENSO), despite some proxies suggesting there could be long-term changes in the power of these oscillations (Landrum et al. 2013). Either the spatial patterns of the MWP and LIA temperature anomalies are influenced by internal variability (for which the models are inconsistent) or some other process that is not included in the models.

Berdahl and Robock (2013) look specifically at how the high Northern Hemisphere cryosphere responds to cooling events in five PMIP3 models. Generally, the models are not found to cool enough, reflected in the Baffin Island and North Atlantic region by a lack of snow accumulation and sea ice growth. The reason for the mismatch in cooling is either that the models do not respond strongly enough to forcing or they start with too warm a background climate prior to the cooling. CCSM4 produces the most snow accumulation and ice growth (in line with what reconstructions suggest), mainly because it is the model with coldest background state in the region. Additionally, Landrum et al. (2013) suggested that although CCSM4 captured the reconstructed changes at the LIA, such as drying in North America and cooling in Europe and North America, the model may be over-sensitive to large volcanic eruptions based upon its simulation of other events in the record. In general, the models do not sustain the cold temperatures after volcanic events for more than a decade, unlike reconstructions which suggest a long legacy from major events (Berdahl and Robock 2013). Clearly some processes are missing and this highlights the difficulties in modelling specific events in a relatively small region.

Atwood et al. (2016) analyse the forcings and feedbacks driving the LIA in seven PMIP3 models. They find that the volcanic forcing is most important (causing 65% of the total forcing effect), with land use, GHGs and insolation making up the rest of the forced variability. In total, forcings contribute 47% of change, with the rest due to feedbacks such as water vapour, snow-albedo etc. Two particularly large uncertainties they highlight with interpreting reconstructions of the last millennium are the characterisation of volcanic forcing (in terms of timing, location, magnitude of events and effect on the models' aerosols and radiative balance) and reconstructed changes in insolation (which could potentially have a much higher amplitude than imposed in these simulations and have an effect on ozone that is only included in a single PMIP3 model).

Yang and Jiang (2017) analyse changes in model inter-annual variability in temperature and precipitation, and compare how this variability changes between the MWP and LIA from ten PMIP3 models. Inter-annual temperature variation increases at high northern latitudes and precipitation variation increases at lower latitudes. Temperature variability generally decreases in the MWP and increases in the LIA, while precipitation variability generally does the opposite. Volcanic forcing has more of an effect on the variability of temperature than precipitation and this could explain why there is more temperature variability for the LIA (when there was increased volcanic forcing) compared to the MWP.

In summary, these model studies suggest that temperature variation during the last millennium was mostly driven by volcanic forcing, with TSI, GHG and other variations playing a lesser but still important role. However, there is still a large degree of uncertainty in the prescribed forcing schemes, models fail to capture the spatial patterns of change indicated by reconstructions and there is a large degree of inter-model variability in responses to forcings.

3.2.2 The Holocene and the last deglaciation

The deglaciation period at the end of the Pleistocene (Figure 3.4a) represents a complex challenge for modelling and data communities to understand. Changes in the global climate were substantial, asynchronous, and there are questions regarding leads and lags in the system. The initial trigger of deglaciation is an effect of insolation changes and is better understood as part of longer transient simulations, and so will be discussed in greater detail in the next section. However, asynchronous hemispheric events such as the Bølling-Allerød (B-A; approx. 14.5 kyr BP) are likely linked through changes in ocean circulation, specifically through fluctuations in the AMOC and have been the focus of numerous recent modelling studies. There are also studies into AMOC stability using idealised semi-empirical, EMIC and GCM modelling approaches (e.g. varying freshwater perturbations on an equilibrium climate, Renssen et al. 2002). Here, however, the focus is on some of the more realistic simulations of the last deglaciation.

Liu et al. (2009) use the fully coupled GCM CCSM3 to simulate the warming between the LGM and the B-A. The model is forced with varying insolation, GHGs, ice sheet sizes, coasts (in response to sea level change) and melt water fluxes. Between 22–19 kyr BP the modelled climate varies slowly with insolation. The extensive glacial state is associated with a reduced AMOC and shallower NADW relative to present. From 19–17 kyr BP the melt water forcing to the North Atlantic increases, causing the model to simulate a further slowdown of the AMOC. This results in a bipolar seesaw reduction in heat transport to the Northern Hemisphere (causing cooling of 4 °C) and an increase in heat transport to the Southern Hemisphere (causing a warming of 2 °C) in good agreement with proxy data. After 17 kyr BP the melt water forcing is decreased either linearly or in abrupt steps, in both cases causing an AMOC recovery and overshoot, which can account for the observed 15 °C temperature increase over Greenland at the B-A (approx. 5 °C of this is from the AMOC overshoot). Unlike previous studies using EMICs

(e.g. Ganopolski and Rahmstorf 2001) they do not find multiple equilibrium states for the AMOC. As a result, to fit the abrupt nature of the observed B-A warming there must be a rapid cessation of the melt water flux on the order of centuries. Simpler models that exhibit hysteresis in the AMOC can exhibit such behaviour under only a gradual forcing.

Knorr and Lohmann (2007) use an ocean model of intermediate complexity and find a similar AMOC overshoot to Liu et al., but with a different mechanism and forcing. Knorr and Lohmann find both a deepening of NADW and an AMOC invigoration, whereas Liu et al. only find an invigoration of the AMOC. As opposed to using an abrupt melt water forcing as in Liu et al., Knorr and Lohmann use a somewhat idealised gradual forcing (representing a linear deglacial warming) and find that a hysteresis effect causes the rapid warming. Although the forcing causes an increase in local ocean buoyancy, the model simulates a change in circulation that transports higher salinity water to the North Atlantic, countering the temperature effect on buoyancy. Once this overcomes the density gradient, deep-water formation occurs, resulting in greater transport of relatively saline water to the region and causing an AMOC overshoot. The inclusion of melt water fluxes into their model can vary and improve the timing of the overshoot so that it coincides with the B-A, but is not necessary to cause such a response. Barker et al. (2010) suggest there is evidence for an AMOC overshoot in some North Atlantic data, based on ^{14}C peak at a site that is currently poorly ventilated and mostly influenced by Antarctic bottom water. The peak suggests there was an intrusion of younger, better-ventilated, northern-sourced water due to an invigorated AMOC. This supports the plausibility of the responses found by Knorr and Lohmann (2007) and Liu et al. (2009), but it is unclear which mechanism is correct.

Shakun et al. (2012) extend the simulations of Liu et al. (2009) up to 6.5 kyr BP, with some additional sensitivity studies in which the forcing was solely CO_2 or orbits, that were run from 17–7 kyr BP. They find that, when all the forcing parameters (insolation, GHGs, ice sheets and melt water) are included, the model produces a good approximation of the global temperature record from a stack of 80 globally distributed sites. The stack shows slightly smaller amplitude variations in temperature compared to the model simulation. The sensitivity simulation with only CO_2 forcing does a better job capturing the temperature trend through the period than the simulation with orbital forcing only. Combined with their analysis of the stacked temperature and CO_2 records, which they suggest shows CO_2 leading temperature changes throughout the record apart from at the onset of deglaciation, this suggests CO_2 is playing a major role in driving the temperature over these timescales. However, neither of these sensitivity simulations capture the ocean circulation changes, showing the importance of melt water in the system.

He et al. (2013) build further upon Liu et al. (2009) and Shakun et al. (2012) by completely breaking down the relative contributions of orbital, GHG, ice sheet and ocean circulation changes across the last deglaciation (22–14.3 kyr BP) using CCSM3. Their simulation with all forcings does a good job of capturing the trends from the LGM through to the onset of the B-A and they find the Southern Hemisphere warming lead starts at 19–18 kyr BP, 1 kyr earlier than over Greenland. They find the last deglaciation was initiated by Northern Hemisphere insolation, with the early part of the record (22–19 kyr BP) matching the orbital only simulation best. This melt then caused a reduction of the AMOC resulting in greater Southern Hemisphere warming from 19–17 kyr BP, with the ocean circulation forcing simulation fitting the spatial and temporal trends of the data best. They propose this resulted in CO_2 degassing in the Southern Hemisphere, producing the global warming with a Southern Hemisphere lead seen throughout the rest of the temperature record (17–15 kyr BP), which fits best with the GHG forcing simulation. Shakun et al. (2015) built further on this work by using the transient simulations to compare local climate of glaciated regions, including the Alps, with moraine data. They found relatively early retreat of the Alpine glaciers, prior even to the CO_2 rise, and high sensitivity of the Alps to climate forcing compared to other glaciers.

After the end of the deglaciation, the Holocene was a relatively stable period, but there were still some significant differences relative to pre-industrial and some major events occurred, such as the desertification of the Sahara during the MH. Claussen et al. (1999) use the EMIC CLIMBER-2 to simulate from 9 kyr BP to the present, with changes in orbital forcing (which are relatively modest over the period) to assess non-linearities that could cause the vegetation of the Sahara to die back. They find that orbital cooling due to changes in perihelion and obliquity around the MH result in cooling in the high Northern Hemisphere, with subsequent feedback with sea ice and a southward migration of the northern treeline. This cooling affects the rest of the hemisphere, reducing the intensity of the African monsoon and causing a drying and loss of vegetation.

Crucifix et al. (2002) use the EMIC MoBidiC, a simple, zonally averaged quasi-geostrophic model with a vegetation model VECODE, to transiently model the last 9 kyr. Snapshot simulations give a reasonable but not perfect fit to observations, with oceans and heat transports like those calculated by GCMs. Over the past 9 kyr annual global mean SAT varies little (fluctuating between 14.55–14.65 °C) with a gradual general global cooling trend due to a non-linear response to obliquity and precession changes, similar to the compiled temperature record shown in Figure 3.4b. Associated with this there is a southward shift in the northern treeline, causing a 200 yr temperature lag relative to the forcing and a large cooling (up to 6 °C) over the high Northern Hemisphere during summer. This cooling is most pronounced after 4 kyr when 80% of forest change occurs. The system mostly remains close to equilibrium, as the changes in vegetation and ocean are relatively slow.

Lorenz et al. (2006) use an ensemble of six runs from an accelerated coupled GCM, ECHO-G, driven solely by insolation changes to simulate the climate of the past 7 kyr. They find heterogeneous cooling of 0.62–4.41 °C in the extra tropics and warming of 0.19–1.47 °C in the tropics over the whole period, with the zonal average broadly in agreement with alkenone based proxy reconstructions. Superimposed upon these general trends they find regional heterogeneities, which are the result of changes such as a weakening of the NAO. Although previous studies with EMICs capture the general trends, they do not identify these subtle (albeit model specific) details.

Timm and Timmermann (2007) simulate the last 21 kyr using an accelerated EMIC, ECBlit-CLIO (LOVECLIM), forced with changing ice sheets, GHGs and orbital configurations. The main aim of the study is to test the impact of the acceleration on the model output. Although some notable issues are identified, for example a damped response in the convective regions in the North Atlantic and bias related to uncertainties in the initial state, the model can capture the general Holocene trends assuming some degree of seasonal bias in the reconstructions. Timmerman et al. (2009) build upon the study of Timm and Timmerman with a more rigorous analysis of the model simulations. In contrast to other studies of the deglacial period, they find that orbital and CO_2 forcing in the Southern Hemisphere started deglacial warming, without a Northern Hemisphere trigger. This is due to insolation driven melt of Southern Ocean sea ice between 19–18 kyr BP, with an associated albedo feedback. They also suggest this could result in a warming-CO_2 release feedback that would exacerbate the change.

Zhang et al. (2016) model the past 11 kyr but focus analysis on the early Holocene from 11.7 – 7 kyr BP, a period over which there was a general warming trend following the end of the deglaciation. They compare proxy reconstructions with transient simulations from LOVECLIM and find that temperature changes are very heterogeneous in space and time. There is some evidence that the model summer temperatures agree better with the proxies, suggesting a seasonal bias in the proxies. Over Europe they find the SAT was 2–5 °C cooler than pre-industrial at 11.5 kyr, warming to a temperature maximum at 7.4 kyr BP. The cool climate of

Europe at the start of the simulation was related to the remnants of the ice sheets that had not fully melted, which had orographic and albedo effects as well as a feedback with the sea ice in the North Atlantic. Vegetation feedbacks also played a small role in affecting the continental temperature, for example over Siberia.

Bakker et al. (2017) attempt to reconcile systematic model underestimation of centennial to multi-millennial scale variability through the Holocene. Using a combination of models (the EMIC LOVECLIM providing the forcing for the ice sheet model PISM, which forces an ocean EMIC UVic), they show that fluctuations in the AIS could be responsible for amplifying low frequency processes of change through the period. Changes in the AIS affect the freshwater balance of the Southern Ocean and affect the formation of Antarctic bottom water, which has far reaching effects globally. These results suggest that reduced variability in transient model simulations could be due to the lack of interactive ice sheets in most simulations.

The Holocene represents a good test of climate models to subtle variabilities in the Earth system. Small changes in orbital insolation and GHGs require interactions from multiple components of the system (e.g. vegetation, ocean circulation and ice sheet dynamics) but models (under appropriate setups) can capture the broad changes in the system (e.g. hemispheric trends). However, more critical analysis shows that there are still problems with the simulations of the period, failing to capture consistent regional patterns (Lorenz et al. 2006), showing muted trends (Liu et al. 2014) and reduced variability (Bakker et al. 2017). Liu et al. (2014) critically analyse the results from three different modelling studies (Timm and Timmermann 2007; Liu et al. 2009; Smith and Gregory 2012). These studies suggested that although the annual mean temperature from the models did not reach a maximum at the MH, as shown in Figure 3.5, seasonally the spring temperatures did and therefore the proxy reconstructions were biased to spring temperatures. Liu et al. question that seasonal bias based upon updated analysis of reconstructions by Shakun et al. (2012) and Marcott et al. (2013), suggesting instead that the discrepancy could be due to a lack of sensitivity in climate models. Understanding of the Earth system through the Holocene is still not complete.

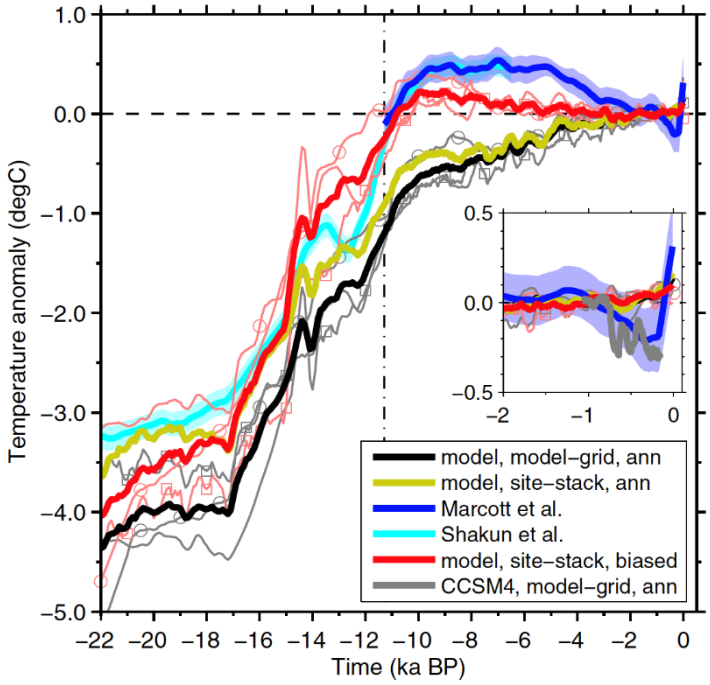

Fig. 3.5: Global temperature relative to pre-industrial from 22-0 kyr BP from two stacked reconstructions (blue lines; Marcott et al. 2013 and Shakun et al. 2012) compared with the annual mean temperature from several model simulations.

The reconstructions suggest a peak around 8-6 kyr BP when the models are still showing warming. Modelled spring temperatures show a similar trend to the reconstructions, questioning if there is seasonal bias in the proxies or insensitivity or missing processes in the models. Figure from Liu et al. 2014.

3.3 Transient simulations of the last ~ 200 kyr

The past 200 kyr covers changes in the Earth's climate over the past two glacial cycles. Explaining the approx. 100 kyr periodicity in ice growth punctuated by rapid deglaciations had been the focus of many studies for decades, particularly trying to identify non-linear interactions

that take place to amplify the 100 kyr eccentricity cycle. The longer time period mostly precludes the use of GCMs for transient simulations (although there are a few exceptions), meaning many studies of this time period use EMICs. There are also some studies that use snapshots of climate from GCMs through the glacial cycle focussing on periods outside of the traditional PMIP time periods (e.g. Pollard and Barron 2003; Singarayer and Valdes 2010). Records of this period come from polar ice cores, with GrIS cores such as NGRIP and NEEM extending through the last glacial cycle (NGRIP Community members 2004, NEEM Community members 2013) and from Antarctica such as Vostok and EPICA Dome C, which extend back 420 kyr and 800 kyr respectively (Petit et al. 1999; Augustin et al. 2004).

Berger et al. (1990) use a 2D model (latitude-height with only longitudinal sectors) to model the past 125 kyr under only an orbital forcing. The highly-parameterised model includes the atmosphere, upper-ocean, sea ice, ice sheets and lithospheric deformation, with the climate-ocean running asynchronously with ice-sheet model (i.e. the ice sheet model is run for 2 kyr then is used to update the atmospheric boundary conditions). The model can generally recreate non-linear amplification of the 100-kyr cycle taken from an equatorial Pacific core. The

magnitude of ice volume change during warm and cold periods of the glacial cycle is somewhat underestimated, likely due to the lack of other processes such as CO_2 change. The rapid deglaciation of the ice sheets is caused by reduced precipitation as they grow, leading to an albedo decrease through the ageing of snow. This makes the ice sheet more sensitive to insolation change and there are subsequent feedbacks that accelerate the deglaciation.

Gallee et al. (1992) use a 2D model for the past 122 kyr forced with both orbital and CO_2 changes. Once again, this model is highly parameterised (with no way to account for clouds, deep water circulation, moisture transport etc.) and it was slightly less sensitive to CO_2 perturbations than the GCMs of the period. The fit to the geologic record is improved with CO_2 inclusion, but orbital forcing has an order of magnitude more influence on the climatic variations. With just the orbit the temperature variations are too small, although the three Northern Hemisphere ice sheets evolve roughly in phase with geologic records. Both ice sheet growth and decline is shown to be non-linear. Increased ablation due to snow ageing is again found to be important for deglaciation, along with some reduction of accumulation through the 'desert altitude effect'. A complete deglaciation is only simulated when the bedrock is sufficiently depressed under a large ice sheet that the base of the ice sheet is situated at low altitudes (i.e. this only occurs at LGM and not at earlier insolation fluctuations).

Berger and Loutre (1997) expand upon the work in the two previous studies by simulating the past 200 kyr using the same 2D asynchronous climate-ice sheet model forced with orbital and CO_2 variations. As shown in Figure 3.6a, low frequency variability (> 5 kyr) is captured but there are some notable issues, such as simulation of too much melt of the Greenland ice sheet at the LIG and subsequent slow regrowth. Variations in orbital forcing can be large over this time period (up to 20% in 10 kyr in June 65 °N insolation) and are about twice as big at the LIG compared to present. Glaciation initiation and termination require both fast and slow feedbacks (e.g. water vapour and land ice-sheet build up) to explain the non-linear 100 kyr cycle. It is also noted that at certain CO_2 values orbit alone can force most of the signal. Whether the internal processes that amplify the 100 kyr signal are driven by external forcings or just phase-locked with the external system is unclear. They suggest the system may have multiple equilibrium states, which could potentially be the cause of the mid-Pleistocene transition.

Loutre and Berger (2000a) use the same model as the previous studies (which by this time was named LLN 2-D NH) to carry out a transient simulation of the past 200 kyr under various constant orbital configurations and varying CO_2 from the Vostok core. They find that although

hemispheric temperature responds directly to CO_2, without orbital changes CO_2 alone cannot reproduce the ice sheet dynamics of the last 200 kyr. However, there is a CO_2 threshold for the build-up of ice at around 230 ppm. Additionally, the simulations were initialised with three different ice sheet states for over Greenland and five different constant insolation schemes. These results suggested that the initial size of the ice sheet has little effect on its behaviour, with the final configuration of the ice sheet defined by the orbital setup.

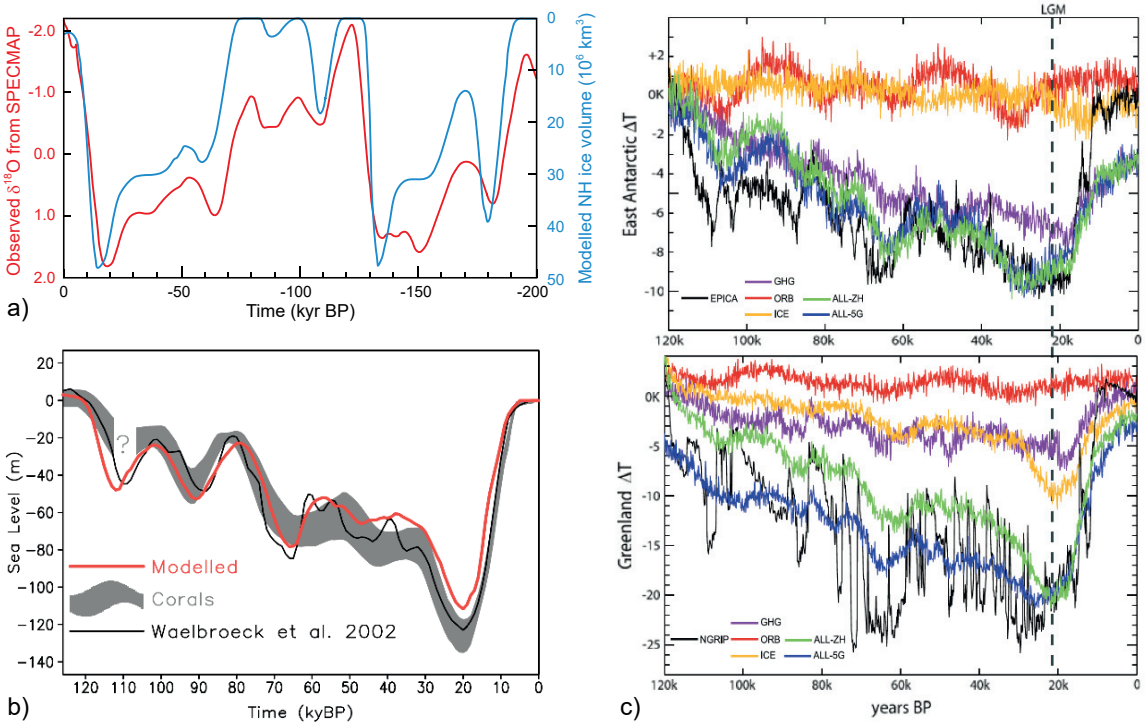

Fig. 3.6: Examples of model performance at simulating global changes.

a) ice volume (Berger and Loutre 1997); b) sea level change (Ganopolski et al. 2010); and c) polar temperatures (Smith and Gregory 2012) compared to various observational datasets. The upper panel of c) is for temperature change over Antarctica, and the bottom panel in c) is for temperature change over Greenland. The LGM is marked with a vertical dotted line. The different coloured lines in (c) show model experiments with different forcings applied (the EPICA and NGRIP observed data are in black), illustrating that orbital changes are less important for temperatures than they are for ice volume. *Note the reversed x axis in (a)

Calov et al. (2009) use the EMIC CLIMBER-2 coupled with the SICOPOLIS ice sheet model to test the sensitivity of idealised glaciation events to model parameters. The insolation forcing (June at 65 °N) was slowly varied for values between 126–115 kyr BP with fixed atmospheric CO_2. The orbital inception threshold is found to be much higher (i.e. ice sheets are more likely to form) if ice dynamics through coupling to an ice sheet model are included, compared to running the climate model component only. The insolation threshold for ice growth with ice dynamics was 477 W m^{-2} compared to 442 W m^{-2} without ice dynamics. This is because ice dynamics allow a fast initial expansion of ice with a snow-albedo feedback, making the model more sensitive to relatively small orbital forcing. It can take over 10 kyr for ice sheets to respond to the orbital forcing, meaning that in transient simulations orbital forcing must be well below the threshold to initiate a glaciation, which contributes to why there was no glaciation in the Holocene (and would not have been even if GHGs had been lower). They find that the rate and magnitude of orbital forcing can affect the growth of the ice and its final size, the ice sheet exhibits hysteresis behaviour and that appropriate CO_2 values were also required to recreate the correct size of glaciation.

Ganopolski et al. (2010) use CLIMBER-2-SICOPOLIS climate-ice sheet model. They use an energy balance model to calculate the ice sheet surface mass balance, which should be more applicable over space and time than simpler positive degree day schemes. The model only includes changing Northern Hemisphere ice sheets and adjusts the land sea mask and elevation relative to sea level. There is a fresh water flux to the ocean from ice sheet calving/melt and a dust deposition rate based upon Mahowald et al. (1999) that affects radiative forcing and snow. CH_4 and nitrous oxide (N_2O) are incorporated as CO_2 equivalent and there are some temperature corrections applied, for example over North America. Some systematic errors could not be eliminated by tuning model parameters, such as an oversensitivity of the Eurasian ice sheet to precession variability and a slightly reduced rate of deglaciation compared to reconstructions, but spatial extent and elevation of ice sheets at the LGM is reasonable as shown in Figure 3.6b. Like Calov et al., they find that during glaciation the ice sheets expand laterally quickly and then thicken. Iceberg calving is noisy due to instability in ice sheets and the AMOC but with no explicit forcing – appearing qualitatively like D-O events. The simulations suggest that the presence of ice sheets can explain approx. 50% of the global cooling, with the rest the result of GHGs, dust, vegetation etc. and they find evidence for a bipolar seesaw effect. Ice sheet evolution is highly sensitive to parameters in the surface energy/mass balance interface and the dust module (e.g. dust, basal sliding of ice, elevation desert effect), however these are poorly constrained.

Singarayer and Valdes (2010) offer the first representation of the last glacial cycle using a GCM, HadCM3. Although not fully transient, they use two sets of 62 simulations spaced from 1–4 kyr apart covering the last 120 kyr to test the roles of fixed or varying ice sheets, orbital forcing and GHGs at driving the climate with no interactive vegetation, dust or freshwater forcing. The magnitude of polar amplification is underestimated compared with data. The difference between the glacial and interglacial temperature is 4.25 °C (or approximately half that when ice sheets are not varied). The ice sheets in the model tend to over-estimate ice extent, as only the thickness is varied linearly with the $\delta^{18}O$ curve. The LIG and Holocene are both warmer than the pre-industrial and there are changes in AMOC at various times through the simulations. Generally, the AMOC is stronger during colder periods due to stronger cooling in the regions of deep convection, but further south due to increased sea-ice, which offsets some of the cooling in western Europe. The only millennial scale event to be modelled is an idealised Heinrich event, represented by a 1 sverdrup (Sv) input of freshwater to the North Atlantic. This freshwater input collapses the AMOC temporarily (the model does not get stuck in a cold mode) causing cooling of 6.5–9 °C over Greenland (not quite as much as reconstructions suggest) and causes a bipolar seesaw effect.

Smith and Gregory (2012) use the coupled GCM FAMOUS (a modified and reduced resolution version of HadCM3), accelerated by a factor of 10 to transiently simulate the past 120 kyr. The effect of orbital insolation, GHGs and ice sheets are modelled separately and in combination (under two ice sheet scenarios) and they find they combine approximately linearly. Changes in solar activity, the AIS, vegetation, sea level changes or melt water forcing are not included, the latter meaning there is no millennial scale variation after the LGM. As shown in Figure 3.6c, generally the model does a good approximation of low frequency (> 10 kyr) variability in the Antarctic records (in terms of rates and magnitude of cooling) and by the end of the simulation the model is within 0.5 K of pre-industrial simulations. Global mean SAT at the LGM is 4.3 °C less than pre-industrial and SST cooling is greatest in North Atlantic. They find anti-correlation between AMOC and Antarctic Circumpolar Current (ACC) strength, but this does not cause a temperature bipolar seesaw. The AMOC strength ranges between 15–20 Sv (up to 4 Sv of variation can be due to ice sheet configuration), reaching a maximum at the LGM, and these changes have a knock-on effect on the ACC. Unlike Singarayer and Valdes (2010), these transient simulations suggest the AMOC and ACC can vary with orbital changes and so the

ocean could be important for transferring many signals, not just those associated with Heinrich events. There are some notable issues in the experiments, including poor representation of sea ice in FAMOUS; the static AIS that affects the regional climate shortly after the LIG; the rapid spatial expansion of the Northern Hemisphere ice sheets (the same issue as Singarayer and Valdes 2010); ocean circulation equilibration time being similar to the accelerated forcing time; general underestimation of Greenland temperatures and a lack of millennial scale variability due to missing processes and the acceleration method. However, in terms of the qualitative response to the forcing, they argue that these should not necessarily have significantly adverse effects on the results.

One final set of snapshot simulations are those of Pollard and Barron (2003), who simulate the climate of Europe during LGM and oxygen isotope stage 3 (OIS3; the middle of last glacial) using the GENESIS GCM (approximately 300 km grid resolution) and the RCM RegCM2 (approximately 60 km grid resolution). The models are set up with the orbital configuration of 30 kyr BP, CO_2 at 200 pm, prescribed ice sheets from ICE-4G and two SST reconstructions (CLIMAP and GLAMAP-2000). The modelled climate of OIS3 is found to be colder than pre-industrial, warmer than the LGM, but with a warm bias relative to OIS3 reconstructions. There are also significant changes in precipitation at OIS3. The LGM and OIS3 have similar orbital forcings and prescribed SST patterns suggesting these are not the cause of the differences between these periods. The size of the ice sheets affects the climate over Europe and could account for some of the differences with proxies by affecting the winter pressure gradients across Europe. During OIS3 pressure gradients and winds are more zonal compared to the LGM, meaning the continental interior is affected more by advection than radiative cooling. This explains why OIS3 is warmer than the LGM in the model, however, given that the ice sheets were smaller at OIS3 there must also be other missing cooling mechanisms. Large sea ice or SST changes are suggested as possible reasons for the model-data mismatch.

3.4 Transient simulations of the last ~ 2 Myr

Both physically-based EMICs and simple conceptual models are used to simulate transient climate changes over timescales of several hundreds of thousands of years or more. Climate forcings taken into account in general include orbital variations and/or natural changes in the atmospheric concentration of CO_2.

DeBlonde and Peltier (1991) used a one dimensional zonally averaged high resolution ice sheet model to project ice volume over the past 1 Ma in response to changes in insolation forcing. A range of physical processes were included in this model, such as ice and Earth physics, and isostatic adjustment of the Earth in response to ice volume. A high resolution $\delta^{18}O$ proxy data set was used to improve the model's simulation of the Pleistocene (Shackleton and Hall 1989), and an additional data set was then compared to the modelled evolution of ice volume over time (Ruddiman et al. 1989). The model was found to be fairly successful in reproducing past changes in ice volume, following the inclusion of an additional feedback process. The study does not address what this feedback process may represent, but it is suggested that it may be linked to the sudden increase in marine ice sheet instability, perhaps due to changes in ocean circulation (Denton and Hughes 1983).

Ganopolski and Calov (2011) used the CLIMBER-2 EMIC to simulate the glacial-interglacial cycles over the last 800 kyr, forced by orbital variations and a range of constant CO_2 concentrations. They find that the 100 kyr periodicity demonstrated by observed changes in ice volume and the timing of ice sheet retreat can be reproduced as highly non-linear responses to changes in just the orbital parameters, assuming that atmospheric CO_2 concentration is lower than its usual interglacial value. In particular, variations in eccentricity are found to be the

primary forcing mechanism for the 100 kyr cycles, and changes in atmospheric CO_2 act to amplify the cyclic variations in ice volume. Additionally, sensitivity simulations with varying sediment cover of the continents suggest that large areas of sediment-free continental rock is required in North America in order to allow the ice sheet to persist through several precessional cycles, and thus produce the long 100 kyr glacial cycles.

Abe-Ouchi et al. (2013) developed and incorporated a climate parameterization into the IcIES three dimensional ice sheet model for the Northern Hemisphere, which was calibrated based on a selection of simulations run using the MIROC GCM with different orbital configurations, CO_2 concentrations, insolation values, and ice sheet extents. This model was then used to simulate the evolution of the Northern Hemisphere ice sheets over the last 400 kyr, forced by variations in insolation and atmospheric CO_2 concentration (Kawamura et al. 2007). When compared to proxy data, the model was found to reproduce the glacial cycles well, including their shape, timing, and intensity, with the greatest variation occurring on a timescale of 100 kyr, in agreement with the data. Sensitivity simulations suggested that this 100 kyr periodicity was robust for a range of values for different model parameters, including those related to isostatic rebound and iceberg calving, as well as a range of constant CO_2 concentrations. It was concluded that, whilst changes in atmospheric CO_2 can affect the intensity of the cycles, and changes in the ice sheets can influence the CO_2 concentration, the glacial-interglacial cycles are not driven by variations in CO_2. For constant CO_2 concentrations of less than 190 ppm and greater than 230 ppm, the Eurasian ice sheet demonstrated orbital forcing with a dominant timescale of 23 and 40 kyr, in contrast to the 100 kyr periodicity evident for a CO_2 value of 220 ppm. Both the Eurasian and North American ice sheets showed hysteresis in their responses to summer insolation, meaning that the insolation forcing required to initiate a change from one equilibrium state to another (e.g. positive to negative mass balance) varies depending on the transition type, which in turn affects the timing of the glacial cycles. It was found that the larger the ice sheets grew, the smaller the insolation forcing that was required to cause a negative mass balance and thus ice sheet retreat. In addition, the model suggested that the Eurasian ice sheet is only stable at either very large or very small extents, with no intermediate ice volumes, due to large variations in summer insolation forcing.

The CLIMBER-2 model was utilized by Ganopolski et al. (2016) to perform simulations with varying orbital configurations and constant CO_2 concentrations of 240 and 280 ppm. Initially, a sensitivity analysis was performed by simulating climate changes for a number of past periods and the Holocene-Future (10–30 kyr after present (AP)) with one model parameter being varied slightly. From the twenty simulations, the four model configurations that simulated climate states in agreement with observations were selected. All four of these configurations projected that the current interglacial ended several thousand years ago for a CO_2 concentration of 240 ppm, with large ice sheets at the present day. The coldest and warmest of the four model configurations were used to calculate the threshold CO_2 concentration which results in glacial inception, derived as a function of summer insolation at 65^{o}N. These models were then forced by orbital variations and CO_2 concentrations (Petit et al. 1999, Augustin et al. 2004) for the last 800 kyr. The critical insolation-CO_2 concentration relationship was found to be valid for the simulated period, with past glaciations occurring when the atmospheric CO_2 concentration fell below the critical threshold value.

A large number of conceptual models have also been developed and used to simulate the glacial-interglacial cycles that have occurred over the last few million years. Only a selection will be discussed here; for a detailed review of changes in climate on orbital timescales and modelling approaches, see Paillard (2015), Ruddiman (2006), or Saltzman (2001). The conceptual models are forced by orbital variations, either via changes in one or more of the main orbital parameters or by changes in insolation (typically at 65^{o}N in June). Some also

include atmospheric CO_2 concentration as a forcing, or another climate feedback that is proposed to influence the glacial-interglacial cycles in some way, such as deep ocean temperature. The models may also have an insolation forcing threshold which, once crossed, results in the initiation of a glacial or interglacial episode, although this is not true of all the models.

Studies based on conceptual models that use only variations in the orbital parameters as a climate forcing include Imbrie and Imbrie (1980), Saltzman and Maasch (1991), Paillard and Parrenin (2004), Huybers (2009), and De Saedeleer et al. (2013). Imbrie and Imbrie (1980), for example, developed a simple non-linear time-dependent model, which was tuned on data for the period 150–0 kyr BP. It accounted for climatic variations on orbital timescales of 19 kyr or lower for one cycle, and thus ignored natural CO_2 forcing. The model performed reasonably well when used to simulate the last 150 kyr, but was less successful is simulating the period 500–150 kyr BP, particularly before 350 kyr BP. The primary shortcomings of the model were that it produced too little variability on 100 kyr timescales, whilst simulating too much variability on precessional (19 and 23 kyr) and obliquity (41 kyr) timescales. The projection of ice volume also deviated from the proxy record at approximately 413 kyr BP, when the last eccentricity minimum occurred.

A conceptual model was developed by Saltzman and Maasch (1991), based on the three function model of Saltzman and Maasch (1990) which calculated ice volume, CO_2 concentration, and deep ocean temperature, but with one less tuneable parameter in the CO_2 equation. The model was forced by changes in insolation, and was able to explain many of the main climatic features of the last 5 Ma, including the mid-Pleistocene transition to 100 kyr cycles.

Paillard and Parrenin (2004) also developed a model based on three functions, calculating Northern Hemisphere ice volume, Antarctic ice area, and atmospheric CO_2 concentration, respectively. Insolation variations were used as the forcing, and were included in the ice volume and CO_2 equations. An additional physical mechanism was proposed, in the form of a non-linear parameterization for Southern Ocean ventilation included in the CO_2 equation, which aimed to link glacial-interglacial changes in climate and CO_2. This mechanism is related to the size of the AIS during periods of maximum glaciation acting to disrupt the process of brine rejection during the formation of sea ice, thus reducing ocean stratification in the Southern Ocean and allowing deep carbon-rich bottom waters, which were previously isolated, to release CO_2 to the atmosphere. The model was applied to the last 500 kyr, and was found to be relatively successful in reproducing the last four glacial cycles when compared to proxy data for sea level (Shackleton et al. 1990, Bassinot et al. 1994, Tiedemann et al. 1994, Petit et al. 1999). In agreement with the data, changes in atmospheric CO_2 led changes in ice volume by several thousand years at glacial terminations, which occurred after the AIS reached its maximum extent, and the 100 kyr cycles were reproduced. The introduction of a small drift in the parameter for bottom water formation efficiency also meant that the model was able to capture most of the glacial-interglacial transitions over the last few million years. It was suggested that this mechanism, related to glacial deep stratification, may be vital in explaining the climate transitions of the past (Paillard and Parrenin 2004, Sigman et al. 2004).

Huybers (2009) used a modified version of the Imbrie and Imbrie (1980) model, in which the rate of deglaciation was influenced by the prior ice volume. A simulation of the last 2 Ma showed that this model produced transitions between different ice sheet states with periodicities of 80 kyr and 120 kyr, resulting in an average 100 kyr timescale. The model was also able to reproduce the mid-Pleistocene transition from short 40 kyr glacial cycles to longer 100 kyr cycles.

A range of simple models also include atmospheric CO_2 concentration as a climate forcing, including Pisias and Shackleton (1984) and Crucifix (2013). Pisias and Shackleton (1984) utilised a simple ice model (Imbrie and Imbrie 1980), which they modified to allow atmospheric CO_2 variations to affect the evolution of the ice sheet. The inclusion of CO_2 forcing improved the ability of the model to simulate observed changes in ice volume over the last 340 kyr compared to when only orbital forcing was used. It was also concluded that other components of the climate system may play a role in variations in ice volume.

Conceptual models which include a critical insolation threshold include those of Paillard (1998), Parrenin and Paillard (2003), Huybers and Wunsch (2005), Tziperman et al. (2006), Imbrie et al. (2011), Parrenin and Paillard (2012), and Tzedakis et al. (2017). Two simple models were presented by Paillard (1998), which used insolation forcing to predict changes in ice volume. Three different climate states were represented (glacial, mild glacial and full glacial), and the transitions between these states occurred when different thresholds were passed. The model results for the last 2 Ma compared reasonably well with proxy data (Tiedemann et al. 1994), with most of the climate state transitions being simulated correctly, along with the onset of 100 kyr cycles (Figure 3.7).

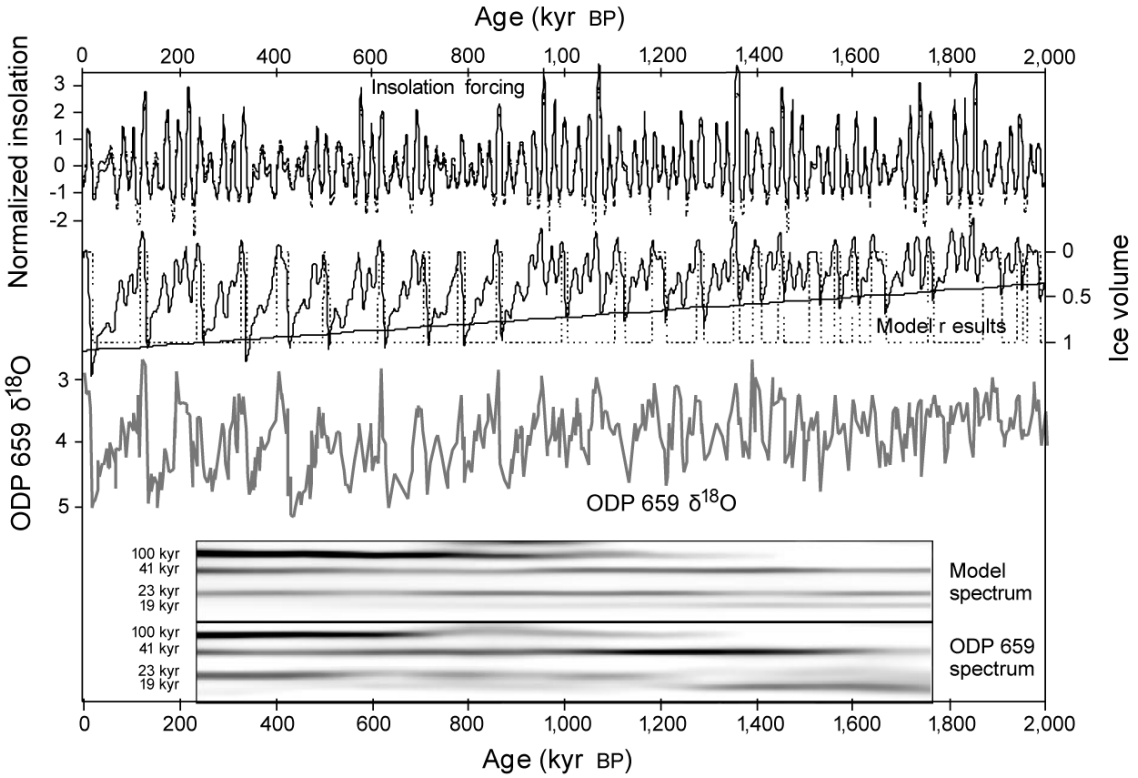

Fig 3.7: Results from the Paillard (1998) conceptual model (middle curve), with a time-varying threshold (oblique line).

The transitions are triggered by threshold crossings of the insolation (upper curve). The oxygen isotope record from ODP site 659 is used for comparison (lower curve, Tiedemann et al 1994). An evolutive spectral analysis of the two series is performed (lowest panel) using the maximum entropy method and a sliding time window of 500 kyr. In both spectra, the 100-kyr periodicity appears around 1 Myr BP. Many aspects of the two series are quite similar, both in the time and frequency domains.

Huybers and Wunsch (2005) modelled glacial variability over the period 700–0 kyr BP using deterministic and stochastic variants of a simple model forced by obliquity. The model included an ice volume threshold that, once exceeded, initiated deglaciation. They found that both models were capable of describing climate variability over the time period examined. They also suggested that in general, Pleistocene climate tends towards a glacial state, with glacial terminations occurring near to obliquity maxima, although this was not true for all transitions.

Imbrie et al. (2011) used a two dimensional 'phase-space' model, containing a threshold for deglaciation which was a function of ice volume and its rate of change. Obliquity and precession were used as climate forcings, with the strength of the orbital forcing being dependent on the ice volume. Many of the features evident in paleo ice volume data for the last 1.5 Ma (Lisiecki and Raymo 2007) were reproduced by the model, particularly the timings and amplitudes of deglaciations from 1 Myr–0 kyr BP. The switch from 40 kyr glacial cycles to 100 kyr cycles at around 1 Ma was also captured, and a mechanism for explaining the anticorrelation between eccentricity and the 100 kyr cycles that is observed at times in the proxy data (Lisiecki 2010) was presented, relating to the impact of eccentricity extremes on the deglaciation threshold.

Tzedakis et al. (2017) presented a simple model forced by peak summer caloric insolation and the time since the start of the last interglacial period. Summer caloric insolation is the amount of energy integrated over the half of the year during which mean insolation on any day is higher than mean insolation of any day in the winter half (known as caloric summer half year). An insolation threshold for deglaciation was also included. The model was able to correctly reproduce all complete deglaciations for the last million years, in addition to the increased dominance of the 100 kyr glacial cycles in the mid-Pleistocene. The results also suggested that the observed series of past glacial terminations is one of a small number of possible evolutions, meaning that small climate differences may have resulted in a number of changes to past deglaciation events which were accompanied by weaker summer insolation.

The conceptual threshold models of Raymo (1997) and Archer and Ganopolski (2005) included both orbital and atmospheric CO_2 as climate forcings. Archer and Ganopolski (2005), for example, calculated the critical insolation threshold leading to glacial inception based on simulations run using CLIMBER-2 with a range of orbital and CO_2 forcings. This model was based on that of Paillard (1998), but modified to allow atmospheric CO_2 to impact the insolation threshold. They then simulated the evolution of ice volume over the last 500 kyr under observed changes in atmospheric CO_2 concentration (Petit et al. 1999). Temperature estimates derived from proxy ice volume data and modelled ice volume compared reasonably well, although there were some discrepancies between the projected timings of a number of climate transitions.

4 Simulations of the next 1 million years

Unlike for the past climates discussed so far in this report, no observational data exists for the future; as such, we are reliant entirely on models for our predictions. This necessitates a careful consideration of the uncertainties inherent in the predictions, which encompass the evolution of atmospheric carbon dioxide on both short (10–1,000 years) and long (1,000–1,000,000 years) timescales in response to carbon cycle processes, and the climatic response to carbon dioxide and variations in Earth's orbital parameters.

In this section, following a summary of the main controls on future climate (Section 4.1), modelling studies that attempt to project future climatic changes are reviewed, with a particular focus on their uncertainties. This section is structured based on the length of time considered: the evolution of climate on the order of centuries (up to 2300 CE; Section 4.2), tens of thousands of years (up to 50 kyr; Section 4.3), a hundred thousand years (100 kyr; Section 4.4), and a million years (1 Ma; Section 4.5) AP. These timescales are chosen in part due to their relevance to the disposal of nuclear wastes, and also because they generally require the use of different modelling techniques and/or focus on different features of the Earth system and climate (see Section 2.3). In general, simulations up to 2300 CE have used full complexity ESMs and GCMs in the context of the IPCC, those up to 50kyr have focussed on CO_2-induced climate warming and ignored orbital forcings; simulations up to 100 kyr have focussed on the onset of the next glaciation using EMICs, and those up to 1 million years have used conceptual models to predict future glacial-interglacial cycles.

4.1 Controls on future climate

As discussed in Section 2.1, the dominant controls on long-term (up to ~ 1 Ma) climate are changes in atmospheric CO_2 concentration and variations in the orbital characteristics of the Earth. For both the past and future, the development of the three orbital parameters (precession, obliquity and eccentricity), which affect the spatial and temporal distribution of insolation received at the top of the Earth's atmosphere, can be calculated with relatively little uncertainty for up to tens of millions of years (Laskar et al. 2004). For the next ~ 100 kyr, the eccentricity of the Earth's orbit will be relatively low, which will reduce the impact of precessional changes and will result in obliquity having a greater influence on climate (Ganopolski et al. 2016, Lord et al., In review). Minima in June insolation at 65^{o}N in the next 100 kyr occur at approximately 17, 54, 77 and 97 kyr AP, making glacial inception more likely around these times. However, as will be discussed later, increased radiative forcing due to higher atmospheric CO_2 concentrations may result in a delay in glacial inception for one glacial cycle or more.

There is a significant amount of uncertainty relating to the future evolution of atmospheric CO_2 concentration. Firstly, it is not possible to know how anthropogenic CO_2 emissions will develop over the next few hundred years or longer in response to human activities. However, it is likely that, at least for the remaining part of the 21st century, CO_2 emissions will continue to be released to the atmosphere, and thus atmospheric CO_2 concentration will continue to increase (IPCC 2013). CO_2 emissions scenarios are often developed for use in modelling studies, based on different assumptions about future socioeconomic developments that aim to cover the range of possible futures. For example, AR5 (IPCC 2013) uses four Representative Concentration Pathways (RCPs), which describe changes in radiative forcing over time, and have different year 2100 radiative forcing targets, of 2.6, 4.5, 6.0 and 8.5 W/m^2. These end-of-century targets roughly represent low (RCP2.6), medium (RCP4.5 and RCP6.0) and high (RCP8.5) levels of climate forcing, and extensions to the scenarios also exist which project emissions to 2300 CE.

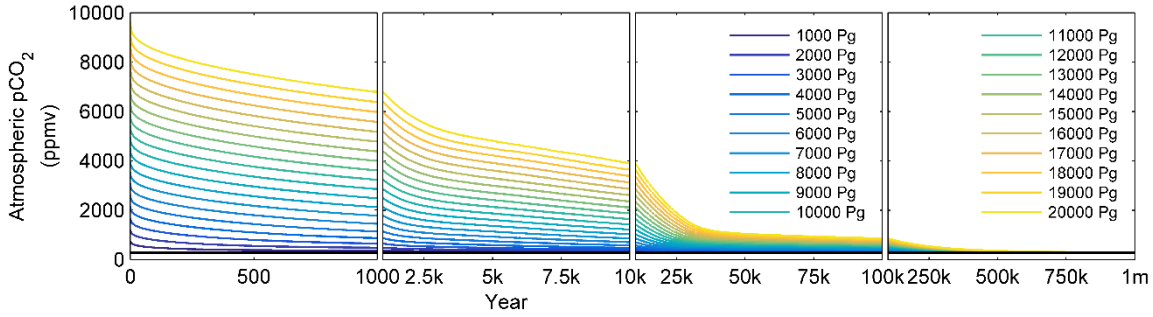

Fig. 4.1: Atmospheric pCO_2 predicted by the cGENIE model for the next million years, for CO_2 scenarios with pulse emissions of 1000–20,000 Pg C.

Pre-industrial CO_2 concentrations are shown in black. Figure 2 (p.8) of Lord et al. (2016).

Secondly, there is uncertainty about the atmospheric lifetime of emitted fossil fuel CO_2, in particular related to how long it will remain in the atmosphere before it is removed by the natural carbon cycle, thus returning CO_2 concentrations back towards pre-industrial values. There is increasing evidence that a significant proportion will remain in the atmosphere for very long timescales, as illustrated in Figure 4.1, due to its removal over tens to hundreds of thousands of years by a range of carbon cycle processes (Archer et al. 1997, Archer 2005, Lenton and Britton 2006, Ridgwell and Hargreaves 2007, Lord et al. 2016). Transient simulations performed using EMICs containing representations of the long-term carbon cycle suggest that, even 10 kyr after CO_2 emissions have ceased, between 15 and 30% of emissions remain in the atmosphere following total cumulative emissions of approximately 200–5000 petagrams of carbon (Pg C; 1 Pg = 10^{15} g) (Eby et al. 2009), and between 7 and 38% for total emissions of 1000–20,000 Pg C (Lord et al. 2016). It is estimated that it may take up to 1 Ma or more for pre-industrial CO_2 values to be restored following an anthropogenic CO_2 perturbation (Lenton and Britton 2006, Colbourn et al. 2015, Lord et al. 2015 Lord et al. 2016), with higher total emissions taking a greater amount of time to be removed. The long-term evolution of an atmospheric CO_2 perturbation is found to be dependent on the total emissions released, rather than the rate of release (Eby et al. 2009, Lord et al. 2016), hence the amount of CO_2 released over the coming centuries will affect the lifetime of the perturbation. However, based on current emissions trends, CO_2 originating from combustion of fossil fuels is expected to act as a significant forcing on climate for the next few tens of thousands of years, in addition to variations in the orbital parameters. Notwithstanding this, it is also important to consider scenarios in which humanity carries out large-scale carbon-cycle geoengineering, in which anthropogenic CO_2 is effectively reduced to zero, and the system follows a 'natural' trajectory as it would have in the absence of human industrialisation.

A third source of uncertainty is associated with natural variations in the carbon cycle. In the absence of anthropogenic emissions, atmospheric CO_2 concentrations have fluctuated over the past few million years, often demonstrating a strong correlation with temperature (Petit et al. 1999, Luthi et al. 2008). During the late Quaternary, atmospheric CO_2 has varied between ~ 180 and 280 ppm on glacial-interglacial timescales, and it is expected that fluctuations will continue into the future, although by an unknown magnitude.

The response of the Greenland and Antarctic ice sheets to changes in SAT and precipitation is also uncertain, as are the resulting impacts on climate and global sea level. However, changes in sea level are not relevant to the sites being considered here, and changes in SAT generally only occur locally to these two ice sheets (Lunt et al. 2004, Toniazzo et al. 2004, Ridley et al. 2005, Lord et al. in review), which is not relevant to any Swiss sites.

As a result of these uncertainties, modelling studies must make a range of assumptions or empirical estimates about the future, which may include, but are not limited to, anthropogenic CO_2 emissions (total emissions and timescale of release), the timing and magnitude of natural CO_2 variations, the evolution of atmospheric CO_2 in response to anthropogenic and natural variations (in the absence of an interactive coupled carbon cycle), and the response of the ice sheets to climate change (in the absence of an interactive coupled ice sheet model).

4.2 Climate evolution until 2300 CE

Changes in climate that occur on timescales of decades to several centuries are relevant to policy decisions, and hence have been addressed in detail by a wide range of studies. Therefore, only a brief description of the key findings will be presented here; for a more detailed summary of current knowledge and understanding, please refer to the Fifth Assessment Report (AR5) of the IPCC (2013).

Based on the Coupled Model Intercomparison Project Phase 5 (CMIP5; (Taylor et al. 2012) climate projections, for which a range of state-of-the-art GCMs were forced using four RCP emissions scenarios, IPCC (2013) concluded that the global annual average surface air temperature (SAT) for 2081–2100 will be higher than for the 1986–2005 reference period, by 0.3–1.7 °C (RCP2.6), 1.1–2.6 °C (RCP4.5), 1.4–3.1 °C (RCP6.0) and 2.6–4.8 °C (RCP8.5), as illustrated in Figure 4.2. The range in predictions for each RCP scenario is a result of the differences in the models used to make each prediction (see Section 2.3.2). At the end of the 21st century, globally averaged changes over land will be greater than changes over the ocean, and the greatest warming is projected to occur in the Arctic region, assuming that there is not a strong reduction in AMOC. A reduction in Northern Hemisphere snow cover and retreat of permafrost will occur over the course of the century, in response to increased global temperatures and changes in precipitation and ablation.

High latitude regions are projected to experience an increase in temperature and precipitation by almost all climate models (IPCC 2013), which generally results in high latitude surface waters becoming less dense and hence more stable, potentially affecting the strength of the AMOC. Surface air temperatures in Central Europe are very likely to continue to increase over the next hundred years, based on the results of the CMIP5 simulations (IPCC 2013). Under the RCP4.5 scenario, annual mean temperatures in Central Europe are projected to have increased by 2-3.1 °C (25th–75th percentiles of model simulations) in 2081–2100 compared to the period 1986–2005, whilst annual mean precipitation increases by 0–6% for the same period. The length, frequency, and/or intensity of warm spells or heat waves are also very likely to increase in this region.

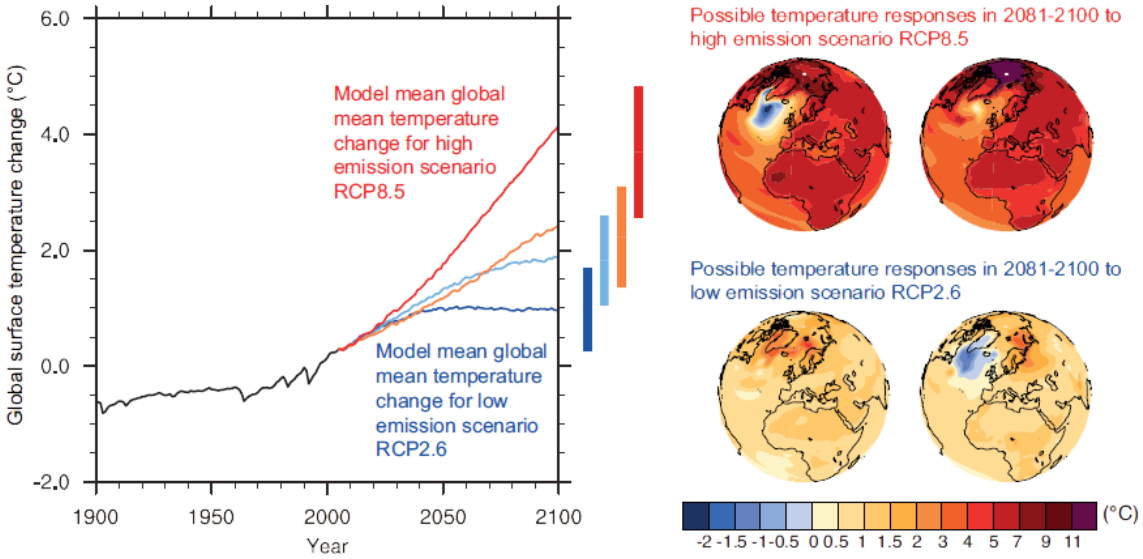

Fig. 4.2: Change in global mean temperature averaged across all CMIP5 models (relative to 1986–2005) for the four RCP scenarios.

RCP2.6 (dark blue), RCP4.5 (light blue), RCP6.0 (orange) and RCP8.5 (red) (left). Likely ranges for global temperature change by the end of the 21st century are indicated by vertical bars. Note that these ranges apply to the difference between two 20-year means, 2081–2100 relative to 1986–2005, which accounts for the bars being centred at a smaller value than the end point of the annual trajectories. For the highest (RCP8.5) and lowest (RCP2.6) scenario, illustrative maps of surface temperature change at the end of the 21st century (2081–2100 relative to 1986–2005) are shown for two CMIP5 models (right). These models are chosen to show a rather broad range of response, but this particular set is not representative of any measure of model response uncertainty. Figure 1 of FAQ12.1 (p.1037) of Collins et al. (2013).

An ensemble of high-resolution (12.5 km) climate simulations run on a range of regional climate models (RCMs) driven by data from GCMs were produced as part of the World Climate Research Program Coordinated Regional Downscaling Experiment (EURO-CORDEX) initiative (http://euro-cordex.net/index.php.en). These projections, shown in Figure 4.3, suggest an increase in annual mean temperature over Europe of 1–4.5 °C for RCP4.5, and 2.5–5.5 °C for RCP8.5 for the period 2071–2100 compared to 1971–2000 (Jacob et al. 2014). For Switzerland, warming appears to be in the range of 2–2.5 °C and 3.5–5.5 °C for the two scenarios, respectively, with the largest temperature increases experienced over south-eastern Alpine regions. Precipitation over Switzerland appears to show little change in some areas, or a slight increase in others.

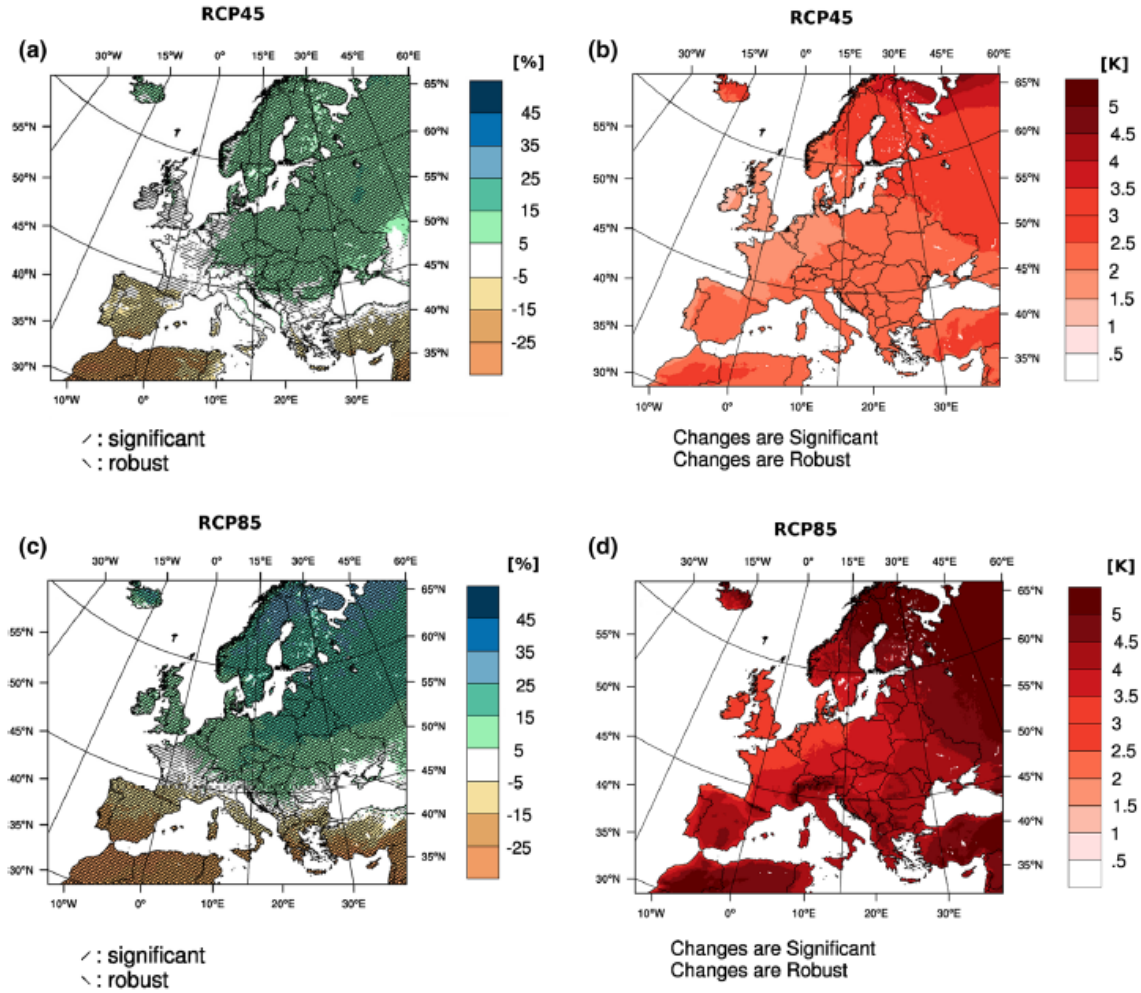

Fig. 4.3: Changes in total annual precipitation (%; left) and annual mean temperature (K; right) averaged across all EURO-CORDEX models for 2071-2100 relative to 1971–200 for two RCP scenarios: RCP4.5 (a, b) and RCP8.5 (c, d).

Hatched areas indicate regions with robust and/or statistically significant change (a, c). Changes are robust and significant across the entire European continent (b, d). Figure 1 (p.567) of Jacob et al. (2014).

4.3 Evolution until 50 kyr AP

A consequence of the slow removal of excess atmospheric CO_2, combined with the slow response times of parts of the climate system, is that changes in global climate are projected to continue to occur long after anthropogenic CO_2 emissions have been reduced or have stopped entirely. In fact, the lag in the response of SAT to changes in radiative forcing caused by increasing atmospheric CO_2 means that, even if radiative forcing were stabilized, global SAT would only reach steady state after several centuries to millennia (IPCC 2013). This means that a large proportion of the climate change that will occur over the next hundred years or so is unavoidable, unless net CO_2 emissions are strongly negative for a significant period of time (IPCC 2013), such as through the development of carbon-neutral energy production accompanied by the removal from the atmosphere and long-term storage of excess CO_2 (carbon sequestration through geoengineering). Variations in emissions of other gases will further affect the global temperature response, with a termination of aerosol emissions likely to contribute to

warming. Conversely, a termination of emissions of GHGs with relatively short-lifetimes, such as methane (~ 10 years), nitrous oxide (~ 100 years) and hexofluoroethane (~ 10 kyr), will have a cooling effect.

For modelling timescales of tens of thousands of years, models of a lower complexity and/or resolution, such as EMICs, are often used in place of GCMs. This is because their relatively fast running time generally makes them more suitable for simulations that cover long periods of time, as well as for running larger ensembles of simulations. In terms of future climate forcings, it is likely that atmospheric CO_2 will act as a dominant influence for at least several tens of thousands of years, due to its relatively high concentration and slow uptake time by the carbon cycle (Shaffer et al. 2009; Ganopolski et al. 2016; Lord et al. in review). Only when atmospheric CO_2 declines back towards pre-industrial values are orbital variations likely to become increasingly influential.

A range of modelling studies have addressed the subject of climate change on multimillennial timescales of up to 50 kyr AP. These studies have generally focussed on the response of climate to fossil fuel emissions up to ~ 10 kyr AP, along with a number of studies which investigate the longer-term impact of climate change on the GrIS. In these studies, anthropogenic CO_2 is emitted to the atmosphere, either as an instantaneous pulse (Frolicher et al. 2014), or over decades to centuries, where emissions or atmospheric CO_2 concentration are initially increased before they are either held constant (Huybrechts et al. 2011, Li et al. 2013) or reduced to zero over various timescales (e.g. several hundred years) (Lenton 2000; Lenton et al. 2006; Mikolajewicz et al. 2007; Solomon et al. 2009; Friedlingstein et al. 2011; National Research Council 2011; Clark et al. 2016), or a combination of these approaches (Plattner et al. 2008; Vizcaino et al. 2008; Eby et al. 2009; Zickfeld et al. 2013). Many of the studies prescribe CO_2 emissions and use models that include a representation of the carbon cycle in order to predict atmospheric CO_2 concentrations, while others prescribe atmospheric CO_2 concentrations directly (Huybrechts et al. 2011 Li et al. 2013), or else use an empirical response function to project the evolution of atmospheric CO_2 following emissions (Charbit et al. 2008).

In the simulations, changes in climate occur long after CO_2 emissions have declined or been reduced to zero. Peak warming generally occurs several decades to millennia after the peak CO_2 concentration is reached (Eby et al. 2009; Friedlingstein et al. 2011, Frolicher et al. 2014), due to the slow response time of the oceans. The amount of warming that occurs in response to increased atmospheric CO_2 ultimately depends on the sensitivity of the climate to a doubling of CO_2, which is estimated [likely/highly likely] to be in the range 1.5 °C and 4.5 °C (IPCC 2013). In the simulations, the maximum warming ranges from 0.32 °C to 10.8 °C, depending on the CO_2 scenario and model used. Following the initial period of warming, global temperature then generally begins to slowly decline, excluding simulations where atmospheric CO_2 concentration is held at a constant elevated value. Some studies demonstrate a temporary reversal of this cooling trend several hundreds to thousands of years into the simulation, which is attributed to changes in ocean processes (Vizcaino et al. 2008; Eby et al. 2009). At the end of 10 kyr AP, Eby et al. (2009) find that 15–20% of the atmospheric CO_2 perturbation remains, whilst up to 75% of the maximum temperature anomaly persists, suggesting that the lifetime of warming may be significantly longer than that of excess atmospheric CO_2.

Increased global temperatures will have further impacts on other parts of the climate and Earth system, including changes in precipitation, storm events and sea level (Vizcaino et al. 2008; Kjellström et al. 2009; Solomon et al. 2009; National Research Council 2011). A number of studies suggest that the AMOC may weaken in response to warming, resulting in cooling over the North Atlantic and parts of north-western Europe (Mikolajewicz et al. 2007; Vizcaino et al. 2008; Kjellström et al. 2009). The reduction in strength of the AMOC is found to be generally dependent on the magnitude of warming (Lenton et al. 2006), and whilst some studies suggest

that it recovers following this weakening within the time period studied (Plattner et al. 2008; Li et al. 2013), others find that higher CO_2 reduces this recovery (Vizcaino et al. 2008; Zickfeld et al. 2013). Mikolajewicz et al. (2007) find that high CO_2 emissions result in a collapse of the AMOC, which does not recover for several thousand years. It has also been suggested that deglaciation of Greenland may occur when global mean temperature increases of 1.9–4.6 °C occur (Meehl et al. 2007), or local warming of higher than 2.5 °C (Huybrechts and de Wolde 1999), with the rate and magnitude of melt increasing with increased warming. Many studies simulate a partial or complete melt of the GrIS within the next 50 kyr for various CO_2 scenarios (Ridley et al. 2005; Lenton et al. 2006; Huybrechts et al. 2011), with some showing no regrowth within the simulation time of up to 20 kyr (Charbit et al. 2008; Vizcaino et al. 2008). Melting of the GrIS may cause local increases in temperature, accompanied by cooling in winter over the Barents sea due to changes in sea ice cover, atmospheric circulation and poleward heat transport (Lunt et al. 2004). Winkelmann et al. (2015) estimate a substantial melting of the Antarctic ice sheet (> 50 metres of sea level equivalent) after 10,000 years under the most extreme CO_2 emissions scenarios, using the PISM ice sheet model.

4.4 Evolution until ~ 100 kyr AP

On timescales of up to 100 kyr, variations in the orbital parameters act as a significant forcing on climate, through their impact on the seasonal and latitudinal distribution of insolation received by the Earth. In Sections 3.3 and 3.4, it was shown that glacial-interglacial cycles have been a dominant feature of the Earth's climate system for several million years, and such cycles are expected to continue into the future. However, it is possible that these natural cycles will be disrupted by anthropogenic climate change, although to what extent is currently uncertain.

As with modelling of multimillennial timescales, EMICs are often used for transient simulations on 100 kyr timescales, although a small number of studies use GCMs to simulate snapshots of climate at specific times and/or conditions in the future, and some studies make use of conceptual models. The models are forced by changes in future insolation and a range of natural and anthropogenic CO_2 scenarios are considered, often with the aim of predicting when the next glacial inception may occur.

Imbrie and Imbrie (1980) forced a simple conceptual non-linear model, tuned on data from the last 150 kyr, with climatic variations on orbital frequencies (lower than 19 kyr for one cycle), thus ignoring anthropogenic and natural CO_2 forcing. The 100 kyr future simulation suggested that, purely under orbital forcing, the current interglacial may have ended ~ 6 kyr BP, when a global cooling trend began. This cooling is projected to continue for the next 23 kyr, with the next glacial maximum occurring at ~ 60 kyr AP.

Loutre and Berger (2000b) used the Louvain-la-Neuve two-dimensional Northern Hemisphere climate model (LLN 2-D NH), an EMIC, to simulate the possible evolution of climate over the next 130 kyr. A range of simulations were performed with a modern day GrIS configuration, with constant natural CO_2 concentrations ranging from 210 to 290 ppm. In addition, a number of scenarios with variable CO_2 were performed, including one where CO_2 linearly increased to 750 ppm within 200 years, before decreasing to natural values by 1 kyr AP, and a second 'natural' scenario, using CO_2 concentrations derived from Vostok ice core data, but shifted towards future by 130 kyr (Jouzel et al. 1993). This natural scenario was also used to force a version of the model with no Greenland ice sheet, along with three other constant CO_2 scenarios of 210, 250 and 290 ppm. For a constant CO_2 concentration of 210 ppm, glacial inception is imminent, with increases in ice beginning at present day. The next glaciation occurs at around 50 kyr AP when atmospheric CO_2 is 270 ppm or lower, whilst if it is higher than this, no inception occurs before 130 kyr AP at the earliest.

A subsequent study by Berger and Loutre (2002) also used the LLN 2-D NH model to simulate the climate from 200 kyr BP to 130 kyr AP under a number of CO2 forcing scenarios. Two natural scenarios were simulated, one with a constant CO2 concentration of 210, and one using CO_2 concentrations derived from the Vostok ice core (Jouzel et al. 1993), as in Loutre and Berger (2000b). The 'global warming' scenario of Loutre and Berger (2000b) was also modelled, where CO_2 increased to 750 ppm within 200 years, before decreasing to natural values by 1 kyr AP. Consistent with the results of Loutre and Berger (2000b), ice growth occurred almost continuously from present day in the simulation with a CO_2 concentration of 210 ppm, whereas glacial inception is delayed until after 50 kyr AP in the anthropogenic and natural variable CO_2 scenarios.

BIOCLIM (2003a) used a GCM, the IPSL_CM4_D model, to carry out snapshot simulations of 67 and 178 kyr AP in the context of the BIOCLIM project. These time periods were chosen because they represent super-interglacial orbital conditions, and a future glaciated state, respectively. The 178kyr simulation showed a cooling relative to modern in the Central European region of the order of 0.5 and 1 °C in DJF and JJA (June-July-August) respectively. This was primarily due to the presence of a Fennoscandian ice sheet, as the CO2 concentration was the same as pre-industrial (280 ppmv). The BIOCLIM project also carried out dynamical downscaling using an RCM (BIOCLIM 2003b), and found that in the RCM, the winter temperature change was significantly greater over Europe than in the GCM, decreasing by as much as 4 °C compared with modern.

Berger et al. (2003) simulated the coming 130 kyr using the LLN 2-D NH model for a range of CO_2 scenarios, including constant natural CO_2 concentrations of 210, 250 and 290 ppm and variable natural CO_2 derived from the Vostok ice core (Jouzel et al. 1993). Two variable fossil fuel scenarios were also modelled, following the same trajectory as the 'global warming' scenario of Loutre and Berger (2000b), but reaching maximum CO_2 concentrations of 550 and 750 ppm. For constant atmospheric CO_2 concentrations of 210 ppm, glacial inception was imminent. However, in all other scenarios the current interglacial lasted until at least 50 kyr AP.

A study by Cochelin et al. (2006), using the 'green' McGill Paleoclimate Model (MPM), an EMIC which simulates the area between 75°S and 75°N, included a range of natural CO_2 scenarios with constant atmospheric CO_2 of between 240 and 300 ppm. Additionally, a number of fossil fuel scenarios were modelled, for which an initial increase in CO_2 was followed by a gradual reduction until constant concentrations of 280, 290 and 300 ppm were achieved. In the absence of anthropogenic CO_2 emissions, three possible future climate evolutions were identified. Glacial inception was predicted to be imminent for atmospheric constant CO_2 concentrations of 270 ppm or less, was predicted to occur at ~ 50 kyr AP for CO_2 of 280-290 ppm, and does not occur within the next 100 kyr for CO_2 concentrations over 300 ppm. Similar development pathways also occurred for the simulations which included a period of intense global warming. For CO_2 concentrations of 290 ppm or lower, glaciation occurs at ~ 50 kyr AP, whilst for 300 ppm or higher the current interglacial period lasts for at least the next 100 kyr. These results suggest the atmospheric CO_2 threshold for the next glacial inception may lie between 290 and 300 ppm.

A study by Pimenoff et al. (2011) investigated the evolution of climate over the next 120 kyr as part of an assessment into long-term repository safety for the planned spent nuclear fuel repository at Olkiluoto, Finland. Natural and fossil fuel CO_2 scenarios were simulated using the CLIMBER-2-SICOPOLIS model, with constant atmospheric CO_2 concentrations of 280 and 400 ppm, respectively. Ice sheet growth was projected to begin from present day for the 280 ppm scenario, particularly over North America and large areas of Fennoscandia. This glacial period is followed by a period of interglacial conditions, before ice sheet growth occurs again at the insolation minima at ~ 54 kyr and 100 kyr AP, when most of Fennoscandia is covered by ice sheets. When atmospheric CO_2 is 400 ppm, significantly less ice sheet development occurs over the next 120 kyr compared to the 280 ppm scenario, likely linked to the significantly warmer global temperatures. During the insolation minima at ~ 17 kyr AP, only a small amount of ice is projected over the Scandinavian mountains, whereas at the 54 kyr AP minima, a limited ice sheet extends from the Scandinavian mountains to Lapland and parts of Northern Ostrobothnia.

Vettoretti and Peltier (2011) used a GCM, the National Center for Atmospheric Research Community Climate Model Version 3 (NCAR CCSM3), to produce a number of snapshot simulations of future climate under natural CO_2 forcing. The first simulation had orbital conditions suitable for 10 kyr AP, whilst the second had orbital conditions for 51 kyr AP, and both had atmospheric CO_2 concentrations of 260 ppm. Glacial inceptions are produced in both simulations, with the 51 kyr AP glaciation being of a stronger magnitude.

Tzedakis et al. (2012) proposed that the onset of bipolar-seesaw variability acts as a constraint on the minimum age of a glacial inception. This variability is instigated when Northern Hemisphere ice sheets reach a sufficient size to produce iceberg discharges that disrupt Meridional Ocean Circulation (MOC), resulting in warming over Antarctica and cooling over the North Atlantic. These temperature trends are then reversed once MOC is re-established. Based on statistical analysis of paleo ice core and marine data, and the assumption that ice growth is mainly driven by insolation and CO_2 forcing, they suggested that the current interglacial will end within the next 1.5 kyr, on the condition that atmospheric CO_2 concentrations are less than 240 ±5 ppm.

Ganopolski et al. (2016) performed simulations with the CLIMBER-2 EMIC, by forcing it with varying orbital values and constant CO_2 concentrations of 240 and 280 ppm. Initially, simulations were run of a number of past periods and the Holocene-Future (-10–30 kyr AP), and only model configurations which simulated climate states that agreed with observations were selected, resulting in selection of four model configurations. Of these, all four model configurations predicted the end of the current interglacial several thousand years ago for CO_2 of 240 ppm, with large ice sheets at the present day. For CO_2 of 280 ppm, glaciation occurs at ~ 50 kyr AP in three of the simulations. The threshold CO_2 concentration which results in glacial inception was calculated, based on summer insolation at 65°N and using the coldest and warmest of the four model configurations. These models were then forced by orbital variations and CO_2 for a number of scenarios, including natural and fossil fuel emissions, for the next 100 kyr, with a glaciation being initiated when atmospheric CO_2 falls below the critical threshold for the given insolation value. None of the scenarios projected glacial inception within the next 50 kyr, due to low eccentricity. In the simulation with no CO_2 emissions, atmospheric CO_2 gradually decreases from the starting concentration of 280 ppm, undergoing some minor orbital-timescale variations, but the Earth system remains in an interglacial state for tens of thousands of years. For emissions of greater than 1000 Pg C, the next glacial inception is likely to be delayed for at least the next 100 kyr.

Brandefelt et al. (2013) used an EMIC and an GCM (LOVECLIM 1.2 and NCAR CCSM4) to run a selection of transient and snapshot simulations of future climate up to 61 kyr AP, for varying CO_2 forcings. The snapshot simulations were for orbital conditions at 17 kyr AP and 54 kyr AP, which coincide with minima in insolation forcing. For both models and time periods, simulations with CO_2 concentrations of 280 ppm or lower had cooler global annual average temperatures than the pre-industrial control simulation, whilst CO_2 values of 320–400 ppm were warmer. A general decrease in temperature at northern high latitudes was evident in LOVECLIM, particularly in the 280 ppm simulations, due to changes in the orbital parameters at these times. The decrease in temperature in the snapshot CCSM4 simulations was significantly larger than in the equivalent LOVECLIM simulations, due to the higher equilibrium climate sensitivity (ECS) in CCSM4. In the GCM simulations, the greatest cooling was experienced in northern high latitudes and the Southern Ocean. In the region of Central Europe, both LOVECLIM and CCSM4 appear to predict a cooling in annual average temperature of 0–2 °C for both time periods with a CO_2 concentration of 280 ppm, whilst LOVECLIM shows a warming of 0–2 °C for a CO_2 of 400 ppm. Transient simulations of climate from 0–61 kyr AP with atmospheric CO_2 of 200 and 400 ppm demonstrated global cooling at a similar time to the insolation minima, as a response to changes in orbital forcing.

4.5 Evolution until ~ 1 Myr AP

Model simulations of timescales of up to a million years generally follow very similar approaches to those modelling periods of up to 100 kyr; EMICs or simple conceptual models are used for transient simulations, and GCMs for snapshot simulations. The simulations generally take into account both atmospheric CO_2 and orbital forcings, as both are relevant on these timescales, and the main results relating to the onset of the next glaciation are detailed in Table 4.1 and illustrated in Figure 4.4.

The BIOCLIM project (Texier et al. 2003) employed two EMICs to simulate climate for the next 200 kyr. Orbital variation and three CO_2 scenarios were used to force the MoBidiC climate model (Louvain-la-Neuve), an improved and extended version of the LLN model, and CLIMBER-2.3-GREMLINS (an EMIC that includes an ice sheet). One natural CO_2 scenario and two fossil fuel CO_2 scenarios were included, for which atmospheric CO_2 trajectories including a low (3160 GtC) and high (5160 GtC) fossil fuel CO_2 contribution calculated using the response function of (Archer et al. 1997) were added to the natural CO_2 scenario (BIOCLIM 2001). The two models produced very different future climate evolutions under the different forcing scenarios. For the natural CO_2 scenario, MoBidiC simulated that the current interglacial will last until after 100 kyr AP, when continental ice will begin to build up. On the other hand, CLIMBER-GREMLINS projected that from 50 kyr AP American ice sheets will begin to grow, experiencing almost constant growth for the remaining 150 kyr period. No ice growth is simulated over Eurasia for this simulation. For the two fossil fuel scenarios, both models suggest that there will be no ice sheet cover in the Northern Hemisphere for most of the 200 kyr time span. At ~ 167 kyr AP, Northern Hemisphere ice sheet growth occurs in both models, at a faster rate for the scenario with a low fossil fuel contribution. However, no ice is projected to grow over Fennoscandia within the next 200 kyr by either model. This study also suggests that atmospheric CO_2 concentrations will remain above natural values until at least 200 kyr AP, as the CO_2 perturbation about pre-industrial values at the end of the simulation is still 60 ppm.

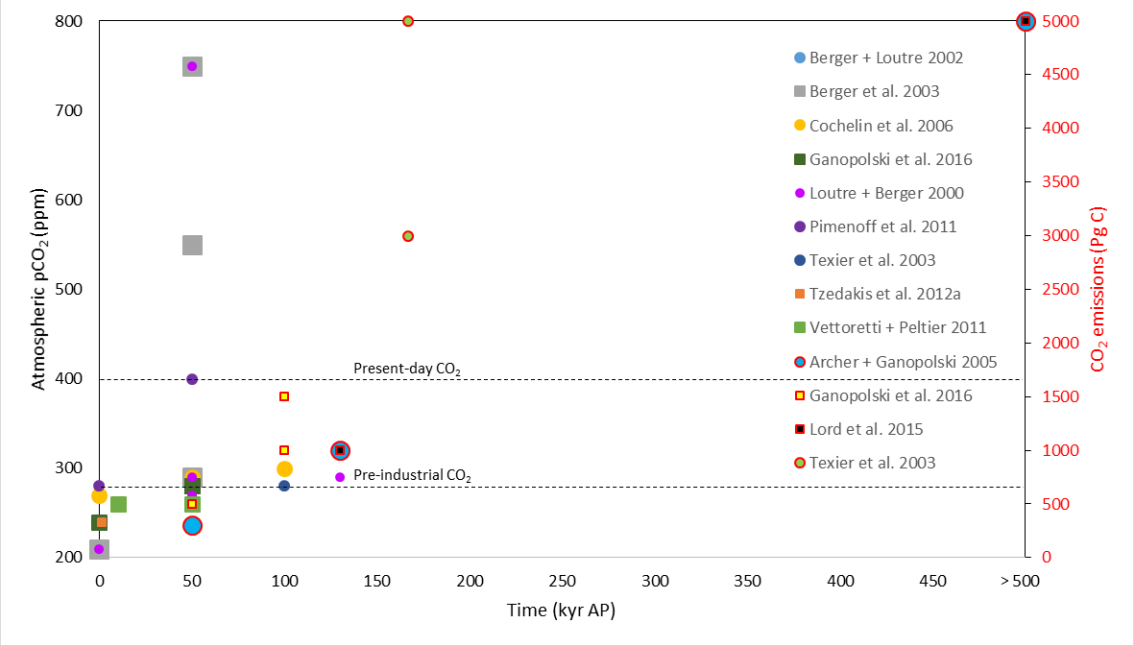

Fig 4.4: Approximate timing of the next glacial inception for different CO_2 scenarios, based on atmospheric CO_2 concentration (left axis) or fossil fuel CO_2 emissions (right axis; red border), for the studies described in this report.

Pre-industrial and present-day CO_2 concentrations are shown in black (dashed). Figure adapted from Figure 1-4 (p.14) of Brandefelt et al. (2013) (circles), but with the inclusion of some additional studies (squares).

Tab. 4.1: Approximate timing of the next glacial inception for different CO_2 scenarios, based on atmospheric CO_2 concentration or fossil fuel CO_2 emissions, for the studies described in this report.

Study	**Model**	**Atmospheric CO_2 concentration (ppm)**	**CO_2 emissions (Pg C)**	**Timing of next glacial inception (kyr AP)**
Imbrie and Imbrie (1980)	Non-linear			0
Loutre and Berger (2000b)	LLN 2-D NH	210		0
		220–270		~ 50
		280–290		> 130
		750 → 280		~ 50
Berger and Loutre (2002)	LLN 2-D NH	210		0
		280		~ 50
		750 → 280		~ 50
Berger et al. (2003)	LLN 2-D NH	210		0
		250–290		~ 50
		550 → 280		~ 50
		750 → 280		~ 50
Texier et al. (2003)	MoBidiC	280		> 100
			3000	~ 167
			5000	~ 167
Texier et al. (2003)	CLIMBER-2.3-GREMLNS	280		~ 50
			3000	~ 167
			5000	~ 167
Archer and Ganopolski (2005)	CLIMBER-2		300	~ 50
			1000	~ 130
			5000	> 500
Cochelin et al. (2006)	McGill Palaeoclimate Model	210–270		0
		280–290		~ 50
		300		> 100
Pimenoff et al. (2011)	CLIMBER-2	280		0
		400		~ 50
Tzedakis et al. (2012a)	Statistical	240		< 1.5
Lord et al. (2015)			1000	~ 130
			5000	> 500
Ganopolski et al. (2016)	CLIMBER-2	240		0
		280		~ 50
			500	~ 50
			1000	> 100
			1500	> 100

Archer and Ganopolski (2005) used the CLIMBER-2 model to calculate the critical insolation threshold leading to glacial inception, under a range of orbital and CO_2 forcings. They then simulated the evolution of atmospheric CO_2 over the next 500 kyr, following fossil fuel emissions of 300, 1000 and 5000 Pg C. In the 300 Pg C emissions scenario, the next glacial inception occurs after ~ 50 kyr AP, whilst for emissions of 1000 Pg C, inception is delayed until ~ 130 kyr AP. No glacial inception is projected to occur within the next 500 kyr for fossil fuel emissions of 5000 Pg C.

Lord et al. (2015) used an EMIC, the cGENIE Earth system model, to project the evolution of atmospheric CO_2 over the next 1 million years following a series of idealized pulse CO_2 emissions of 1000 to 10,000 Pg C. It was found that the CO_2 perturbation was long-lived taking hundreds of thousands of years for atmospheric CO_2 to be returned back towards pre-industrial values. Global annual mean SAT was found to continue to increase following peak atmospheric CO_2 concentration, to a maximum of approximately 2 °C and 7 °C above pre-industrial for the 1000 and 5000 Pg C emissions scenarios, before decreasing gradually over hundreds of thousands of years. Changes in the critical insolation value for glacial inception, derived by (Archer and Ganopolski 2005), were estimated based on the projected CO_2 trajectories. It was suggested that emissions of 1000 Pg C may be sufficient to delay the next glacial inception for approximately 130 kyr, whilst emissions of 5000 Pg C or higher may extend the current interglacial for at least the next 500 kyr.

A recent study by Lord et al. (In review) used the Hadley Centre GCM, HadCM3, to run an ensemble of snapshot simulations with varying orbital configurations and atmospheric CO_2 concentrations, in order to cover the range of possible climate conditions that may occur over the next million years. A statistical emulator was developed based on the climatic data for the GCM simulations. The emulator is able to interpolate between the GCM results, such that it can provide a prediction of the output that the GCM would produce if it were run using a particular input configuration. The benefits of the emulator are that it is able to rapidly simulate the 'continuous' long-term evolution of climate via a series of snapshot simulations (every 1 kyr for example) at the spatial resolution of an GCM, but with significantly lower computational cost than would be required to run an actual GCM. It was used to project the evolution of SAT and precipitation over the next 200 kyr at a number of European sites that have been identified as an adopted or proposed location for the geological disposal of solid radioactive wastes (Forsmark, Sweden and El Cabril, Spain), or simply as a reference location where a suitable site has not yet been identified (Switzerland and the UK). Four fossil fuel CO_2 scenarios were simulated, with emissions of 500, 1000, 2000 and 5000 Pg C. At the start of the simulations, variations in SAT and precipitation are dominated by CO_2 forcing due to its high atmospheric concentration, with peak warming of 4.1–12.2 °C for the Switzerland grid box occurring at 1 kyr AP. After this time, the warming slowly subsides along with the atmospheric CO_2 perturbation, and orbital timescale variations become more evident after ~ 20 kyr, particularly on the obliquity frequency until ~ 120 kyr, followed by the precessional frequency as eccentricity increases. Precipitation is also increased over the Switzerland grid box, and demonstrates fluctuations on an approximately precessional timescale. Both SAT and precipitation are still elevated above pre-industrial values at the end of the 200 kyr period. It should be noted that, whilst this study includes separate climate emulators for both present-day ice sheet configurations and reduced (partially melted) ice sheet configurations, the GCM does not include an ice sheet model, and hence the question of the onset of the next glaciation cannot be directly investigated. However, this issue is being researched as part of a subsequent project in collaboration with Posiva and SKB.

5 Synthesis and Summary

Here, a synthesis and summary of the preceding sections is given. In particular, there is a focus on the implications of the palaeoclimate and future simulations for the European region, and on the likely timing of the next glaciation. In this way, information of relevance to questions (Q1) and (Q4) in Section 1 is highlighted.

- The ultimate forcing of the climate system on timescales of 1 million years is astronomical variations associated with the Earth's orbit, and natural and anthropogenic changes in atmospheric CO_2.
- The Earth system mediates these forcings via a hugely complex web of feedback processes, resulting in complex behavior such as glacial-interglacial cycles.
- A hierarchy of numerical models have been developed to understand these processes, and predict past and future climate change, ranging from the simplest conceptual models to the most complex Earth system models, all of which have strengths and weaknesses.
- Work carried out in the three phases of the Palaeoclimate Modelling Intercomparison project (PMIP) offer valuable insights into the European and global climate of the Last Glacial Maximum (LGM). As PMIP has progressed through its four phases, more processes and more representative boundary conditions have been included in the models, and model resolution has increased. Simultaneously, improved understanding of potential proxy data reconstruction biases has allowed a reasonably consistent picture between models and data to be built up (Ramstein et al. 2007; Hargreaves et al. 2013). The most up to date PMIP3 simulations and model-data comparisons are presented by Harrison et al. (2014), and are summarised in Figure 5.1. Over Europe, the largest remaining discrepancies are in the cold month temperature over western Europe, in that the models are still not as cold as the proxies indicate, an area that also has its precipitation affected by changes in Atlantic storm tracks. The Alps show similar patterns and discrepancies to western Europe, however it is not practical to assess changes on scales much below the regional/sub-continental (Hargreaves et al. 2013), so precise estimations for the Alps and Switzerland require caution. These CMIP5/PMIP3/IPCC AR5 simulations are available for download from the PMIP database (https://pmip3.lsce.ipsl.fr/database). Simulations of the LGM in the framework of PMIP4 (and ultimately IPCC AR6) are in the process of being finalised (Kageyama et al., in review). It is likely that the models that carry out these simulations will be improved on those in PMIP3 primarily due to (a) improved boundary conditions such as the routine inclusion of desert dust forcing and improved ice sheet distribution, (b) the use of models that simulate the Earth system more completely, through the inclusion for example of biogeochmical cycles, and (c) the use of models that run at higher resolution, and as such will begin to resolve some aspects of the Alpine climate.

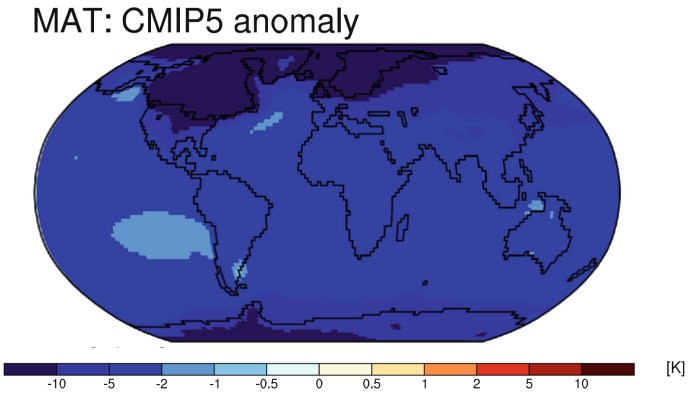

Fig. 5.1: Simulated change (anomalies between the experiment and the pre-industrial control) in mean annual temperature (MAT) at the Last Glacial Maximum (LGM) for the CMIP5 ensemble.

The ocean temperatures are sea-surface temperature, except over areas with sea ice where air temperature is used.

- In the same way as for the LGM, the most state-of-the-art and comprehensive summary of mid-Holocene simulations is associated with PMIP3, and is summarised on a global scale by Harrison et al. (2014). Figure 5.2 provides a summary of the reconstructed and PMIP3 ensemble mean changes in seasonal temperature and precipitation over Europe for the mid-Holocene. For both summer and winter, the reconstructions suggest the Alps warmed by 1-2 °C. The PMIP ensemble shows good agreement within reconstruction uncertainty with the summer temperatures over the Alps (2 °C of warming), but for the winter the ensemble does not capture the warming relative to the pre-industrial. Reconstructions suggest slightly reduced precipitation in summer and slightly increased precipitation in winter over the Alps, both up to approx. 10 mm month^{-1}. The model ensemble does not show any major trends in either season, but this result lies on the margin of the reconstruction uncertainty and is within the uncertainty for the southern and central Alps. Due to the relatively small signal-to-noise ratio (compared to the LGM for example), the MH presents quite a challenge to the modelling community in terms of spatial patterns of reconstructed change. The north-south gradient across Europe is not captured correctly and some processes are misrepresented by models, likely related to large scale circulation changes in the region. The uncertainties in both the modelling and data of the mid-Holocene are sufficiently large for Hargreaves et al (2013) to conclude that on a global scale the models fail to reproduce the observed changes with any degree of skill.
- Very few of the modelling studies of the Last Interglacial (LIG) focus specifically on the climate of Europe, due to the greater uncertainties in other regions and processes, in particular the high latitudes sea level change. However, Lunt et al. (2013) carried out a multi-model intercomparison of a combination of EMIC and GCM simulations of the Last Interglacial, which probably represent the most up to date summary of LIG modelling; comparing the multi-model mean to reconstructions (Figure 3.3) shows that over Europe there is a general warming of up to approx. 1 °C, which is agreed upon by the majority of the models and the data. There are one or two data points that suggest greater temperature increases in the Alps, but mostly the changes appear in line with the rest of Europe. However, the LIG proxy dataset has been shown to be biased, in particular in terms of its weak age control, and robust model-data comparisons of the LIG are currently limited to the North Atlantic and Southern Ocean (Capron et al. 2015; Stone et al. 2016). The numerical

data from the Lunt et al. (2013) simulations can be downloaded from the Supplementary Information of that paper.

- Transient simulations of the Holocene have shown that over short time scales (from decades to centuries) total solar irradiance and volcanic forcing are important for global climate, but for longer time periods they are poorly constrained and generally appear to be of smaller magnitude relative to orbital changes (and subsequent feedback processes) and CO_2 forcing. On timescales of 1000 years, such as for the Last Millennium, internal variability is often of a similar magnitude to the response to external forcing, and as such model-data comparisons are extremely challenging.

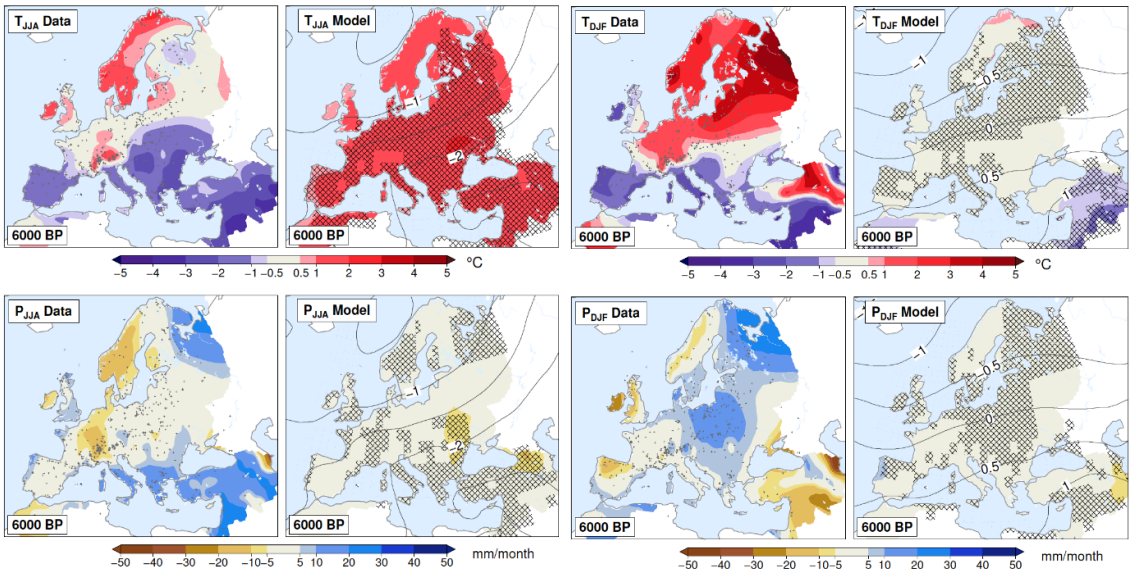

Fig. 5.2: Reconstructed and PMIP3 ensemble mean temperature and precipitation anomalies for the mid-Holocene.

a, b) the reconstructed and modelled summer temperature anomaly respectively; c, d) as a, b but for winter; e, f) as a, b but for precipitation; g, h) as c, d but for precipitation. Hatching shows where the ensemble mean lies outside the range of uncertainty in the reconstructions. Figure from Mauri et al. 2014.

- The last deglaciation represents a considerable challenge as it is at the limit of length of simulation that can be carried out with a full complexity GCM. In this context, the NCAR group have been pioneers, through the 'TraCE-21ka' programme, including simulation of Alpine glaciers through the deglaciation (Liu et al. 2009; Shakun et al. 2012; He et al. 2013; Shakun et al. 2015; see Figure 5.3). Large reorganisations of the Earth system (such as the last deglaciation) have a complex chain of mechanisms (e.g. ocean circulation, overturning and CO_2 outgassing) driving the observed regional and temporal patterns that are not trivial to unpick. Although fully coupled GCMs are excellent tools for assessing the interaction between processes, there is still a large degree of uncertainty behind the dominant processes, due in part to the small number of different fully coupled GCMs that have been applied to this time period due to the computational expense. However, this may change in the future because in the context of PMIP4, new simulations of the deglaciation are being proposed (Ivanovic et al. 2016), and it is expected that several modelling groups will take

part. In addition, the German PalMod project (www.palmod.de) aims to simulate a full glacial cycle in transient mode and with a comprehensive ESM, allowing full interactions between the physical and biogeochemical components of the Earth system, including ice sheets.

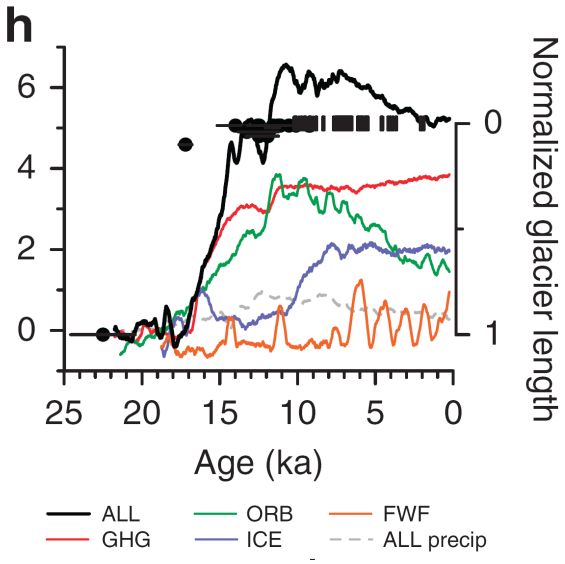

Fig. 5.3: Modelled climate and reconstructed glacier fluctuations in the Alps.

Modelled temperatures from the single-forcing (colored lines) and ALL (black line) simulations from the transient TrACE model simulations (Liu et al. 2009), as well as normalized moraine positions (black dots). Error bars (1 sigma) give the standard.deviation of the boulder ages plus the production-rate uncertainty, added in quadrature. Local modelled summer temperatures are shown on the left-hand y-axis (degrees C). Modelled precipitation from the ALL simulation (grey dashed line) has been scaled to temperature as -25% = 1 °C, and is shown for local winter All model time series are 500-year moving averages and given as anomalies from 19 ka. y-axis on left is temperature and y-axis on right is normalized moraine position, which have been scaled to align maximum (1) and minimum (0) glacier extent with simulated Last Glacial Maximum and modern temperatures, respectively. Adapted from Shakun et al (2015).

- Three main approaches for modelling the past 200 kyr have been discussed in this report: the simple 2D transient modelling approaches from the 1990s and early 2000s (e.g. Figure 3.6a), transient EMIC modelling coupled to ice sheet models (e.g. Figure 3.6b) and attempts to model the full complexity of the system with GCMs (e.g. Figure 3.6c). Although other examples of each approach exist, these studies were selected because they are reasonably representative. Over this time period orbital cycles appear as the main influence for ice sheet growth and decline, with further forcing/feedback from CO_2 to produce global temperature variations. The 100 kyr orbital cycle can be non-linearly reproduced by simple models inducing feedback processes with ice and snow albedo, dust and isostatic deformation. However, fitting the magnitude and rates of change shown by the oxygen isotope reconstructions requires the inclusion of other forcing changes, such as varying CO_2. Although there is qualitatively good agreement between these simple models and global proxy reconstructions, the few higher complexity studies with GCMs show there is a large degree of subtlety in the temperature responses that are currently unable to be categorised fully by the available data or models. In these cases, the geometry of ice sheets and interconnections through ocean circulation become important. The lack of millennial scale variations near the end of the last glacial cycle show that processes that can be included in shorter transient simulations are missing from these simplified modelling approaches.
- In general, conceptual model studies of the last 2 million years suggest that the glacial-interglacial cycles are linked to orbital variations, and atmospheric CO_2 concentration. Various mechanisms have been suggested to explain the timing of transitions and the duration of the different climate states, including orbital forcing alone (e.g. Huybers and Wunsch 2005; Imbrie et al. 2011; Parrenin and Paillard 2012), and a combination of atmospheric CO_2 and orbital forcing (e.g. Pisias and Shackleton 1984; Archer and Ganopolski 2005). A number of studies have proposed that feedbacks in the climate system may play a role in initiating glaciations or deglaciations, such as deep ocean stratification (Paillard and Parrenin 2004) and deep ocean temperature (Saltzman and Maasch 1991; Saltzman and Maasch 1990). It has also been suggested that the size of the ice sheet may contribute to triggering a deglaciation, with larger ice sheets requiring a relatively small increase in insolation to initiate glacial retreat (e.g. Raymo 1997; Parrenin and Paillard 2003; Abe-Ouchi et al. 2013). Overall, it is clear that the mechanisms driving the glacial-interglacial cycles are not yet fully understood. At present, there is no model that is able to simulate glacial-interglacial cycles satisfactorily given purely an orbital forcing, primarily due to uncertainties in simulating the global carbon cycle and the response of ice sheets to forcing. However, progress is being made rapidly, and the CLIMBER model in particular may be close to accurately reproducing glacial-interglacial cycles (Andrey Ganopolski, personal communication). Whilst simple conceptual models may be able to represent the features of paleo data well, they need to be used in conjunction with simulations using more complex physically-based models, in order to improve our understanding of how long-term climate has evolved in the past, and thus provide insights into how it may also change in the future.
- Future climate projections are ultimately controlled by two external forcings – astronomical forcing (which is very well known) and CO_2 concentrations (which are not well known). Uncertainties in CO_2 come from sociological/political/technological uncertainties associated with the rate of future emissions of carbon, and environmental uncertainties associated with the lifetime of atmospheric CO_2. In addition, future societies may choose to actively engage in geoengineering, and reduce atmospheric CO_2 through technological means.

- On timescales of 100–300 years, the IPCC AR5 report provides a comprehensive summary of future climate changes given various emissions scenarios. Regional changes over Europe have also been studied in depth in the CORDEX program, and model output from the CORDEX RCMs is available from their data portal (www.cordex.org/output.html). The results of a number of studies suggests that the IPCC Special Report on Emission Scenarios (SRES; (Nakićenović et al. 2000)) B1, A1B and A2 CO_2 scenarios, which cover low to high emissions, result in annual mean warming in Central Europe of approximately 1–3 °C (Mikolajewicz et al. 2007), with regional warming of 1–1.5 °C for every 1 °C of global annual average warming (National Research Council 2011).
- A range of studies have addressed the evolution of future climate on longer timescales of up to 50,000 years. On these timescales, the CO_2 forcing generally dominates over orbital forcing. A range of model complexities and modelling approaches have been employed, depending on the length of time and aspect of climate being considered, usually with the aim of addressing long-term warming, ocean circulation, and/or sea level change (e.g. Winkelmann et al. 2015). The simulations generally agree that mean global and European temperatures are likely to continue to increase for at least the remaining part of the 21st century, with the ultimate extent and timescale of warming in the following thousands of years being dependent on future anthropogenic CO_2 emissions and the natural carbon cycle. An increase in atmospheric CO_2 concentration to 2x and 4x pre-industrial values appears to result in regional warming of approximately 2–5 °C after 1 kyr in the European region, (Vizcaino et al. 2008), and 8–10 °C following equilibration after 6 kyr for 4x CO2 (Li et al. 2013). Finally, 3000 year long simulations with emissions of 15,000 Pg C performed by Lenton et al. (2006), appear to show an increase in Central European SAT of 9–12 °C. The range in warming estimates may have a number of causes, including the use of different models, different CO_2 assumptions and different modelling approaches, etc.
- On longer timescales, orbital forcing begins to play an ever-increasingly important role. The next glacial inception is generally projected to occur approximately 50 kyr AP under pre-industrial CO_2 concentrations. However, many studies suggest that atmospheric CO_2 concentrations, and thus mean global temperatures, may remain elevated above natural values due to fossil fuel emissions for hundreds of thousands of years. This may result in the onset of the next glaciation being delayed for tens of thousands of years or longer, depending on the degree of warming. The studies, summarized in Table 4.1 and Figure 4.4, generally agree that in the absence of anthropogenic CO_2 forcing and with natural CO_2 concentrations lower than pre-industrial values (< 280 ppm), the current interglacial may come to an end imminently, or that glaciation may have already begun several thousand years ago. On the other hand, when the natural CO_2 concentration is close to the pre-industrial value (~ 280 ppm) or higher, or when fossil fuel CO_2 emissions are taken into account, the timing of the next glacial inception is found to be dependent on the concentration of atmospheric CO_2, with inception within the next 100 kyr decreasingly likely as concentrations increase.

6 References

Abe-Ouchi, A., Saito, F., Kawamura, K., Raymo, M.E., Okuno, J., Takahashi, K. & Blatter, H. 2013. Insolation-driven 100,000-year glacial cycles and hysteresis of ice-sheet volume. Nature, 500, 190-+, DOI: 10.1038/nature12374.

Archer, D. 2005. Fate of fossil fuel CO_2 in geologic time. *Journal of Geophysical Research-Oceans,* 110**,** DOI: 10.1029/2004jc002625.

Archer, D. & Ganopolski, A. 2005. A movable trigger: Fossil fuel CO2 and the onset of the next glaciation. Geochemistry Geophysics Geosystems, 6, Q05003, DOI: 10.1029/2004gc000891.

Archer, D., Kheshgi, H. & Maier-Reimer, E. 1997. Multiple timescales for neutralization of fossil fuel CO_2. *Geophysical Research Letters,* 24**,** 405-408**,** DOI: 10.1029/97gl00168.

Atwood, A.R., WU, E., Frierson, D.M.W., Battisti, D.S. & Sachs, J.P. 2016. Quantifying climate forcings and feedbacks over the Last Millennium in the CMIP5-PMIP3 models. *Journal of Climate*, 29, pp. 1161-1178, DOI: 10.1175/JCLI-D-15-0063.1.

Augustin, L., Barbante, C., Barnes, P.R.F., Barnola, J.M., Bigler, M., Castellano, E., Cattani, O., Chappellaz, J., Dahljensen, D., Delmonte, B., Dreyfus, G., Durand, G., Falourd, S., Fischer, H., Fluckiger, J., Hansson, M.E., Huybrechts, P., Jugie, R., Johnsen, S.J., Jouzel, J., Kaufmann, P., Kipfstuhl, J., Lambert, F., Lipenkov, V.Y., Littot, G.V.C., Longinelli, A., Lorrain, R., Maggi, V., Masson-Delmotte, V., Miller, H., Mulvaney, R., Oerlemans, J., Oerter, H., Orombelli, G., Parrenin, F., Peel, D.A., Petit, J.R., Raynaud, D., Ritz, C., Ruth, U., Schwander, J., Siegenthaler, U., Souchez, R., Stauffer, B., Steffensen, J.P., Stenni, B., Stocker, T.F., Tabacco, I.E., Udisti, R., Van De Wal, R.S.W., Van Den Broeke, M., Weiss, J., Wilhelms, F., Winther, J.G., Wolff, E.W., Zucchelli, M. & Members, E.C. 2004. Eight glacial cycles from an Antarctic ice core. Nature, 429, 623-628, DOI: 10.1038/nature02599.

Bakker, P., Stone, E.J., Charbit, S., Gröger, M., Krebs-Kanzow, U., Ritz, S.P., Varma, V., Khon, V., Lunt, D.J., Mikolajewicz, U., Prange, M., Renssen, H., Schneider, B. & Schulz, M. 2013 Last interglacial temperature evolution – a model inter-comparison. *Climate of the Past*, 9, 605–619, DOI: 10.5194/cp-9-605-2013.

Bakker, P. Clark, P.U., Golledge, N.R., Schmittner, A. & Weber, M.E. 2017. Centennial-scale Holocene climate variations amplified by Antarctic Ice Sheet discharge. *Nature*, 541, pp. 72-76, DOI: 10.1038/nature20582.

Barker, S., Knorr, G., Vautravers, M.L., Diz, P. & Skinner, L.C. 2010. Extreme deepening of the Atlantic overturning circulation during deglaciation. *Nature Geoscience*, 3, pp. 567-571, DOI: 10.1038/NGEO921.

Bartlein, P., Harrison, S., Brewer, S., Connor, S., Davis, B., Gajewski, K., Guiot, J., Harrison-Prentice, T., Henderson, A., Peyron, O., Prentice, I.C., Scholze, M., Seppa A, H., Shuman, B., Sugita, S., Thompson, R.S., Viau, A.E., Williams, J., & WU, H. 2011. Pollen-based continental climate reconstructions at 6 and 21 ka: a global synthesis. *Climate Dynamics*, 37, pp. 775–802.

Bassinot, F.C., Labeyrie, L.D., Vincent, E., Quidelleur, X., Shackleton, N.J. & Lancelot, Y. 1994. The astronomical theory of climate and the age of the Brunhes-Matuyama magnetic reversal. Earth and Planetary Science Letters, 126, 91-108, DOI: 10.1016/0012-821x(94)90244-5.

Berdahl, M. & Robock, A. 2013. Northern Hemispheric cryosphere response to volcanic eruptions in the Paleoclimate Modeling Intercomparison Project 3 last millennium simulations. *Journal of Geophysical Research: Atmospheres*, 118, pp. 12359-12370, DOI: 10.1002/2013JD019914.

Berger, A., Gallee, H., Fichefet, T., Marsiat, I. & Tricot, C. 1990. Testing the astronomical theory with a coupled climate-ice-sheet model. *Palaeogeography, Palaeoclimatology, Palaeoecology. Global and Planetary Change Section*, 89, 3, pp. 125-141.

Berger, A. & Loutre, M.F. 1997. Long-term variations in insolation and their effects on climate, the LLN experiments. *Surveys in Geophysics*, 18, pp. 147-161.

Berger, A. & Loutre, M.F. 2002. An exceptionally long interglacial ahead? *Science,* 297**,** 1287-1288**,** DOI: 10.1126/science.1076120.

Berger, A., Loutre, M.F. & Crucifix, M. 2003. The Earth's climate in the next hundred thousand years (100 kyr). *Surveys in Geophysics,* 24**,** 117-138**,** DOI: 10.1023/A:1023233702670.

Bioclim 2001. Deliverable D3: Global climatic features over the next million years and recommendation for specific situations to be considered, Agence Nationale pour la Gestion des Dechets Radioactifs (ANDRA), Parc de la Croix Blanche, 1/7 rue Jean Monnet, 92298, Châtenay-Malabry, France. Available from: www.andra.fr/bioclim/pdf/d3.pdf.

Bioclim 2001a. Deliverable D4/5: Global climatic characteristics, including vegetation and seasonal cycles over Europe, for snapshots over the next 200,000 years, Agence Nationale pour la Gestion des Dechets Radioactifs (ANDRA), Parc de la Croix Blanche, 1/7 rue Jean Monnet, 92298, Châtenay-Malabry, France. Available from: http://www.andra.fr/bioclim/pdf/d45.pdf.

Bioclim 2003b. Deliverable 6a: Regional climatic characteristics for the European sites at specific times: the dynamical downscaling, Agence Nationale pour la Gestion des Dechets Radioactifs (ANDRA), Parc de la Croix Blanche, 1/7 rue Jean Monnet, 92298, Châtenay-Malabry, France. Available from: http://www.andra.fr/bioclim/pdf/d6a.pdf.

Bonfils, C., Noblet-Ducoudré, N., Guiot, J. & Bartlein, P. 2004. Some mechanisms of mid-Holocene climate change in Europe, inferred from comparing PMIP models to data. *Climate Dynamics*, 23, pp. 79-98, DOI: 10.1007/s00382-004-0425-x.

Braconnot, P., Otto-Bliesner, B., Harrison, S., Joussaume, S., Peterchmitt, J.Y., Abe-Ouchi, A., Crucifix, M, Driesschaert, E., Fichefet, T., Hewitt, C.D, Kageyama, M., Kitoh, A., Laîné, A., Loutre, M.F., Marti, O., Merkel, U., Ramstein, G., Valdes, P.J., Weber, S.L., Yu, Y. & Zhao, Y. 2007 Results of PMIP2 coupled simulations of the Mid-Holocene and Last Glacial Maximum – Part 1: experiments and large-scale features. *Climate of the Past*, 3, pp. 261-277.

Braconnot, P., Harrison, S.P., Kageyama, M., Bartlein, P.J., Masson-Delmotte, V., Abe-Ouchi, A., Otto-Bliesner, B. & Zhao, Y. 2012. Evaluation of climate models using palaeoclimatic data. *Nature Climate Change*, 2, pp. 417-424, DOI: 10.1038/NCLIMATE1456.

Brandefelt, J., Näslund, J.-O., Zhang, Q. & Hartikainen, J. 2013. The potential for cold climate and permafrost in Forsmakr in the next 60,000 years, *SKB Report, TR-13-04.* Svensk Kärnbränslehantering AB, Stockholm, Sweden. Available from: www.skb.com/publication/2652151/TR-13-04.pdf.

Brewer, S., Guiot, J. & Torre, F. 2007. Mid-Holocene climate change in Europe: a data-model comparison. *Climate of the Past*, 3, pp. 499-512.

Broecker, W.S. 1998. Paleocean circulation during the last deglaciation: A bipolar seesaw? *Paleoceanography*, 13, 2, pp. 119-121.

Calov, R., Ganopolski, A., Kubatzki, C. & Claussen, M. 2009. Mechanisms and time scales of glacial inception simulated with an Earth system model of intermediate complexity. *Climate of the Past*, 5, pp. 245-258.

Capron, E., Govin, A., Stone, E.J., Masson-Delmotte, V., Mulitza, S., Otto-Bliesner, B., Rasmussed, T.L., Sime, L.C., Waelbroeck, C. & Wolff, E.W. 2014. Temporal and spatial structure of multi-millennial temperature changes at high latitudes during the Last Interglacial. *Quaternary Science Reviews*, 103, pp. 116-133, DOI: 10.1016/j.quascirev.2014.08.018.

Charbit, S., Paillard, D. & Ramstein, G. 2008. Amount of CO_2 emissions irreversibly leading to the total melting of Greenland. *Geophysical Research Letters,* 35, L12503**,** DOI: 10.1029/2008gl033472.

Clark, P.U., Shakun, J.D., Marcott, S.A., Mix, A.C., Eby, M., Kulp, S., Levermann, A., Milne, G.A., Pfister, P.L., Santer, B.D., Schrag, D.P., Solomon, S., Stocker, T.F., Strauss, B.H., Weaver, A.J., Winkelmann, R., Archer, D., Bard, E., Goldner, A., Lambeck, K., Pierrehumbert, R.T. & Plattner, G.K. 2016. Consequences of twenty-first-century policy for multi-millennial climate and sea-level change. *Nature Climate Change,* 6**,** 360-369**,** DOI: 10.1038/Nclimate2923.

Claussen, M., Kubatzki, C., Brovkin, V. & Ganopolski, A. 1999. Simulation of an abrupt change in Saharan vegetation in the mid-Holocene. *Geophysical Research Letters*, 26, 14, pp. 2037-2040.

Climap 1981. Seasonal reconstructions of the earth's surface at the Last Glacial Maximum. Geophysical Society of America Map Chart Series MC-36, 1-18.

Cochelin, A.S.B., Mysak, L.A. & Wang, Z.M. 2006. Simulation of long-term future climate changes with the green McGill paleoclimate model: The next glacial inception. *Climatic Change,* 79**,** 381-401**,** DOI: 10.1007/s10584-006-9099-1.

Colbourn, G., Ridgwell, A. & Lenton, T. 2015. The time scale of the silicate weathering negative feedback on atmospheric CO_2. *Global Biogeochemical Cycles,* 29**,** 583-596**,** DOI: 10.1002/2014GB005054.

Crowley, T.J. 1992. North Atlantic deep water cools the Southern Hemisphere. *Paleo-ceanography*, 7, pp. 489-497.

Crowley, T.J. 2000. Causes of climate change over the past 1000 years. *Science*, 289, 5477, pp. 270-277, DOI: 10.1126/science.289.5477.270.

Crucifix, M. 2013. Why could ice ages be unpredictable? Climate of the Past, 9, 2253-2267, DOI: 10.5194/cp-9-2253-2013.

Crucifix, M. & Loutre, M.F. 2002. Transient simulations over the last interglacial period (126-115 kyr BP): feedback and forcing analysis. *Climate Dynamics*, 19, pp. 417-433, DOI: 10.1007/s00382-002-0234-z.

Crucifix, M., Loutre, M.F., Tulkens, P., Fichefet, T. & Berger, A. 2002. Climate evolution during the Holocene: a study with an Earth system model of intermediate complexity. *Climate Dynamics*, 19, pp. 43-60, DOI: 10.1007/s00382-001-0208-6.

De Saedeleer, B., Crucifix, M. & Wieczorek, S. 2013. Is the astronomical forcing a reliable and unique pacemaker for climate? A conceptual model study. Climate Dynamics, 40, 273-294, DOI: 10.1007/s00382-012-1316-1.

Deblonde, G. & Peltier, W.R. 1991. A one-dimensional model of continental ice volume fluctuations through the Pleistocene - Implications for the origin of the Mid-Pleistocene climate transition. Journal of Climate, 4, 318-344, DOI: 10.1175/1520-0442(1991)004<0318:Aodmoc>2.0.Co;2.

Denton, G.H. & Hughes, T.J. 1983. Milankovitch theory of ice ages - Hypothesis of ice-sheet linkage between regional insolation and global climate. Quaternary Research, 20, 125-144, DOI: 10.1016/0033-5894(83)90073-X.

Eby, M., Zickfeld, K., Montenegro, A., Archer, D., Meissner, K.J. & Weaver, A.J. 2009. Lifetime of anthropogenic climate change: millennial time scales of potential CO_2 and surface temperature perturbations. *Journal of Climate,* 22**,** 2501-2511**,** DOI: 10.1175/2008jcli2554.1.

Fernández-Donado, L., González-Rouco, J.F., Raible, C.C., Ammann, C.M., Barriopedro, D., García-Bustamante, E., Jungclaus, J.H., Lorenz, S.J., Luterbacher, J., Phipps, S.J., Servonnat, J., Swingedouw, D., Tett, S.F.B., Wagner, S., Yiou, P. & Zorita, E. 2013. Large-scale temperature response to external forcing in simulations and reconstructions of the last millennium. *Climate of the Past*, 9, pp. 393-421, DOI: 10.5194/cp-9-393-2013.

Friedlingstein, P., Solomon, S., Plattner, G.K., Knutti, R., Ciais, P. & Raupach, M.R. 2011. Long-term climate implications of twenty-first century options for carbon dioxide emission mitigation. *Nature Climate Change,* 1**,** 457-461**,**

Frolicher, T.L., Winton, M. & Sarmiento, J.L. 2014. Continued global warming after CO_2 emissions stoppage. *Nature Climate Change,* 4**,** 40-44**,** DOI: 10.1038/Nclimate2060.

Gallee, H., Van Ypresele, J.P., Fichefet, T., Marsiat, I., Tricot, C. & Berger, A. 1992. Simulation of the Last Glacial Cycle by a Coupled, Sectorially Averaged Climate-Ice Sheet Model 2) Response to Insolation and CO_2 Variations. *Journal of Geophysical Research*, 97, D14, pp. 15,713-15,740.

Ganopolski, A., Rahmstorf, S., Petoukhov, V.& Claussen, M. 1998. Simulations of modern and glacial climates with a coupled global model of intermediate complexity. *Nature*, 391, pp. 351-356.

Ganopolski, A. & Rahmstorf, S. 2001 Rapid changes of glacial climate simulated in a coupled climate model. *Nature*, 409, pp. 153-158.

Ganopolski, A., Calov, R. & Claussen, M. 2010. Simulation of the last glacial cycle with a couple climate-ice sheet model of intermediate complexity. *Climate of the Past*, 6, pp. 229-244.

Ganopolski, A. & Calov, R. 2011. The role of orbital forcing, carbon dioxide and regolith in 100 kyr glacial cycles. Climate of the Past, 7, 1415-1425, DOI: 10.5194/cp-7-1415-2011.

Ganopolski, A., Winkelmann, R. & Schellnhuber, H.J. 2016. Critical insolation-CO2 relation for diagnosing past and future glacial inception. Nature, 529, 200-203, DOI: 10.1038/nature16494.

Goosse, H., Brovkin, V., Fichefet, T., Haarsma, R., Huybrechts, P., Jongma, J., Mouchet, A., Selten, F., Barriat, P. -Y., Campin, J. -M., Deleersnijder, E., Driesschaert, E., Goelzer, H., Janssens, I., Loutre, M. -F., Morales Maqueda, M.A., Opsteegh, T., Mathieu, P. -P., Munhoven, G., Pettersson, E.J., Renssen, H., Roche, D.M., Schaeffer, M., Tartinville, B., Timmermann, A. & Weber, S.L. 2010. Description of the Earth system model of intermediate complexity LOVECLIM version 1.2. *Geoscientific Model Development*, 3, pp. 603-633, DOI: 10.5194/gmd-3-603-2010.

Hargreaves, J.C., Annan, J.D., Ohgaito, R., Paul, A. & Abe-Ouchi, A. 2013. Skill and reliability of climate model ensembles at the Last Glacial Maximum and mid-Holocene. *Climate of the Past*, 9, pp. 811-823, DOI: 10.5194/cp-9-811-2013.

Harrison, S.P., Bartlein, P.J., Brewer, S., Prentice, I.C., Boyd, M., Hessler, I., Holmgren, K., Izumi, K. & Willis, K. 2014. Climate model benchmarking with glacial and mid-Holocene climates. *Climate Dynamics*, 43, pp. 671-688, DOI: 10.07/s00382-013-1922.

HE, F., Shakun, J.D., Clark, P.U., Carlson, A.E., Liu, F., Otto-Bliesner, B.L. & Kutzbach, J.E. 2013. Northern Hemisphere forcing of Southern Hemisphere climate during the last deglaciation. *Nature*, 494, pp. 81-85, DOI: 10.1038/nature11822

Hofer, D., Raible, C.C., Merz, N., Dehnert, A. & Kuhlemann, J. 2012a. Simulated winter circulation types in the North Atlantic and European region for preindustrial and glacial conditions. *Geophysical Research Letters*, 39, L15805, DOI:10.1029/2012GL052296

Hofer, D., Raible, C.C., Dehnert, A. & Kuhlemann, J. 2012b. The impact of different glacial boundary conditions on atmospheric dynamics and precipitation in the North Atlantic region. *Climate of the Past*, 8, 935-949.

Huybers, P. 2009. Pleistocene glacial variability as a chaotic response to obliquity forcing. *Climate of the Past*, 5, 481-488.

Huybers, P. & Wunsch, C. 2005. Obliquity pacing of the late Pleistocene glacial terminations. *Nature*, 434, 491-494, DOI: 10.1038/nature03401.

Huybrechts, P. & De Wolde, J. 1999. The dynamic response of the Greenland and Antarctic ice sheets to multiple-century climatic warming. *Journal of Climate,* 12**,** 2169-2188**,** DOI: 10.1175/1520-0442(1999)012<2169:Tdrotg>2.0.Co;2.

Huybrechts, P., Goelzer, H., Janssens, I., Driesschaert, E., Fichefet, T., Goosse, H. & Loutre, M.F. 2011. Response of the Greenland and Antarctic Ice Sheets to Multi-Millennial Greenhouse Warming in the Earth System Model of Intermediate Complexity LOVECLIM. *Surveys in Geophysics,* 32**,** 397-416**,** DOI: 10.1007/s10712-011-9131-5.

Imbrie, J. & Imbrie, J.Z. 1980. Modeling the Climatic Response to Orbital Variations. Science, 207, 943-953, DOI: 10.1126/science.207.4434.943.

Imbrie, J.Z., Imbrie-Moore, A. & Lisiecki, L.E. 2011. A phase-space model for Pleistocene ice volume. Earth and Planetary Science Letters, 307, 94-102, DOI: 10.1016/j.epsl.2011.04.018.

IPCC 2013. Climate Change 2013: The Physical Science Basis. Contribution of Working Group I to the Fifth Assessment Report of the Intergovernmental Panel on Climate Change. *In:* Stocker, T.F., Qin, D., Plattner, G.K., Tignor, M., Allen, S.K., Boschung, J., Nauels, A., Xia, Y., Bex, V. & Midgley, P.M. (eds.). Cambridge, UK and New York, USA: Cambridge University Press.

Ivanovic, R.F., Gregoire, L.J., Kageyama, M., Roche, D.M., Valdes, P.J., Burke, A., Drummond, R., Peltier, W.R. & Tarasov, L. 2016 Transient climate simulations of the deglaciation 21-9 thousand years before present (version 1) – PMIP4 Core experiment design and boundary conditions. *Geoscientific Model Development*, 9, pp. 2563-2587, DOI: 10.5194/gmd-9-2563-2016.

Jacob, D., Petersen, J., Eggert, B., Alias, A., Christensen, O.B., Bouwer, L.M., Braun, A., Colette, A., Deque, M., Georgievski, G., Georgopoulou, E., Gobiet, A., Menut, L., Nikulin, G., Haensler, A., Hempelmann, N., Jones, C., Keuler, K., Kovats, S., Kroner, N., Kotlarski, S., Kriegsmann, A., Martin, E., Van Meijgaard, E., Moseley, C., Pfeifer, S., Preuschmann, S., Radermacher, C., Radtke, K., Rechid, D., Rounsevell, M., Samuelsson, P., Somot, S., Soussana, J.F., Teichmann, C., Valentini, R., Vautard, R., Weber, B. & Yiou, P. 2014. EURO-CORDEX: new high-resolution climate change projections for European impact research. *Regional Environmental Change,* 14**,** 563-578**,** DOI: 10.1007/s10113-013-0499-2.

Jickells, T.D., An, Z.S., Andersen, K.K, Baker, A.R., Bergametti, G., Brooks, N., CAO, JJ., Boyd, P.W., Duce, R.A., Hunter, K.A., Kawahata, H., Kubilay, N., Laroche, J., Liss, P.S., Mahowald, N., Prospero, J.M., Ridgwell, A.J., Tegen, I. & Torres, R. 2005. Global iron connections between desert dust, ocean biogeochemistry, and climate. *Science*, 308, pp. 67-71, DOI: 10.1126/science.1105959.

Jost, A., Lunt, D.J., Kageyama, M., Abe-Ouchi, A., Peyron, O., Valdes, P.J. & Ramstein, G. 2005. High-resolution simulations of the last glacial maximum climate over Europe: a solution to discrepancies with continental palaeoclimatic reconstructions? *Climate Dynamics*, 24, pp. 577-590, DOI: 10.1007/s00382-005-0009-4.

Joussaume, S. & Taylor, K. 1995. Status of the Paleoclimate Modelling Intercomparison Project (PMIP). *Proceedings of the First International AMIP Scientific Conference*, Monterey, CA, WRCP, Tech. Rep. 27, 217 pp.

Jouzel, J., Barkov, N.I., Barnola, J.M., Bender, M., Chappellaz, J., Genthon, C., Kotlyakov, V.M., Lipenkov, V., Lorius, C., Petit, J.R., Raynaud, D., Raisbeck, G., Ritz, C., Sowers, T., Stievenard, M., Yiou, F. & Yiou, P. 1993. Extending the Vostok ice-core record of paleoclimate to the penultimate glacial period. *Nature,* 364**,** 407-412**,** DOI: 10.1038/364407a0.

Jungclaus, J.H., Lorenz, S.J., Timmreck, C., Reick, C.H., Brovkin, V., Six, K., Segschneider, J., Giorgetta, M.A., Crowley, T.J., Pongratz, J., Krivova, N.A., Vieira, L.E., Solanki, S.K., Klocke, D., Botzet, M., Esch, M., Gayler, V., Haak, H., Raddatz, T.J., Roeckner, E., Schnur, R., Widmann, H., Claussen, M., Stevens, B. & Marotzke, J. 2010. Climate and carbon-cycle variability over the last millennium. *Climate of the Past*, 6, pp. 723–737, DOI: 10.5194/cp-6-723-2010.

Kageyama, M., Valdes, P.J., Ramstein, G., Hewitt, C.D. & Wyputta, U. 1999. Northern hemisphere storm-tracks in present day and last glacial maximum climate simulations: a comparison of European PMIP models, *Journal of Climate*, 12 pp. 742-760.

Kageyama, M., Peyron, O., Pinot, S., Tarasov, P., Guiot, J., Joussame, S. & Ramstein, G. 2001. The Last Glacial Maximum climate over Europe and western Siberia: a PMIP comparison between models and data. *Climate Dynamics*, 17, pp. 23-43.

Kageyama, M., Laîné, A., Abe-Ouchi, A., Braconnot, P., Cortijo, E., Crucifix, M., De Vernal, A., Guiot, J., Hewitt, C.D., Kitoh, A., Kucera, M., Marti, O., Ohgaito, R., Otto-Bliesner, B., Peltier, W.R., Modell-Melé, A., Vettoretti, G., Weber, S.Lo., Yu, Y. & Margo PROJECT MEMBERS 2006. Last Glacial Maximum temperatures over the North Atlantic, Europe and western Siberia: a comparison between PMIP models, MARGO sea-surface temperatures and pollen-based reconstructions. *Quaternary Science Reviews*, 25, pp. 2082-2102, DOI: 10.1016/j.quascirev.2006.02.010.

Kageyama, M., Albani, S., Braconnot, P., Harrison, S.P., Hopcroft, P.O., Ivanovic, R.F., Lambert, F., Marti, O., Peltier, W.R., Peterschmitt, J. -Y., Roche, D.M., Tarasov, L., Zhang, X., Brady, E.C., Haywood, A.M., Legrande, A.N., Lunt, D.J., Mahowald, N.M., Mikolajewicz, U., Nisancioglu, K.H., Otto-Bliesner, B.L., Renssen, H., Tomas, R.A., Zhang, Q., Abe-Ouchi, A., Bartlein, P.J., Cao, J., Lohmann, G., Ohgaito, R., SHI, X., Volodin, E., Yoshida, K., Zhang, X. & Zheng, W. (in review). The PMIP4 contribution to CMIP6 – Part 4: Scientific objectives and experimental design of the PMIP4-CMIP6 Last Glacial Maximum experiments and PMIP4 sensitivity experiments. *Geoscientific Model Development*, DOI: 10.5194/gmd-2017-18.

Kawamura, K., Parrenin, F., Lisiecki, L., Uemura, R., Vimeux, F., Severinghaus, J.P., Hutterli, M.A., Nakazawa, T., Aoki, S., Jouzel, J., Raymo, M.E., Matsumoto, K., Nakata, H., Motoyama, H., Fujita, S., Goto-Azuma, K., Fujii, Y. & Watanabe, O. 2007. Northern Hemisphere forcing of climatic cycles in Antarctica over the past 360,000 years. Nature, 448, 912-914, DOI: 10.1038/Nature06015.

Kjellström, E., Strandberg, G., Brandefelt, J., Näslund, J.-O., Smith, B. & Wohlfarth, B. 2009. Climate conditions in Sweden in a 100,000-year time perspective, *SKB Report, TR-09-04.* Svensk Kärnbränslehantering AB, Stockholm, Sweden. Available from: www.skb.com/publication/1925516/TR-09-04.pdf.

Knorr, G. & Lohmann, G. 2007. Rapid transitions in the Atlantic thermohaline circulation triggered by global warming and meltwater during the last deglaciation. *Geochemistry Geophysics Geosystems*, 8, 12, Q12006, DOI: 10.1029/2007GC001604.

Lambert, F., Delmonte, B., Petit, J.R., Bigler, M., Kaufmann, P.R., Hutterli, M.A., Stocker, T.F., Ruth, U., Steffensen, J.P. & Maggi, V. Dust-climate couplings over the past 800,000 years from the EPICA Dome C ice core. *Nature*, 452, pp. 616-619, DOI: 10.10378/nature06763.

Landrum, L., Otto-Bliesner, B.L., Wahl, E.R., Conley, A., Lawrence, P.J., Rosenbloom, N. & TENG, H. 2013. Last Millennium climate and its variability in CCSM4. *Journal of Climate*, 26, pp. 1085-1111, DOI: 10.1175/JCLI-D-11-00326.1.

Langebroek, P.M. & Nisancioglu, K.H. 2014. Simulating last interglacial climate with NorESM: role of insolation and greenhouse gases in the timing of peak warmth. *Climate of the Past*, 10, pp. 1305-1318, DOI: 10.5194/cp-10-1305-2014.

Laskar, J., Robutel, P., Joutel, F., Gastineau, M., Correia, A.C.M. & Levrard, B. 2004. A long-term numerical solution for the insolation quantities of the Earth. *Astronomy & Astrophysics,* 428**,** 261-285**,** DOI: 10.1051/0004-6361:20041335.

Lenton, T.M. 2000. Land and ocean carbon cycle feedback effects on global warming in a simple Earth system model. *Tellus Series B-Chemical and Physical Meteorology,* 52**,** 1159-1188**,** DOI: 10.1034/j.1600-0889.2000.01104.x.

Lenton, T.M. & Britton, C. 2006. Enhanced carbonate and silicate weathering accelerates recovery from fossil fuel CO_2 perturbations. *Global Biogeochemical Cycles,* 20, GB3009**,** DOI: 10.1029/2005gb002678.

Lenton, T.M., Williamson, M.S., Edwards, N.R., Marsh, R., Price, A.R., Ridgwell, A.J., Shepherd, J.G., Cox, S.J. & Team, T.G. 2006. Millennial timescale carbon cycle and climate change in an efficient Earth system model. *Climate Dynamics,* 26**,** 687-711**,** DOI: 10.1007/s00382-006-0109-9.

LI, C., Von Storch, J.S. & Marotzke, J. 2013. Deep-ocean heat uptake and equilibrium climate response. *Climate Dynamics,* 40**,** 1071-1086**,** DOI: 10.1007/s00382-012-1350-z.

Lisiecki, L.E. 2010. Links between eccentricity forcing and the 100,000-year glacial cycle. Nature Geoscience, 3, 349-352, DOI: 10.1038/Ngeo828.

Lisiecki, L.E. & Raymo, M.E. 2007. Plio-Pleistocene climate evolution: trends and transitions in glacial cycle dynamics. Quaternary Science Reviews, 26, 56-69, DOI: 10.1016/j.quascirev.2006.09.005.

Liu, Z., Otto-Bliesner, B.L., He, F., Brady, E.C., Tomas, R., Clark, P.U., Carlson, A.E., Lynch-Stieglitz, J., Curry, W., Brook, E., Erickson, D., Jacob, R., Kutzbach, J. & Cheng, J. 2009. Transient Simulation of Last Deglaciation with a New Mechanism for Bølling-Allerød Warming. *Science*, 325, 5938, pp. 310-314, DOI: 10.1126/science.1171041.

Liu, Z., Zhu, J., Rosenthal, Y., Zhang, X., Otto-Bliesner, B.L., Timmermann, A., Smith, R.S., Lohmann, G., Zheng, W. & Timm, O.E. 2014. The Holocene temperature conundrum. *PNAS*, E3501-3505, DOI: 10.1073/pnas.1407229111.

Lord, N.S., Crucifix, M., Lunt, D.J., Thorne, M.C., Bounceur, N., Dowsett, H., O'brien, C.L. & Ridgwell, A. In review. Emulation of long-term changes in global climate: Application to the mid-Pliocene and future. *Climate of the Past***,**

Lord, N.S., Ridgwell, A., Thorne, M.C. & Lunt, D.J. 2015. The 'long tail' of anthropogenic CO_2 decline in the atmosphere and its consequences for post-closure performance assessments for disposal of radioactive wastes. *Mineralogical Magazine,* 79**,** 1613-1623**,** DOI: 10.1180/minmag.2015.079.6.37.

Lord, N.S., Ridgwell, A., Thorne, M.C. & Lunt, D.J. 2016. An impulse response function for the "long tail" of excess atmospheric CO_2 in an Earth system model. *Global Biogeochemical Cycles,* 30**,** 2-17**,** DOI: 10.1002/2014gb005074.

Lorenz, S.J., Kim, J.H., Rimbu, N., Schneider, R.R. & Lohmann, G. 2006. Orbitally driven insolation forcing on Holocene climate trends: Evidence from alkenone data and climate modelling. *Paleoceanography*, 21, PA1002, DOI: 10.1029/2005PA001152.

Loutre, M.F. & Berger, A. 2000a. No glacial-interglacial cycle in the ice volume simulated under a constant astronomical forcing and a variable CO_2. *Geophysical Research Letters*, 27, 6, pp. 783-786.

Loutre, M.F. & Berger, A. 2000b. Future climatic changes: Are we entering an exceptionally long interglacial? *Climatic Change,* 46**,** 61-90**,** DOI: 10.1023/A:1005559827189.

Loutre, M.F., Fichefet, T., Goosse, H., Huybrechts, P., Goelzer, H. & Capron, E. 2014. Factors controlling the last interglacial climate as simulated by LOVECLIM1.3. *Climate of the Past*, 10, pp. 1541-1565, DOI: 10.5194/cp-10-1541-2014.

Ludwig, P., Schaffernicht, E.J., Shao, Y. & Pinto, J.G. 2016. Regional atmospheric circulation over Europe during the Last Glacial Maximum and its links to precipitation. *Journal of Geophysical Research: Atmospheres*, 121, pp. 2130-2145, DOI: 10.1002/2015JD024444.

Lunt, D.J., De Noblet-Ducoudre, N. & Charbit, S. 2004. Effects of a melted Greenland ice sheet on climate, vegetation, and the cryosphere. *Climate Dynamics,* 23**,** 679-694**,** DOI: 10.1007/s00382-004-0463-4.

Lunt, D.J., Ridgwell, A., Sluijs, A., Zachos, J., Hunter, S. & Haywood, A. 2011. A model for orbtial pacing of methane hydrate destabilization during the Palaeogene. *Nature Geoscience*, 4, pp. 775-778, DOI: 10.1038/ngeo1266.

Lunt, D.J., Abe-Ouchi, A., Bakker, P., Berger, A., Braconnot, P., Charbit, S., Fischer, N., Herold, N., Jungclaus, J.H., Khon, V.C., Krebs-Kanzow, U., Langebroek, P.M., Lohmann, G., Nisancioglu, K.H., Otto-Bliesner, B.L., Park, W., Pfeiffer, M., Phipps, S.J., Prange, M., Rachmayani, R., Renssen, H., Rosenbloom, N., Schneider, B., Stone, E.J., Takahashi, K., Wei, W., Yin, Q. & Zhang, Z.S. 2013. A multi-model assessment of last interglacial temperatures. *Climate of the Past*, 9, pp. 699–717, DOI: 10.5194/cp-9-699-2013.

Luthi, D., Le Floch, M., Bereiter, B., Blunier, T., Barnola, J.M., Siegenthaler, U., Raynaud, D., Jouzel, J., Fischer, H., Kawamura, K. & Stocker, T.F. 2008. High-resolution carbon dioxide concentration record 650,000-800,000 years before present. *Nature,* 453**,** 379-382**,** DOI: 10.1038/Nature06949.

Mahowald, N., Kohfeld, K., Hansson, M., Balkanski, Y., Harrison, S.P., Prentice, I.C., Schulz, M. & Rodhe, H. 1999. Dust sources and deposition during the last glacial maximum and current climate: A comparison of model results with paleodata from ice cores and marine sediments. *Journal of Geophysical Research*, 104, D13, pp. 15895-15916.

Marcott, S.A., Shakun, J.D., Clark, P.U. & Mix, A.C. 2013. A reconstruction of regional and global temperature for the past 11,300 years. *Science*, 339, pp. 1198-1201, DOI: 10.1126/science.1228026.

Margo Project Members 2009. Constraints on the magnitude and patterns of ocean cooling at the Last Glacial Maximum. *Nature Geoscience*, 2, pp. 127–132, DOI: 10.1038/NGEO411.

Masson, V., Cheddadi, R., Braconnot, P., Joussaume, S., Texier, D. & Pmip Participants 1999. Mid-Holocene climate in Europe: what can we infer from PMIP model-data comparisons? *Climate Dynamics*, 15, pp. 163-182.

Mauri, A., Davis, B.A.S., Collins, PM. & Kaplan, J.O. 2014. The influence of atmospheric circulation on the mid-Holocene climate of Europe: a data-model comparison. *Climate of the Past*, 10, pp. 1925-1938, DOI: 10.5194/cp-10-1925-2014.

Meehl, G.A., Covey, C., Delworth, T., Latif, M., Mcavaney, B., Mitchell, J.F.B., Stouffer, R.J. & Taylor, K.E. 2007. The WCRP CMIP3 multimodel dataset - A new era in climate change research. *Bulletin of the American Meteorological Society,* 88**,** 1383-1394**,** DOI: 10.1175/Bams-88-9-1383.

Mikolajewicz, U., Groger, M., Maier-Reimer, E., Schurgers, G., Vizcaino, M. & Winguth, A.M.E. 2007. Long-term effects of anthropogenic CO_2 emissions simulated with a complex earth system model. *Climate Dynamics,* 28**,** 599-631**,** DOI: 10.1007/s00382-006-0204-y.

Nakićenović, N., Alcamo, J., Davis, G., De Vries, B., Fenhann, J., Gaffin, S., Gregory, K., Grübler, A., Jung, T.Y., Kram, T., Lebre La Rovere, E., Michaelis, L., Mori, S., Morita, T., Pepper, W., Pitcher, H., Price, L., Riahi, K., Roehrl, A., Rogner, H.-H., Sankovski, A., Schlesinger, M., Shukla, P., Smith, S., Swart, R., Van Rooijen, S., Victor, N. & Dadi, Z. 2000. *Emissions Scenarios. A special report of Working Group III of the Intergovernmental Panel on Climate Change.,* Cambridge, UK, Cambridge University Press.

National Research Council 2011. *Climate stabilization targets: emissions, concentrations, and impacts over decades to millennia,* Washington, D.C., USA, The National Academies Press.

Neem Community Members 2013. Eemian interglacial reconstructed from a Greenland folded ice core. *Nature*, 493, pp. 489-494, DOI: 10.1038/nature11789.

Ngrip Community Members (North Greenland Ice Core Project Members) 2004. High-resolution record of Northern Hemisphere climate extending to the last interglacial period. *Nature*, 431, pp. 147-151, DOI: 10.1038/nature02805.

Nikolova, I., Yin, Q., Berger, A., Singh, U.K. & Karami, M.P. 2013. The last interglacial (Eemian) climate simulated by Loveclim and CCSM3. *Climate of the Past*, 9, pp. 1789-1806, DOI: 10.5194/cp-9-1789-2013.

Paillard, D. 1998. The timing of Pleistocene glaciations from a simple multiple-state climate model. Nature, 391, 378-381, DOI: 10.1038/34891.

Paillard, D. 2015. Quaternary glaciations: from observations to theories. Quaternary Science Reviews, 107, 11-24, DOI: 10.1016/j.quascirev.2014.10.002.

Paillard, D. & Parrenin, F. 2004. The Antarctic ice sheet and the triggering of deglaciations. Earth and Planetary Science Letters, 227, 263-271, DOI: 10.1016/j.epsl.2004.08.023.

Parrenin, F. & Paillard, D. 2003. Amplitude and phase of glacial cycles from a conceptual model. Earth and Planetary Science Letters, 214, 243-250, DOI: 10.1016/S0012-821x(03)00363-7.

Parrenin, F. & Paillard, D. 2012. Terminations VI and VIII (similar to 530 and similar to 720 kyr BP) tell us the importance of obliquity and precession in the triggering of deglaciations. Climate of the Past, 8, 2031-2037, DOI: 10.5194/cp-8-2031-2012.

Pedersen, R.A., Langen, P.L. & Vinther, B.M. 2016 The last interglacial climate: comparing direct and indirect impacts of insolation changes. *Climate Dynamics*, DOI: 10.1007/s00382-016-3274-5.

Peltier, W.R. 1994. Ice age paleotopography. *Science*, 265, pp.195-201.

Peltier, W.R. 2004. Global glacial isostacy and the surface of the iceage Earth: the ICE-5G (VM2) model and GRACE. *Annual Review of Earth and Planetary Science*, 32, pp. 111-149.

Petit, J.R., Jouzel, J., Raynaud, D., Barkov, N.I., Barnola, J.M., Basile, I., Bender, M., Chappellaz, J., Davis, M., Delaygue, G., Delmotte, M., Kotlyakov, V.M., Legrand, M., Lipenkov, V.Y., Lorius, C., Pepin, L., Ritz, C., Saltzman, E. & Stievenard, M. 1999. Climate and atmospheric history of the past 420,000 years from the Vostok ice core, Antarctica. Nature, 399, 429-436, DOI: 10.1038/20859.

Pfeiffer, M. & Lohmann, G. 2016. Greenland Ice Sheet influence on Last Interglacial climate: global sensitivity studies performed with an atmosphere-ocean general circulation model. *Climate of the Past*, 12, pp. 1313-1338, DOI: 10.5194/cp-12-1313-2016.

Pimenoff, N., Venäläinen, A. & Järvinen, H. 2011. Climate scenarios for Olkiluoto on a time scale of 120,000 years, *Report POSIVA, 2011-04.* Posiva Oy, Eurajoki, Finland. Available from: www.posiva.fi/files/2763/POSIVA_2011-04web.pdf.

Pisias, N.G. & Shackleton, N.J. 1984. Modeling the Global Climate Response to Orbital Forcing and Atmospheric Carbon-Dioxide Changes. Nature, 310, 757-759, DOI: 10.1038/310757a0.

Plattner, G.K., Knutti, R., Joos, F., Stocker, T.F., Von Bloh, W., Brovkin, V., Cameron, D., Driesschaert, E., Dutkiewicz, S., Eby, M., Edwards, N.R., Fichefet, T., Hargreaves, J.C., Jones, C.D., Loutre, M.F., Matthews, H.D., Mouchet, A., Muller, S.A., Nawrath, S., Price, A., Sokolov, A., Strassmann, K.M. & Weaver, A.J. 2008. Long-term Climate commitments projected with climate-carbon cycle models. *Journal of Climate,* 21**,** 2721-2751**,** DOI: 10.1175/2007jcli1905.1.

Pollard, D. & Barron, E.J. 2003. Causes of model-data discrepancies in European climate during oxygen isotope stage 3 with insights from the last glacial maximum. *Quaternary Research*, 59, pp. 108-113.

Prentice, I.C., Jolly, D. & Biome 6000 Participants 2000. Mid-Holocene and glacial-maximum vegetation geography of the northern continents and Africa. *Journal of Biogeography*, 27, pp. 507-519.

RAHMSTORF, S. 2007. A semi-empirical approach to projecting future sea-level rise. *Science*, 315, pp. 368-370, DOI: 10.1126/science.1135456.

Ramstein, G., Kageyama, M., Guiot, J., Wu, H., Hely, C., Krinner, G. & Brewer, S. 2007. How cold was Europe at the Last Glacial Maximum? A Synthesis of the progress achieved since the first PMIP model-data comparison. *Climate of the Past*, 3, 2, pp. 331-339.

Raymo, M.E. 1997. The timing of major climate terminations. *Paleoceanography*, 12, 577-585, DOI: 10.1029/97pa01169.

Renssen, H., Goosse, H. & Fichefet, T. 2002. Modeling the effect of freshwater pulses on the early Holocene climate: The influence of high-frequency climate variability. *Paleoceanography*, 17, 2, pp. 1020-1035, DOI: 10.1029/2001PA0006419.

Ridgwell, A. & Hargreaves, J.C. 2007. Regulation of atmospheric CO_2 by deep-sea sediments in an Earth system model. *Global Biogeochemical Cycles,* 21, GB2008**,** DOI: 10.1029/2006gb002764.

Ridley, J.K., Huybrechts, P., Gregory, J.M. & Lowe, J.A. 2005. Elimination of the Greenland ice sheet in a high CO_2 climate. *Journal of Climate,* 18**,** 3409-3427**,** DOI: 10.1175/Jcli3482.1.

Ruddiman, W.F. 2006. Orbital changes and climate. Quaternary Science Reviews, 25, 3092-3112, DOI: 10.1016/j.quascirev.2006.09.001.

Ruddiman, W.F., Raymo, M.E., Martinson, D.G., Clement, B.M. & Backman, J. 1989. Pleistocene evolution: Northern Hemisphere ice sheets and North Atlantic Ocean. Paleoceanography, 4, 353-412, DOI: 10.1029/PA004i004p00353.

Saltzman, B. 2001. Dynamical paleoclimatology: Generalized theory of global climate change, San Diego, CA, Academic Press.

Saltzman, B. & Maasch, K.A. 1990. A first-order global model of late Cenozoic climatic change. Transactions of the Royal Society of Edinburgh-Earth Sciences, 81, 315-325,

Saltzman, B. & Maasch, K.A. 1991. A first-order global model of late Cenozoic climatic change - Part II: Further analysis based on a simplification of CO2 dynamics. Climate Dynamics, 5, 201-210, DOI: 10.1007/BF00210005.

Servonnat, J., Yiou, P., Khodri, M., Swingedouw, D. & Denvil, S. 2010. Influence of solar variability CO_2 and orbital forcing between 1000 and 1850 AD in the IPSLCM4 model. *Climate of the Past*, 6, pp. 445-460, DOI: 10.5194/cp-6-445-2010

Shackleton, N.J., Berger, A. & Peltier, W.R. 1990. An alternative astronomical calibration of the Lower Pleistocene timescale based on ODP Site 677. Transactions of the Royal Society of Edinburgh-Earth Sciences, 81, 251-261,

Shackleton, N.J. & Hall, M.A. (eds.) 1989. Stable isotope history of the Pleistocene at ODP site 677, College Station, TX: Ocean Drilling Program.

Shaffer, G., Olsen, S.M. & Pedersen, J.O.P. 2009. Long-term ocean oxygen depletion in response to carbon dioxide emissions from fossil fuels. *Nature Geoscience,* 2**,** 105-109**,** DOI: 10.1038/Ngeo420.

Shakun, J.D., Clark, P.U., HE, F., Marcott, S.A., Mix, A.C., Liu, Z., Otto-Bliesner, B., Schmittner, A. & Bard, E. 2012. Global warming preceded by increasing carbon dioxide concentrations during the last deglaciation. *Nature*, 484, pp. 49-54, DOI: 10.1038/nature10915.

Shakun, J.D., Clark, P.U., HE, F., Lifton, N.A., Liu, Z. & Otto-Bliesner, B.L. 2015. Regional and global forcing of glacier retreat during the last deglaciation. *Nature Communications*, 6, 8059, DOI: 10.1038/ncomms9059.

Sigman, D.M., Jaccard, S.L. & Haug, G.H. 2004. Polar ocean stratification in a cold climate. Nature, 428, 59-63, DOI: 10.1038/nature02357.

Singarayer, J.S. & Valdes, P.J. 2010. High-latitude climate sensitivity to ice-sheet forcing over the last 120 kyr. *Quaternary Science Reviews*, 29, pp. 43-55, DOI: 10.1016/j.quascirev.2009.10.011

Smith, R.S. & Gregory, J. 2012. The last glacial cycle: transient simulations with an AOGCM. *Climate Dynamics*, 38, pp. 1545-1559, DOI: 10.1007/s00382-011-1283-y.

Smith, R.S., Gregory, J.M. & Osprey, A. 2008. A description of the FAMOUS (version XDBUA) climate model and control run. *Geoscientific Model Development*, 1, pp. 53-68.

Solomon, S., Plattner, G.K., Knutti, R. & Friedlingstein, P. 2009. Irreversible climate change due to carbon dioxide emissions. *Proceedings of the National Academy of Sciences of the United States of America,* 106**,** 1704-1709**,** DOI: 10.1073/pnas.0812721106.

Stenni, B., Buiron, D., Frezzotti, M., Albani, S., Barbante, C., Bard, E., Barnola, J.M., Baroni, M. And Baumgartner, M. And Bonazza, M. And Capron, E. And Castellano, E., Chappellaz, J., Delmonte, B., Falourd, S., Genoni, L., Iacumin, P., Jouzel, J., Kipfstuhl, S., Landais, A., Lemieux-Dudon, B., Maggi, V., Masson-Delmotte, V., Mazzola, C., Minster, B., Montagnat, M., Mulvaney, R., Narcisi, B., Oerter, H., Parrenin, F., Petit, J.R., Ritz, C., Scarchilli, C., Schilt, A., Schupbach, S., Schwander, J., Selmo, E., Severi, M., Stocker, T.F. & Udisti, R. 2010. Expression of the bipolar see-saw in Atlantic climate records during the last deglaciation. *Nature Geoscience*, 4, pp. 46-49, DOI: 10.1038/NGEO1026.

Stocker, T.F. 1998. Climate change – the seesaw effect. *Science*, 282, pp. 61-62.

Stone, E.J., Lunt, D.J., Annan, J.D. & Hargreaves, J.C. 2013. Quantification of the Greenland ice sheet contribution to Last Interglacial sea level rise. *Climate of the Past*, 9, pp. 621-639, DOI: 10.5194/cp-9-621-2013.

Stone, E.J., Capron, E., Lunt, D.J., Payne, A.J., Singarayer, J.S., Valdes, P.J. & Wolff, E.W. 2016. Impact of meltwater on high-latitude early Last Interglacial climate. *Climate of the Past*, 12, pp. 1919-1932, DOI: 10.5194/cp-12-1919-2016.

Taylor, K.E., Stouffer, R.J. & Meehl, G.A. 2012. An Overview of CMIP5 and the experiment design. *Bulletin of the American Meteorological Society,* 93**,** 485-498**,** DOI: 10.1175/Bams-D-11-00094.1.

Tegen, I. 2003. Modelling the mineral dust aerosol cycle in the climate system. *Quaternary Science Reviews*, 22, pp. 1821-1834.

Texier, D., Degnan, P., Loutre, M.F., Paillard, D. & Thorne, M.C. 2003. Modelling sequential BIOsphere systems under CLIMate change for radioactive waste disposal. Project BIOCLIM. Proceedings of the 10th International High-Level Waste Management Conference, 30 March – 2 April 2003 Las Vegas, Nevada.

Tiedemann, R., Sarnthein, M. & Shackleton, N.J. 1994. Astronomic timescale for the Pliocene Atlantic δ18O and dust flux records of Ocean Drilling Program Site 659. Paleoceanography, 9, 619-638, DOI: 10.1029/94pa00208.

Timm, O. & Timmermann, A. 2007. Simulation of the last 21000 years using accelerated transient boundary conditions. *Journal of Climate*, 20, pp. 4377-4401, DOI: 10.1175/JCLI4237.1.

Timmermann, A., Timm, O., Stott, L. & Menviel, L. 2009. The roles of CO_2 and orbital forcing in driving southern hemispheric temperature variations during the last 21000 yr. *Journal of Climate*, 22, pp. 1626-1640, DOI:10.1175/2008JCLI2161.1.

Toniazzo, T., Gregory, J.M. & Huybrechts, P. 2004. Climatic impact of a Greenland deglaciation and its possible irreversibility. *Journal of Climate,* 17**,** 21-33**,** DOI: 10.1175/1520-0442(2004)017<0021:Cioagd>2.0.Co;2.

Tzedakis, P.C., Channell, J.E.T., Hodell, D.A., Kleiven, H.F. & Skinner, L.C. 2012. Determining the natural length of the current interglacial. *Nature Geoscience,* 5**,** 138-141**,** DOI: 10.1038/Ngeo1358.

Tzedakis, P.C., Crucifix, M., Mitsui, T. & Wolff, E.W. 2017. A simple rule to determine which insolation cycles lead to interglacials. Nature, 542, 427-432, DOI: 10.1038/nature21364.

Tziperman, E., Raymo, M.E., Huybers, P. & Wunsch, C. 2006. Consequences of pacing the Pleistocene 100 kyr ice ages by nonlinear phase locking to Milankovitch forcing. Paleoceanography, 21, Pa4206, DOI: 10.1029/2005pa001241.

Vettoretti, G. & Peltier, W.R. 2011. The impact of insolation, greenhouse gas forcing and ocean circulation changes on glacial inception. *Holocene,* 21**,** 803-817**,** DOI: 10.1177/0959683610394885.

Vizcaino, M., Mikolajewicz, U., Groger, M., Maier-Reimer, E., Schurgers, G. & Winguth, A.M.E. 2008. Long-term ice sheet-climate interactions under anthropogenic greenhouse forcing simulated with a complex Earth System Model. *Climate Dynamics,* 31**,** 665-690**,** DOI: 10.1007/s00382-008-0369-7.

Warren, S.G. 1984. Impurities in snow: effects on albedo and snowmelt (review). *Annals of Glaciology*, 5, pp. 177-179.

Winkelmann, R., Levermann, A., Ridgwell, A. & Caldeira, K. 2015. Combustion of available fossil fuel sources sufficient to eliminate the Antarctic Ice Sheet. *Science Advances*, 1, 8, e1500589, DOI: 10.1126/sciadv.1500589.

Wolff, E.W., Chappellaz, J., Blunier, T., Rasmussen, S.O. & Svensson, A. Millennial-scale variability during the last glacial: the ice core record. *Quaternary Science Review*, 29, pp. 2828-2838, DOI: 10.1016/j.quascirev.2009.10.013.

Yang, K. & Jiang, D. 2017 Interannual climate variability change during the Medieval Climate Anomaly and Little Ice Age in PMIP3 Last Millennium simulations. *Advances in Atmospheric Sciences*, 34, pp 497-508, DOI: 10.1007/s00376-016-6075-1.

Zhang, X., Lohmann, G., Knorr, G. & Xu, X. 2013. Different ocean states and transient characteristics in Last Glacial Maximum simulations and implications for deglaciation. *Climate of the Past*, 9, pp. 2319-2333, DOI: 10.5194/cp-9-2319-2013.

Zhang, Y., Renssen, H. & Seppä, H. 2016. Effects of melting ice sheets and orbital forcing on the early Holocene warming in the extratropical Northern Hemisphere. *Climate of the Past*, 12, pp. 1119-1135, DOI: 10.5194/cp-12-1119-2016.

Zickfeld, K., Eby, M., Weaver, A.J., Alexander, K., Crespin, E., Edwards, N.R., Eliseev, A.V., Feulner, G., Fichefet, T., Forest, C.E., Friedlingstein, P., Goosse, H., Holden, P.B., Joos, F., Kawamiya, M., Kicklighter, D., Kienert, H., Matsumoto, K., Mokhov, I.I., Monier, E., Olsen, S.M., Pedersen, J.O.P., Perrette, M., Philippon-Berthier, G., Ridgwell, A., Schlosser, A., Von Deimling, T.S., Shaffer, G., Sokolov, A., Spahni, R., Steinacher, M., Tachiiri, K., Tokos, K.S., Yoshimori, M., Zeng, N. & Zhao, F. 2013. Long-Term Climate Change Commitment and Reversibility: An EMIC Intercomparison. *Journal of Climate,* 26**,** 5782-5809**,** DOI: 10.1175/Jcli-D-12-00584.1.